June 24, 2021
SBK-L-21049
GL 2004-02

U. S. Nuclear Regulatory Commission
Attn: Document Control Desk
Washington DC 20555-0001

RE: Seabrook Station
Docket No. 50-443
Renewed Facility Operating License No. NPF-86

Revision to Updated Final Response to NRC Generic Letter 2004-02

References:

1. NextEra Energy Seabrook, LLC, Letter SBK-L-18010, "Updated Final Response to NRC Generic Letter 2004-02," January 31, 2018 (ADAMS Accession No. ML18031B248)

2. Point Beach Nuclear Plant, Units 1 and 2; Seabrook Station, Unit No. 1; St. Lucie Plant, Units 1 and 2; and Turkey Point Nuclear Generating Units 3 and 4 - Audit Report Regarding Generic Letter 2004-02, "Potential Impact of Debris Blockage on Emergency Recirculation During Design Basis Accidents at Pressurized-Water Reactors" Closure Methodology (EPID 2017-LRC-0000), December 2, 2019 (ADAMS Accession ML19217A003)

In Reference 1, NextEra Energy Seabrook, LLC (NextEra) provided on behalf of the Seabrook Station, Unit No. 1 (Seabrook), an updated final response to Generic Letter (GL) 2004-02, Potential Impact of Debris Blockage on Emergency Recirculation During Design Basis Accidents at Pressurized-Water Reactors (ADAMS Accession No. ML18031B248). Included within were NextEra 's statement of compliance with the *Applicable Regulatory Requirements* of GL 2004-02, a description of completed plant modifications and process changes, and an evaluation of the 16 issue areas identified in the NRC's 'Revised Content Guide for Generic Letter 2004-02 Supplemental Responses (ADAMS Accession No. ML073110389), including a summary of the significant margins and conservatisms utilized in supporting analyses to demonstrate regulatory compliance.

During January 15, 2019 through January 17, 2019, the NRC staff conducted an audit of NextEra's updated final response to GL 2004-02 at NextEra's Juno Beach facility. In Reference 2, the NRC staff reported their audit results. For Seabrook, Reference 2 identified several open issues that NextEra determined would require additional testing and analyses, and performing new evaluations for Seabrook.

Enclosure 1 contains information proprietary to Westinghouse Electric Company LLC ("Westinghouse"), it is supported by an Affidavit signed by Westinghouse, the owner of the information. The Affidavit sets forth the basis on which the information may be withheld from public disclosure by the Nuclear Regulatory Commission ("Commission") and addresses with specificity the considerations listed in paragraph (b)(4) of Section 2.390 of the Commission's regulations. Accordingly, it is respectfully requested that the information which is proprietary to Westinghouse be withheld from public disclosure in accordance with 10 CFR Section 2.390 of the Commission's regulations.

Correspondence with respect to the copyright or proprietary aspects of the items listed above or the supporting Westinghouse Affidavit should reference CAW-21-5181 and should be addressed to Camille Zozula, Manager, Regulatory Compliance & Corporate, Westinghouse Electric Company, 1000 Westinghouse Drive, Cranberry Township, Pennsylvania 16066.

Enclosure 1 to this letter replaces the updated final response to GL 2004-02 provided in Reference 1. Section 1 of Enclosure 1 provides NextEra's statement of compliance with the Applicable Regulatory Requirements section of GL 2004-02 on behalf of Seabrook. Section 2 of Enclosure 1 describes the corrective actions that were completed in response to GL 2004-02, summarizes the remaining actions that need to be completed, and lists significant margins and conservatisms that were utilized in the analyses. Compared with the January 2018 submittal of Reference 1, Sections 1 and 2 are updated for consistency with the implementation guidance of Pressurized Water Reactor Users Group (PWROG) 16073-P, "TSTF-567 Implementation Guidance, Evaluation of In-Vessel Debris Effects, Submittal Template for Final Response to Generic Letter 2004-02 and FSAR Changes" (Proprietary). Section 3 of Enclosure 1 summarizes the methodologies, key assumptions and results of the Seabrook analyses and testing in each of the sixteen areas identified in the NRC's Revised Content Guide for GL 2004-02 (ADAMS Accession No. ML073110389). Section 3 provides the basis for a deterministic resolution and closure of GL 2004-02 for Seabrook. All changes from the January 2018 submittal of Reference 1 are identified with change bars, with the exception of formatting and non-technical changes.

Enclosure 2 to this letter provides a non-proprietary (redacted) version of the evaluations and conclusions provided in Enclosure 1.

Enclosure 3 provides the Westinghouse Application for Withholding Proprietary Information from Public Disclosure CAW-21-5181 affidavit supporting the proprietary withholding request. The request is supported by an affidavit signed by Westinghouse, the owner of the information. The affidavit sets forth the basis on which the information may be withheld from public disclosure by the Nuclear Regulatory Commission ("Commission") and addresses with specificity the considerations listed in paragraph (b)(4) of Section 2.390 of the Commission's regulations. Accordingly, NextEra requests that the information which is proprietary to Westinghouse be withheld from public disclosure in accordance with 10 CFR Section 2.390 of the Commission's regulations. Correspondence with respect to the copyright or proprietary aspects of the items listed above or the supporting Westinghouse affidavit should reference CAW-21-5181 and be addressed to Camille Zozula, Manager, Regulatory Compliance & Corporate, Westinghouse Electric Company, 1000 Westinghouse Drive, Suite 165, Cranberry Township, Pennsylvania 16066.

As stated in Reference 1, changes to the Seabrook licensing basis have been implemented which allowed NextEra to complete plant modifications that enhanced Seabrook's capabilities with respect to the information in GL 2004-02. Accordingly, the assumptions and inputs used to establish the bases for GL 2004-02 closure are consistent with the Seabrook licensing basis and no new changes pursuant to 10 CFR 50.90 are being proposed as a result of this submittal. Upon NRC acceptance of NextEra's closure of GL 2004-02, the updated final safety analysis reports (UFSARs) for Seabrook will be revised to reflect the final closure information in accordance with 10 CFR 50.71(e).

This letter contains the following regulatory commitment.

Commitment	Type		Scheduled Completion Date
	One-Time	Continuing Compliance	
NextEra will modify the Seabrook Station refueling canal drain and drain lines and update relevant sections of the UFSAR accordingly.	X	--	By no later than November 2021

As this submittal was being prepared, NextEra learned of a non-conservatism in the Seabrook debris transport evaluation that supported the Reference 1 submittal. Specifically, the non-conservatism occurred when determining the debris transport fractions for the reactor nozzle breaks, which incorrectly applied the pool fill-up transport fractions for selected debris types, resulting in non-conservative transported debris quantities. However, this non-conservatism did not impact the limiting break scenarios evaluated in Reference 1. The issue has been entered into the Seabrook Corrective Action Program (CAP). Moreover, the calculation containing the non-conservatism has been revised, and updated debris transport fractions are presented in this submittal.

Should you have any questions regarding this submission, please contact Mr. Matthew Levander, Licensing Manager, at 603-773-7631.

I declare under penalty of perjury that the foregoing is true and correct.

Executed on the 24TH day of June 2021.

Sincerely,

Brian Booth

Brian Booth
Nuclear Site VP – Seabrook Nuclear Power Station
NextEra Energy Seabrook, LLC

Enclosures:

Enclosure 1 - Updated Final Response to NRC Generic Letter 2004-02 Seabrook Nuclear Power Plant (Proprietary)

Enclosure 2 - Updated Final Response to NRC Generic Letter 2004-02 Seabrook Nuclear Power Plant (Non-Proprietary)

Enclosure 3 - Application for Withholding Proprietary Information from Public Disclosure

cc: USNRC Region I Administrator
USNRC Project Manager
USNRC Senior Resident Inspector

Director Homeland Security and Emergency Management
New Hampshire Department of Safety
Division of Homeland Security and Emergency Management
Bureau of Emergency Management
33 Hazen Drive
Concord, NH 03305

Katharine Cederberg, Lead Nuclear Planner
The Commonwealth of Massachusetts
Emergency Management Agency
400 Worcester Road
Framingham, MA 01702-5399

Enclosure 2 - Updated Final Response to NRC Generic Letter 2004-02 Seabrook Nuclear Power Plant (Non-Proprietary)

Enclosure 2 Updated Final Response to NRC Generic Letter 2004-02 Seabrook Nuclear Power Plant (Non-Proprietary)

Table of Contents

Section **Page**

Enclosure 2
Updated Final Response to NRC Generic Letter 2004-02
(Non-Proprietary)

This enclosure replaces the Updated Final Response to Generic Letter (GL) 2004-02 (Reference 1) submitted January 31, 2018 (Reference 2) by NextEra Energy Seabrook, LLC (NextEra) for the Seabrook Nuclear Station (Seabrook). Section 1 of the enclosure provides NextEra's statement of compliance with the Applicable Regulatory Requirements section of GL 2004-02 on behalf of Seabrook. Section 2 of the enclosure describes the corrective actions that were completed in response to GL 2004-02, summarizes the remaining actions that need to be completed, and lists significant margins and conservatisms that were utilized in the analyses. Compared with the January 2018 submittal, Sections 1 and 2 are updated in consistency with the Pressurized Water Reactor Users Group (PWROG) guidance (Reference 3). Section 3 summarizes the methodology, key assumptions and results of the Seabrook analyses and testing in each of the sixteen areas identified in the NRC's Revised Content Guide for GL 2004-02 (Reference 4). This enclosure provides the basis for a deterministic resolution of GL 2004-02 for Seabrook. All changes from the January 2018 submittal (Reference 2) are identified with change bars, except for formatting and non-technical changes.

1. Overall Compliance

Provide information requested in GL 2004-02 <u>Requested Information</u> Item 2(a) regarding compliance with regulations.

<u>GL2004-02 Requested Information Item 2(a)</u>
Confirmation that the ECCS and CSS recirculation functions under debris loading conditions are or will be in compliance with regulatory requirements listed in the Applicable Regulatory Requirements section of this GL. This submittal should address the configuration of the plant that will exist once all modifications required for regulatory compliance have been made and this licensing basis has been updated to reflect the results of the analysis described above.

Response to 1:

On January 31, 2018, NextEra submitted a response to GL 2004-02 for Seabrook to the NRC (Reference 2). The NRC performed an audit of the submittal and issued an audit report on December 2, 2019 (Reference 8). Following the audit, NextEra performed new strainer head loss and fiber bypass testing for Seabrook, and completed all necessary analyses.

This submittal reflects the new testing and analysis results, and uses a deterministic approach to demonstrate that the Seabrook emergency core cooling system (ECCS) and containment building spray (CBS) have the capability to provide long-term cooling following a LOCA and therefore meet the regulatory requirements of Title 10 of the Code of Federal Regulations Section 50.46 (10 CFR 50.46) and relevant General Design Criteria (GDCs) in Appendix A to 10 CFR Part 50, as discussed in the "Applicable Regulatory Requirements" section of GL 2004-02 (Reference 1).

1.1 Overview of NextEra Resolution to GL 2004-02 for Seabrook

The key aspects of the approach chosen by NextEra to resolve the GL 2004-02 concerns for Seabrook are summarized in this section and are presented in Section 3 with more details.

- Extensive design modifications to significantly reduce the potential effects of post-accident debris and latent material on the functions of the ECCS and CBS system during the recirculation phase of accident mitigation.
- Extensive testing and analysis to determine break locations, identify and quantify debris sources, quantify debris transport, determine upstream and downstream effects, and confirm the recirculation function.
- Changes to the Seabrook updated final safety analysis report (UFSAR) to reflect the plant modifications that addressed the GL 2004-02 concerns.
- Extensive changes to plant programs, processes, and procedures to limit the introduction of materials into containment that could adversely impact the recirculation function.
- Addition of monitoring programs to ensure containment conditions will continue to support the recirculation function.
- Application of conservative methodology, inputs and assumptions in analyses and testing for the GL 2004-02 resolution.

<u>Analyses</u>

Since the previous submittal (Reference 2), NextEra has revised existing analyses and performed new evaluations for Seabrook to address the questions raised by the NRC in their audit report (Reference 8), as summarized below.

A revision to the Seabrook debris generation calculation has been made since the previous submittal (Reference 2) to update the coatings debris loads, as discussed in the response to Section 3.h.

Since the previous submittal (Reference 2), NextEra has revised the containment sump water level calculation for Seabrook. This revision updated the holdup volumes considered in the minimum sump water level evaluation and resulted in reductions in water levels, compared with the previous submittal. Refer to the response to Section 3.g for details.

After the NRC audit, NextEra has revised the debris transport analysis for Seabrook. The computational fluid dynamics (CFD) models for evaluating recirculation transport were rerun to incorporate washdown through the refueling canal drains and reduced water level. This change reflects the planned configuration with the modified refueling canal drains. Additionally, debris holdup is no longer credited by any of the debris interceptors inside the containment. Refer to the response to Section 3.e for details.

Since the previous submittal (Reference 2), NextEra has performed new strainer head loss testing (including chemical effects) and fiber bypass testing for Seabrook using NRC reviewed protocols. Additional discussion is provided in the responses to Sections 3.f, 3.n and 3.o.

A new hydraulic model was developed for the Seabrook ECCS and CBS system to quantify the residual heat removal (RHR) and CBS pump flow rates required for the analysis. Using the latest pump flow rates and head loss testing data, NextEra analyzed strainer head losses for Seabrook in a new calculation. The head loss results were then applied to determine the RHR and CBS pump net positive suction head (NPSH) margin and to demonstrate that the head loss will not challenge structural integrity of the strainer. A new strainer degasification analysis was also prepared to determine the worst void fraction at the RHR and CBS pump suctions. Refer to the responses to Sections 3.f and 3.g for details.

NextEra has also performed a new in-vessel downstream effects evaluation for Seabrook to determine the worst-case in-vessel fiber loads using the latest fiber bypass testing data. The evaluation also followed the latest NRC review guidance on in-vessel effects (Reference 9) to demonstrate that accumulation of debris within the reactor core will not challenge long term core cooling using the results from Revision 1 of WCAP-17788 (Reference 10; 11). Refer to Section 3.n for details.

<u>Changes to UFSAR</u>

NextEra had previously updated the Seabrook UFSAR to recognize the modifications and evaluations performed to address the effect of post-accident debris on the ECCS and CBS recirculation function. The UFSAR will be reviewed after NRC acceptance of information presented in this submittal to determine if any further changes are necessary. If changes are determined to be necessary, the UFSAR updates will occur after receipt of the final closeout letter from the NRC. This is discussed in the response to Section 3.p.

The Technical Specification (TS) surveillance requirements were updated to expand the recirculation sump inspection requirements to include the entire sump strainer system. This is discussed in the response to Section 3.p.

<u>Improvements in Processes and Programs</u>

NextEra has completed a review of procedures, processes, and programs, and has performed updates accordingly to ensure the analysis inputs and assumptions can be maintained. This is discussed in the response to Section 3.i.

Margins and Conservatisms

Specific conservatisms adopted in the methodology, inputs and assumptions for the Seabrook GL 2004-02 analyses and testing are summarized in the response to Section 2 under Margins and Conservatisms.

1.2 Correspondence Background

The following provides a listing of correspondences issued by the NRC or submitted by NextEra for Seabrook on the subject of GL 2004-02 since 2018:

Table 1-1 NextEra GL 2004-02 Correspondences for Seabrook

Document Date	ADAMS Accession Number	Document
January 31, 2018	ML18031B248 (Reference 2)	Updated final response to GL 2004-02 using the alternate break methodology
May 31, 2018	ML18136A905 (Reference 12)	Meeting summary for request for exemption from single-failure requirement
August 30, 2018	ML18243A043 (Reference 13)	Request for exemption from single-failure requirement
November 26,2018	ML18331A033 (Reference 14)	NRC audit plan
September 4, 2019	ML19228A011 (Reference 9)	NRC review guidance on in-vessel effects
December 2, 2019	ML19217A003 (Reference 8)	NRC audit report
November 19, 2020	ML20324A623 (Reference 15)	Withdrawal of request for exemption from single-failure requirement
December 21, 2020	ML20346A089 (Reference 16)	Withdrawal of request for exemption from single-failure requirement

1.3 General Plant System Description

Seabrook has a Westinghouse four loop pressurized water reactor (PWR) design. The RHR pumps, Safety Injection (SI) pumps, and Centrifugal Charging Pumps (CCPs) are automatically started by the safety injection signal following a loss of coolant accident (LOCA). Operation of the CBS pumps is initiated by high containment pressure. Recirculation is initiated by the RWST Lo-Lo level signal. Upon receipt of this signal, the RHR and CBS pumps are automatically re-aligned to take suction from the recirculation sumps. The CCPs and SI pumps are then re-aligned to take suction from the RHR pumps' discharge ("piggyback" mode). Approximately 5 to 6 hours after the accident, the SI and RHR pumps are aligned to hot leg recirculation supplying flow to the RCS hot legs. The CCPs continue to supply flow to the cold legs.

1.4 General Description of Containment Sump Strainers

Seabrook has two separate and independent containment sump recirculation strainers designed by General Electric (GE). Each strainer is installed in a separate sump and supplies flow to one ECCS train and CBS train. A strainer consists of 20 strainer disk assemblies (4 disks per assembly or 80 disks total) installed vertically on top of a plenum and a doghouse assembly. The doghouse also provides connections to the suction piping supplying flow to the RHR and CBS pumps. The previous NextEra submittal for Seabrook showed an unobstructed surface area of 2,412 ft^2 (Reference 2 pp. E1-78), which was calculated based on the Sump A strainer and excluded the surface area of perforated plates on the strainer doghouse. This strainer surface area was increased to 2,445 ft^2 after including the perforated sides of the strainer doghouse. Refer to the response to Section 3.j.1 for details.

2. General Description of and Schedule for Corrective Actions:

Provide a general description of actions taken or planned, and dates for each. For actions planned beyond December 31, 2007, reference approved extension requests or explain how regulatory requirements will be met as per Requested Information Item 2(b). (Note: All requests for extension should be submitted to the NRC as soon as the need becomes clear, preferably no later than October 1, 2007.)

> *GL 2004-02 Requested Information Item 2(b)*
> *A general description and implementation schedule for all corrective actions, including any plant modifications that you identify while responding to this generic letter. Efforts to implement the identified actions should be initiated no later than the first refueling outage starting after April 1, 2006. All actions should be completed by December 31, 2007. Provide justification for not implementing the identified actions during the first refueling outage starting after April 1, 2006. If corrective actions will not be completed by December 31, 2007, describe how the regulatory requirements discussed in the Applicable Regulatory Requirements section will be met until the corrective actions are completed.*

Response to 2:

The corrective actions to address the concerns identified in GL 2004-02 at Seabrook consisted of plant modifications, testing and analysis, changes to plant programs and processes, and changes to the UFSAR. These actions have been completed in accordance with NextEra regulatory commitments and NRC-approved extensions.

Plant Modifications and Walkdowns

The original sump screens have been removed and replaced with new strainer systems. These systems ensure adequate NPSH during recirculation with margin for chemical effects. This modification was performed in Spring 2008. Debris interceptors within containment was installed for Seabrook in Fall 2006 to limit the transported quantities of debris that could reach the sump strainers.

Containment spray drain tubing downstream of the drain valves was rerouted and supported from the top of the “B” sump platform to support installation of the new sump strainers.

Walkdowns have been performed to confirm the absence of potential choke points in the flow path from potential break locations to the recirculation strainers.

NextEra plans to install strainers over all refueling canal drains, add a new drain line, and enlarge the existing drain line to ensure the drains will not be clogged during recirculation (see the response to Section 3.e.1). This is shown as a regulatory commitment in the response to Section 3.p.

Testing and Analyses

NextEra completed new strainer head loss and fiber bypass testing for Seabrook in 2019. All of the analyses that are required to address GL 2004-02 concerns were completed in 2020. Section 3 provides summarizes of the relevant testing programs and analyses.

Plant Programs and Processes

Significant program and process changes necessary to address the GL 2004-02 concerns were completed by Spring 2008.

The containment and containment spray recirculation sump surveillance procedure requires inspection of all accessible areas to verify that no loose debris, fibrous materials that could degrade into loose debris, or bubbling/chipping paint is present prior to setting containment integrity. In addition, any entry performed while containment integrity is set requires that any materials brought into the containment during the entry are tracked by an accountability log to ensure they are removed upon departure.

The maintenance director is responsible for maintaining the general housekeeping of containment, which includes tracking the overall cleanliness of containment and promptly correcting identified deficiencies.

Foreign material exclusion programmatic controls are in place, which ensure that proper work control is specified for debris-generating activities within the containment building. This assists in preventing introduction of foreign material into containment, which could challenge the containment recirculation function. Additionally, the foreign material exclusion program requires that engineering be consulted any time foreign material covers are placed on, or modifications are performed on, the containment sump strainers. Lastly, the containment entry procedure provides additional controls to evaluate foreign materials to be brought into containment and ensure they are removed during at-power entries.

Engineering change processes and procedures for Seabrook ensure modifications that may affect the ECCS, including sump performance, are evaluated for GL 2004-02 compliance. During engineering change preparation, the process requires specific critical attributes be listed, evaluated, and documented when affected. This includes the introduction of materials into containment that could affect sump performance or lead to equipment degradation. It also includes repair, replacement, and installation of coatings inside containment, including installing coated equipment.

NextEra has adopted the industry's standard change process for Seabrook, including the industry procedure IP-ENG-001. The standard process and tools are intended to facilitate sharing of information, solutions and design changes throughout the industry. This process requires activities that affect UFSAR described structure, system, or component (SSC) design functions to be evaluated as a design change in accordance with NextEra's 10 CFR 50 Appendix B program. This includes modifications that would impact the containment sump. Design changes require a final impact review meeting (i.e., final design workshop) and assessment in accordance with 10 CFR 50.59. Additional meetings may be required based on complexity and risk of the change. A failure modes and effects analysis is required if the design change introduces any new failure modes or changes failure modes for the affected SSCs.

Temporary configuration changes are controlled by plant procedure, which maintain configuration control for non-permanent changes to plant structures, systems, and components while ensuring the applicable technical and administrative reviews and approvals are obtained.

In accordance with 10 CFR 50.65 (Maintenance Rule), an assessment of risk resulting from the performance of maintenance activities is required. Prior to performing maintenance, NextEra assesses and manages the increase in risk for Seabrook that may result from the proposed maintenance activities. In general, the risk assessment ensures that the maintenance activity will not adversely impact a dedicated/protected train, which ensures a system is capable of performing its intended safety function.

Licensing Basis

The licensing basis changes performed to address the GL 2004-02 concerns consisted of changes to the UFSAR reflecting the plant modifications and evaluations performed to address GL 2004-02, as well as changes to the TS surveillance procedure to include inspection of the strainers and debris interceptors for visible damage or corrosion, and to confirm that there is no debris present on the strainers or debris interceptors.

Following receipt of a GL 2004-02 final closure letter, the UFSAR will be updated in accordance with 10 CFR 50.12 (e).

Margins & Conservatisms

The following list documents the margins and conservatisms utilized in the GSI-191/ GL 2004-02 analysis.

Debris Generation

Margins:

- The amount of latent debris at Seabrook was conservatively increased, rather than using the actual walkdown value.
- The amount of miscellaneous debris (e.g. tags and labels) at Seabrook was conservatively increased, rather than using the actual walkdown value.

Conservatisms:

- Shadowing by the reactor or structures was not considered for reactor nozzle breaks. ZOIs at these breaks were truncated to the primary shield wall and a line-of sight cone projecting out the closest primary shield penetration to the radius of the ZOI sphere.
- Unqualified coatings were assumed to fail for all breaks, conservatively maximizing the potential unqualified coatings load in the recirculation pool.
- Qualified epoxy inside the ZOI was assumed to fail as 100% particulate, conservatively treating it as the most easily transportable debris type.

Debris Transport

Margins:

- During pool fill, the transport to the inactive cavity (reactor cavity) was conservatively limited to 15% for fine debris. Note that the transport to the inactive cavity without the limitation was calculated to be 37%.

Conservatisms:

- It was conservatively assumed that all unqualified coatings are located in lower containment and are present in the pool at the start of recirculation. This conservatively results in 100% transport of this debris.
- Unless held up by grating or concrete, all debris blown to upper containment was conservatively assumed to be washed back down by the containment spray flow. This conservatively includes debris blown up onto holdup areas protected from the containment spray path (on the primary shield walls, the shield walls around the pressurizer, and the bottom side of the over-head floor slabs).
- Small pieces of debris landing on the operating deck and other concrete structures after blowdown in upper containment were assumed to wash to lower containment without any retention on grating.

- Additional levels of grating below the operating deck were neglected during washdown. This is conservative, since the maximum amount of debris will be washed down to lower containment without any credit for additional retention on gratings.
- Turbulent kinetic energy (TKE) and velocity plots were created to determine the recirculation transport fractions. The threshold velocity used to make the plots for small and large fiberglass debris is the incipient tumbling velocity (minimum required to initiate motion of one piece of debris) rather than the bulk tumbling velocity (minimum required to induce motion of all debris pieces). The incipient tumbling velocity is lower than the bulk tumbling velocity and results in conservatively higher transport area.
- It was assumed that the debris interceptors in the bioshield would become completely blocked with debris in the CFD model. This conservatively causes all of the flow from inside the bioshield to exit to the annulus via the open passageway on the east side of containment, which increases the velocity in the annulus.
- The flow of water falling from the reactor coolant system breach was assumed to do so without encountering any structures before reaching the containment pool. This is conservative since any impact with structures would dissipate the momentum of the water and decrease the turbulent energy in the pool.
- Holdup of debris by the debris interceptors is not credited when calculating recirculation transport fractions.

<u>Water Volume and Level</u>

Conservatisms:

- The maximum containment free volume is used when calculating atmospheric steam holdup, conservatively neglecting portions that contain liquid water.

<u>NPSH</u>

Conservatisms:

- The NPSH margin is calculated using a combination of minimum containment water level for a pressurizer surge line break and maximum LBLOCA strainer head loss. Combining these inputs in the analysis is conservative, as they would not happen simultaneously.
- The minimum NPSH margins were calculated at a sump pool temperature of 211.27°F which occurs for a short period of time at the beginning of recirculation. Additionally, this high pool temperature was conservatively assumed to be coincident with the strainer head loss due to the full conventional debris loads.
- It was assumed that during recirculation following a large-break LOCA the RCS is completely depressurized, causing RCS pressure to be equal to the containment pressure, thus maximizing flow through the system.
- For sump temperatures at or above 211.27°F, the containment pressure was assumed to be equal to the vapor pressure at the corresponding sump

temperature, conservatively neglecting any accident pressure or air partial pressure of the containment atmosphere.

Strainer Structural Analysis

Margins:

- The strainer structure analysis provides margin to design allowable stresses, which ensures that the strainer system will perform its function as long as necessary following an event that requires its use. Table 3.k.2-1 in the response to Section 3.k.2 contains an itemized strainer component list and the margin for each component.

Conservatisms:

- Use of the code of record provides the conservatism inherent within the code itself (Reference 17).

Head Loss

Margins:

- The tested debris loads for both full debris load and thin bed head loss tests are higher than the largest transported debris loads for the worst breaks postulated for Seabrook.
- The head loss tests were performed at approach velocities higher than that of the plant strainer.

Conservatisms:

- Head loss test conditions were selected to result in maximum strainer head loss.
- Testing demonstrated that small conventional debris resulted in an increase in conventional debris head loss but decreased the head loss impact of chemical debris. Strainer head loss was evaluated by including the impact of small pieces of fiberglass on conventional debris head loss but using chemical debris head loss data gathered without small debris.
- In the absence of flow sweep data for the chemical debris bed during the full debris load test, it was conservatively assumed that the flow through the debris bed is completely laminar when adjusting the measured chemical debris head loss from testing conditions to plant conditions. This results in a conservatively higher debris head loss.

Vortexing Evaluation

Conservatisms:

- The strainer approach velocities used during vortex testing for both the clean screen and debris laden conditions are higher than the maximum approach velocity expected for the plant strainer.
- The clean strainer and debris laden vortexing test were performed at zero submergence, which is conservative when compared to the minimum strainer submergence at the plant.

Fiber Bypass Testing

Conservatisms:

- Bypass test conditions were selected to result in maximum fiber bypass.
- No particulate debris was used in the fiber bypass testing. Particulate debris hastens bed formation by filling gaps and plugging holes within the network of entangled fibers on the strainer. This would increase head loss across the debris bed, causing bed compression. The combination of these effects results in a reduction of available paths for fiber to traverse its way through the debris bed and through the strainer perforations. Thus, the exclusion of particulate debris for bypass testing is conservative.
- Only fiber fines were used in bypass testing. In the sump pool, larger sized fiber debris (e.g., small and large pieces) and miscellaneous debris that transport to the strainer are unlikely to penetrate the small perforations of the strainer but could block portions of the strainer, preventing fiber fines from penetrating. Therefore, exclusion of debris types other than fine fiber in testing is conservative.
- The fiber introduction schedule used in bypass testing promoted slow bed development and utilized small batch sizes when the strainer was clean and when the debris bed was small, which maximized the opportunity for fiber bypass via shedding and prompt bypass.

Chemical Effects

Margins:

- The quantities of submerged and unsubmerged aluminum used for the chemical effects analysis included design contingencies.
- The quantity of Nukon used for the chemical effects analysis included a design contingency over the maximum E-Glass debris predicted in the debris generation calculation.

Conservatisms:

- Debris quantities bound the maximum amount of debris predicted from the bounding LOCA break.
- Maximum pH values were conservatively used to increase the calculated aluminum release, and minimum pH values were conservatively used to decrease the calculated aluminum solubility.
- The maximum containment sump pool mass was conservatively used for the 30-day post-LOCA event to increase the calculated aluminum release. The minimum containment sump pool mass was used to maximize the aluminum concentration for the purpose of conservatively maximizing the aluminum precipitation temperature.
- Maximum temperature profiles were conservatively used for the 30-day post LOCA event to increase the calculated aluminum release.
- The containment sprays were assumed to be active for the full 30-day event to conservatively maximize aluminum release.
- All destroyed and latent debris was conservatively assumed to be submerged.
- It was conservatively assumed that the submerged quantity of aluminum would be available to interact with the sump pool and that the unsubmerged quantity of aluminum would be available to interact with the containment spray. This is conservative because some of the listed materials would not be sprayed or would be submerged in a portion of the pool that does not interact with the fluid that recirculates through the containment sump strainer.
- The total quantity of aluminum in solution was assumed to precipitate as AlOOH after the concentration exceeds the calculated solubility limit.

<u>In-Vessel Downstream Effects</u>

Margin:

- A conservative transportable fiber debris load was used for in-vessel analyses. This allows for a margin for future discovery of transportable fibrous debris within containment.

Conservatisms:

- The in-vessel analysis considered several RHR and CBS flow configurations to determine the configuration that resulted in the maximum in-vessel fiber load. The effect of containment spray operation was minimized by using the minimum CBS flow rate and the minimum CBS operation time. The maximum RHR flow rate corresponding to the selected CBS configuration was used. This increases the fraction of debris that reaches the reactor vessel (RV) by limiting the debris diverted away from the reactor.

- The in-vessel analysis determined that the maximum sump volume resulted in a higher in-vessel fiber load than the minimum sump volume. The maximum sump volume was used to conservatively increase the in-vessel fiber load.
- The bypass curve-fit uncertainty was added to the final in-vessel debris loads. This conservatively increases the in-vessel fiber loads.
- All fiber that reaches the RV was assumed to accumulate at the core inlet while, in reality, some fiber may penetrate through the core inlet or be diverted away from the core inlet through the alternate flow paths (AFPs).
- In the in-vessel analysis, no transportable fine fiber is held up in any locations other than the sump strainers and RV. No settling of transportable debris is credited in the sump pool, or inside the RCS, ECCS, or CBS piping and equipment. Therefore, the maximum amount of debris is available to reach the core.

<u>Ex-Vessel Downstream Effects</u>

Conservatisms:

- Rather than using the transported quantities of Nukon and coatings associated with a specific break, it was conservatively assumed that the maximum quantities of both Nukon and coatings transport to the strainer, regardless of break. This means that the debris quantities presented do not represent a single break, but instead maximize the amount of Nukon and coatings analyzed, conservatively bounding all break scenarios.
- The minimum sump pool volume following a small-break LOCA (SBLOCA) was combined with the maximum debris loads from an LBLOCA to determine debris concentration. This is conservative because minimizing the mass of recirculating water maximizes the debris concentration, and thus the amount of wear. Additionally, water volumes such as portions of the RCS inventory or the volume of water in the RHR piping could also be proven to be part of the recirculation flow path, but were conservatively excluded for the downstream effects calculations.
- Although the actual maximum spherical particulate size that could penetrate the strainer is 0.068 inches, the maximum particulate size that penetrates the strainer was assumed to be 0.100 inches for the downstream effects evaluations.
- The downstream effects evaluations were performed using conservative overall fiber and particulate concentrations. The total maximum initial debris concentration used in the evaluations was 4557.65 ppm. The actual maximum initial debris concentration is determined to be 1,587.89 ppm, which is approximately three times less than the concentration used in the downstream effects evaluations.

3. Specific Information Regarding Methodology for Demonstrating Compliance

3.a Break Selection

The objective of the break selection process is to identify the break size and location that present the greatest challenge to post-accident sump performance.

3.a.1 Describe and provide the basis for the break selection criteria used in the evaluation.

Response to 3.a.1:

The debris generation calculation performed for Seabrook followed the methodology of NEI 04-07 and associated NRC SE (Reference 18 pp. 3-5 - 3-26, 4-1 - 4-5; 19 pp. 12-35, 85-91), with the exception that it analyzed a full range of breaks, rather than just the worst-case breaks as suggested by NEI 04-07. The purpose of the debris generation calculation was to obtain debris quantities for the full range of possible break scenarios. This method ensures that the most challenging break can be identified. The calculation evaluated debris generation quantities for breaks on every ISI weld within the Class 1 pressure boundary inside the first isolation valve, including breaks at the reactor nozzles. The following types of LOCA breaks were considered:

1. Double-ended guillotine breaks (DEGBs) with the largest break being a 31" DEGB,
2. Partial breaks, orientated 45 degrees apart, at size increments of 0.5, 2, 4, 6, 8, 10, 12, 14, 17, 20, 23, and 26 inches,
3. Single-ended guillotine breaks (SEGBs) within 10 pipe diameters of a normally closed isolation valve or termination point.

In the debris generation calculation, a three-dimensional computer-aided design (CAD) model of the Seabrook containment building was updated to work with ENERCON's BADGER software. BADGER was used to place ZOIs representing possible breaks on every 0.5" or larger ISI weld identified in containment inside the first isolation valve. Figure 3.a.1-1 shows the graphical representation of these weld locations for Seabrook.

Per Section 3.3.5.2 of the NRC SE of NEI 04-07, evaluating breaks at equal increments is "only a reminder to be systematic and thorough" (Reference 19 p. 17). The use of Class 1 ISI welds as break locations is both systematic and thorough because they are closer to the components that contain the greatest quantity of debris sources as opposed to a span of straight pipe further away from these sources (see Figure 3.a.1-1). Also, welds are almost exclusively recognized as likely failure locations because they can have relatively high residual stress, are preferentially-attacked by many degradation mechanisms, and are most likely to have preexisting fabrication defects (Reference 20 p. xviii). Since each of the weld locations were evaluated for determination of the quantity of debris that would be generated, these locations, by observation, represent the limiting break locations.

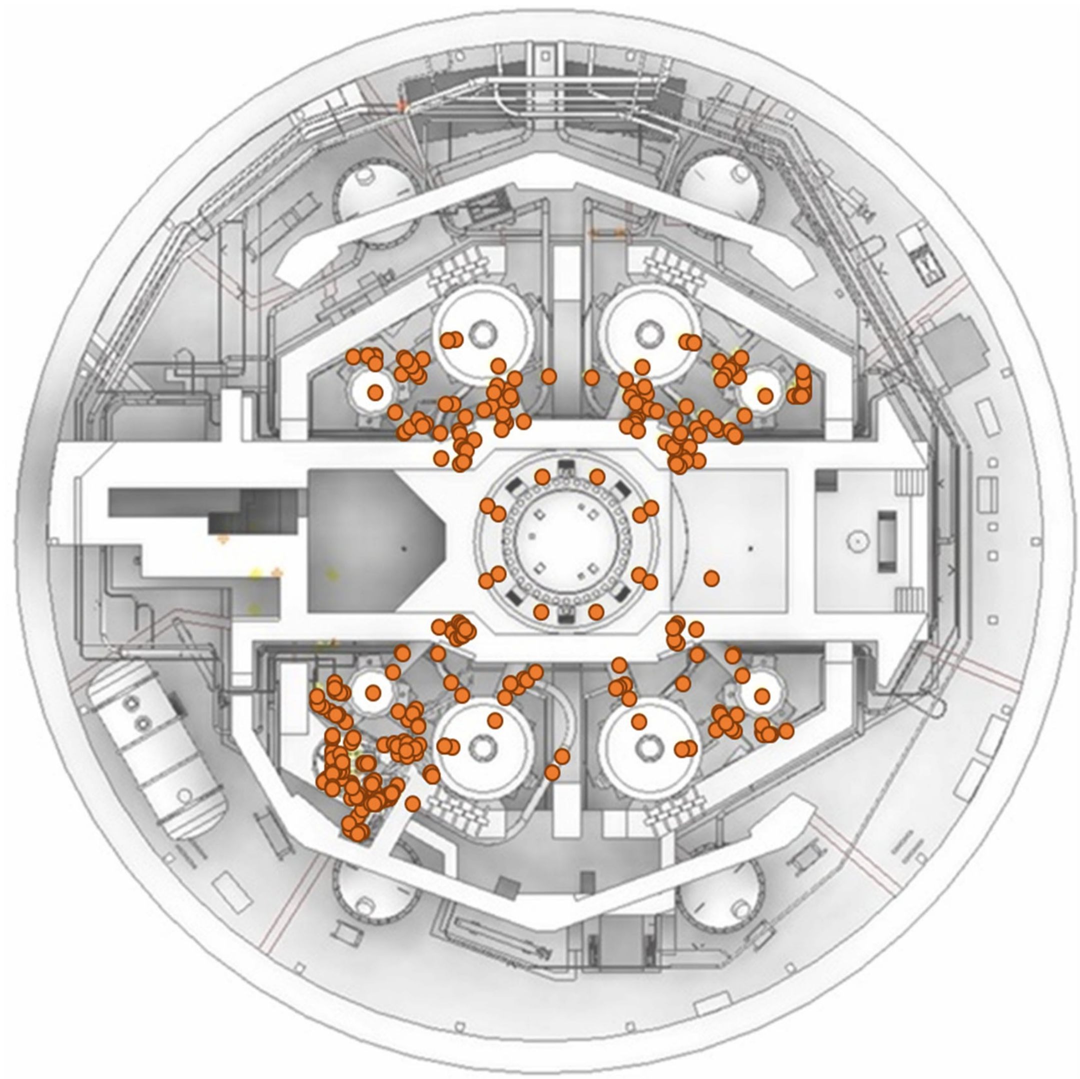

Figure 3.a.1-1: Weld Locations Where Postulated LOCAs Occur

The most limiting breaks are those that contain sufficient fiber to result in the highest head loss across the strainer. Strainer head loss testing was used to determine the debris quantities that would result in either acceptable or unacceptable strainer head loss (see the response to Section 3.f.4).

3.a.2 State whether secondary line breaks were considered in the evaluation (e.g., main steam and feedwater lines) and briefly explain why or why not.

Response to 3.a.2:

Feedwater and main steam piping were not considered for potential break locations because ECCS in recirculation mode is not required for Main Steam or Feedwater line breaks (Reference 21 p. 5).

3.a.3 Discuss the basis for reaching the conclusion that the break size(s) and locations chosen present the greatest challenge to post-accident sump performance.

Response to 3.a.3:

The quantities of debris generated by the full range of breaks has been determined for Seabrook (see the Responses to 3.a.1 and 3.b.4). The debris generation calculation performed for Seabrook takes into account a spectrum of break sizes on every ISI weld within the Class 1 pressure boundary inside the first isolation valve. The purpose of this calculation is to characterize the debris generation for the range of possible break scenarios. This includes the debris generated by the worst-case scenario LOCAs (DEGBs on the main loop piping).

Given that most large breaks generate similar quantities of debris from latent dirt/dust, miscellaneous debris (e.g., stickers, tags, labels, and tape), and unqualified coatings, the breaks that present the greatest challenge to post-accident sump performance are breaks that generate limiting amounts of fibrous debris and qualified coatings debris. Therefore, areas with the potential to generate significant quantities of fibrous and qualified coatings debris were identified.

The generated debris quantities for all postulated breaks were multiplied by the debris transport fractions (see the response to Section 3.e) to determine the quantity of debris transported to the containment sump strainers. The breaks that resulted in the most limiting debris loads for the head loss and in-vessel analyses were selected and presented in this submittal, as listed in Table 3.a.3-1. The selection of these breaks for their respective analyses is discussed in the Responses to 3.f and 3.n.

Table 3.a.3-1: Bounding Breaks for Seabrook

Limiting Debris Type	Weld Location	Location Description
DEGB with High Fiber Debris Loads	RC-0001-01-03	Loop 1 Hot Leg at SG Nozzle
DEGB with High Fiber Debris Loads	RC-0007-01-03	Loop 3 Hot Leg at SG Nozzle
DEGB with High Particulate Debris Loads	RC-0005-01-04	Loop 2 Crossover Leg
DEGB with High Particulate Debris Loads	RC-0008-01-03	Loop 3 Crossover Leg

3.b Debris Generation/Zone of Influence (excluding coatings)

The objective of the debris generation/ZOI process is to determine, for each postulated break location: (1) the zone within which the break jet forces would be sufficient to damage materials and create debris; (2) the amount of debris generated by the break jet forces.

3.b.1 Describe the methodology used to determine the ZOIs for generating debris. Identify which debris analyses used approved methodology default values. For debris with ZOIs not defined in the guidance report/SE, or if using other than default values, discuss method(s) used to determine ZOI and the basis for each.

Response to 3.b.1:

In a pressurized water reactor (PWR) reactor containment building, the worst-case pipe break would typically be a DEGB. In a DEGB, jets of water and steam would blow in opposite directions from the severed pipe. One or both jets could be reflected by obstacles in different directions. To take into account the double jets and potential jet reflections, NEI 04-07 (Reference 18 pp. 1-3; 19 p. vii) proposes using a spherical ZOI centered at the break location to determine the quantity of debris that could be generated by a given line break.

For DEGBs, the ZOIs are defined in the analysis as a spherical volume about the break in which the jet pressure is higher than the destruction/damage pressure for certain types of insulation, coatings, or other materials impacted by the break jet.

For any break smaller than a DEGB (i.e., a partial break), NEI 04-07, Volume 2, accepts the use of a hemispherical ZOI centered at the edge of the pipe (Reference 19 p. 117). Because these types of breaks could occur anywhere along the circumference of the pipe, the partial breaks were analyzed using hemispheres at eight different angles that are 45 degrees apart from each other around the pipe.

Because different insulation types have different destruction pressures, different ZOIs were determined for each type of insulation. Table 3.b.1-1 shows the primary side break equivalent ZOI radii divided by the break diameter (L/D) for each representative material in the Seabrook containment building. Note that the reactor vessel has Microtherm and Temp-Mat insulation installed on the top head and bottom head, respectively. However, neither insulation would be affected by the breaks because the top head is shielded from all breaks by the reactor cavity seal ring, and the bottom head is not within any break ZOIs.

Table 3.b.1-1: Primary Side Break ZOI Radii for Seabrook Insulation Types

Insulation Type	Destruction Pressure (psi)	ZOI Radius/Break Diameter (L/D)
Unjacketed and Jacketed Nukon	6*	17.0*
Transco RMI	114*	2.0*
Qualified Coatings on Steel and Concrete Surfaces (excluding Westinghouse Equipment and Supports)	40***	4.0**
Qualified Coatings on Westinghouse Equipment and Supports	-	10.0****

*NRC SE for NEI 04-07 (Reference 19 p. 30)
**Revised Guidance Regarding Coatings Zone of Influence for Review of Final Licensee Responses to Generic Letter 2004-02 (Reference 22 p. 2)
***40 psi corresponds to a 4D ZOI in Table 3-1 of the SER (Reference 19 p. 27)
****See additional discussion in the response to Section 3.h.5

In some cases, if the ZOI for a particular material is very large (i.e., it has a low destruction pressure or is located on a large pipe), the radius of the sphere may extend beyond robust barriers located near the break. Robust barriers consist of structures, such as concrete walls that are impervious to jet flow and prevent further expansion of the jet. Insulation in the shadow of large robust barriers can be assumed to remain intact to a certain extent (Reference 18 pp. 3-14 through 3-15). Due to the compartmentalization of containment in Seabrook, the insulation on the opposite side of the compartment walls can be assumed to remain intact. However, the steam generator (SG) compartments share an opening where a break jet could extend, so this was accounted for by including destruction of some of the insulation in these areas. The ZOIs were truncated to account for robust barriers per NEI 04-07 Volume 2 (Reference 19 p. vii).

For reactor nozzle breaks, the ANSI 58.2-1988 jet model methodology (Reference 23) was implemented to evaluate the ZOI length of a nozzle break subjected to partial separation of the two pipe ends. ANSI 58.2-1988 postulates two break types and determines the jet impingement pressures resulting from a high-energy line break: fully separated breaks with unrestrained pipe ends and partially separated breaks with highly restrained pipe ends. The fully separated breaks were analyzed in the NRC SE of NEI 04-07 to derive the ZOI radii found in the SE by solving for isobaric impingement pressures radially and axially from the jet centerline and converted to a volume-equivalent spherical ZOI radius (Reference 19 p. 30). One limitation of the ANSI Jet methodology is that the maximum radial separation of a partially separated break is one pipe wall thickness before defaulting to a full sized break. For breaks with radial separation larger than a pipe wall, a combination of the two break methodologies must be used to increase the ZOI size appropriately. This was performed by applying a crescent shaped jet profile to the area generated by a partially offset break bounded by the inside diameter of the pipe and the outer diameter of the pipe wall from the offset half. The volume of the jet generated by the equivalent fully offset break is combined with the volume of the jet generated by the axial offset to conservatively calculate the ZOI volume.

Table 3.b.1-2 contains the maximum allowable separation distances for hot and cold leg breaks and the ZOI dimensions for reactor nozzle breaks.

Table 3.b.1-2: ZOI Adjustments for Partially Separated Reactor Nozzle Breaks

	Hot Leg Nozzles	**Cold Leg Nozzles**
Pipe I.D. (in)	29	27.5
Pipe O.D. (in)	33.9	32.22
Axial Separation (in)	0.09	2.82
Radial Separation (in)	7.83	8.05
Insulation	**ZOI Radius**	
Nukon	7.2D	8.4D
Epoxy	1.8D	2.3D
Transco RMI	0.9D	1.2D

The ZOI for a reactor nozzle break was truncated at the external surface of the primary shield wall and included a line of sight extension through the primary shield wall penetration for the broken leg. As a result, the destruction of materials within all of the penetrations was considered without crediting any shielding by the reactor vessel. Extending the ZOI only through the penetration with the broken pipe is reasonable because the other penetrations are at angles such that most of the energy would be removed from the break flow as it changes direction before reaching the other penetrations.

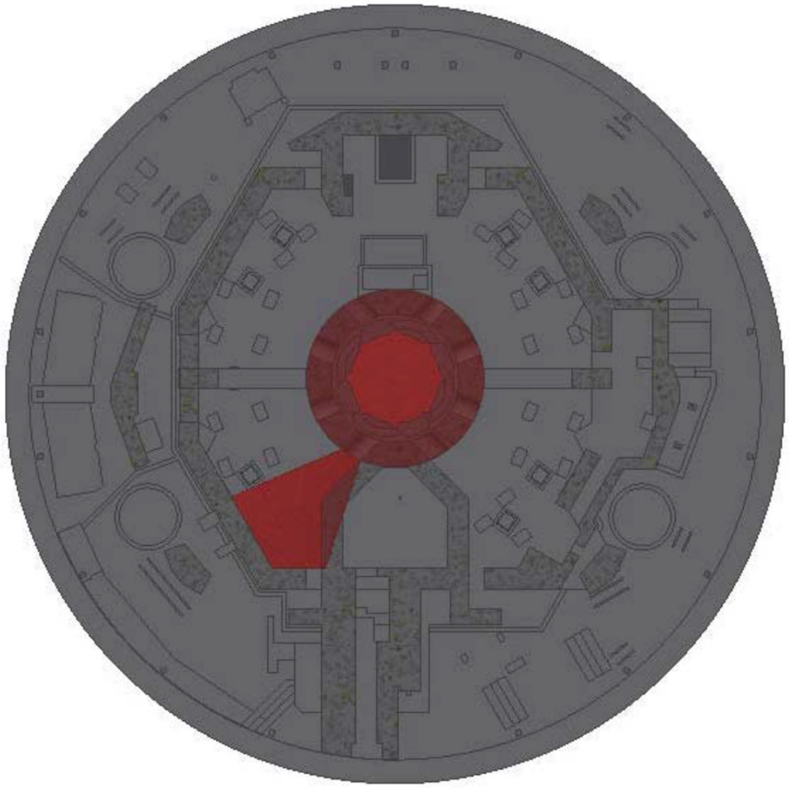

Figure 3.b.1-1: Example Reactor Nozzle Break ZOI for Loop 4 Cold Leg

3.b.2 Provide destruction ZOIs and the basis for the ZOIs for each applicable debris constituent.

Response to 3.b.2:

See the response to Section 3.b.1.

3.b.3 Identify if destruction testing was conducted to determine ZOIs. If such testing has not been previously submitted to the NRC for review or information, describe the test procedure and results with reference to the test report(s).

Response to 3.b.3:

NextEra applied the ZOI refinement discussed in NEI 04-07 Volume 2 (Reference 18 p. Section 4.2.2.1.1) for Seabrook, which allows the use of debris-specific spherical ZOIs. No new destruction testing was used to determine the ZOIs listed above.

For reactor nozzle breaks, the ANSI 58.2-1988 jet model methodology was implemented to evaluate the ZOI length of a nozzle break subjected to partial separation of the two pipe ends. See the response to Section 3.b.1 for additional information.

The only ZOI that is being used that is different from those listed in NEI 04-07 is that for qualified coatings on the steel and concrete surfaces, excluding Westinghouse equipment and supports. This is discussed in the response to Section 3.h.5.

3.b.4 Provide the quantity of each debris type generated for each break location evaluated. If more than four break locations were evaluated, provide data only for the four most limiting locations.

Response to 3.b.4:

Using the ZOIs listed in this section, the breaks selected in the response to Section 3.a, and the size distribution provided in the response to Section 3.c of this enclosure, quantities of generated debris for each break case were calculated for each type of insulation. Table 3.b.4-1 shows the quantities of debris generated for the two worst-case fiber breaks and two worst-case particulate breaks, as determined in debris generation calculation. Note that, for coatings debris, the table only shows the generated quantities for the qualified coatings. The generated quantities of the unqualified coatings are shown in the response to Section 3.h.1. The quantities of the latent debris are shown in the response to Section 3.d.3.

Table 3.b.4-1: Generated Debris Quantities for Worst-Case DEGBs

Break Location			**RC-0007-01-03**	**RC-0001-01-03**	**RC-0005-01-04**	**RC-0008-01-03**
Location Description			Loop 3 Hot Leg at SG Nozzle	Loop 1 Hot Leg at SG Nozzle	Loop 2 Crossover Leg	Loop 3 Crossover Leg
Break Size			31"	31"	31"	31"
Break Type			DEGB	DEGB	DEGB	DEGB
Nukon (lb)		Fine	738.5	758.8	293.3	508.2
		Small	2493.3	2648.8	938.6	1660.4
		Large	1318.7	1104.8	672.2	1066.7
		Intact	1424.8	1193.5	726.4	1152.6
Transco RMI (ft^2)		Small (<4")	0	0	0	0
		Large (≥ 4")	0	0	0	0
Qualified Epoxy Coatings excluding Westinghouse Equipment and Supports (ft^3)	**K&L #6548**	Particulate	0.58	0.25	0.90	0.91
	K&L #D-1 / K&L E-1	Particulate	0.49	0.25	0.85	0.85
	K&L #4000	Particulate	0.48	0.48	1.44	1.41
Qualified Coatings on Westinghouse Equipment and Supports (ft^3)	**IOZ**	Particulate	3.06	3.06	3.06	3.06
	epoxy	Particulate	1.06	1.06	1.06	1.06

3.b.5 Provide total surface area of all signs, placards, tags, tape, and similar miscellaneous materials in containment.

Response to 3.b.5:

Labels, tags, stickers, placards and other miscellaneous or foreign materials were evaluated via two walkdowns at Seabrook. The amount of miscellaneous foreign materials found by the walkdowns was 39.8 ft^2. However, for conservatism, a total surface area of 133 ft^2 was assumed in the debris generation analysis performed for Seabrook.

3.c Debris Characteristics

The objective of the debris characteristics determination process is to establish a conservative debris characteristics profile for use in determining the transportability of debris and its contribution to head loss.

3.c.1 Provide the assumed size distribution for each type of debris.

Response to 3.c.1:

A summary of the material properties of the accident generated debris types found within containment are listed in Table 3.c.1-1 below (Reference 18 pp. 3-22, Tables 3-2 and 3-3). Note that the reactor vessel has Microtherm and Temp-Mat insulation installed on the top head and bottom head, respectively; however, neither insulation type would become a source of debris, as noted in the response to Section 3.b.1.

Table 3.c.1-1: Debris Material Properties

Debris	Distribution	Density (lbm/ft³)	Characteristic Size (µm)
Nukon	See section below	2.4 (bulk) 159 (fiber)	7
Transco RMI	75% small pieces 25% large Pieces	-	<4” ≥4”
Qualified Coatings for non-Westinghouse Equipment and Support	100% Particulate	See Table 3.h.1-1	10
Qualified Coatings on Westinghouse Equipment and Support	100% Particulate	See Table 3.h.1-1	10
Unqualified Coatings	100% Particulate	See Table 3.h.1-2	10

<u>Nukon Insulation</u>

The debris characteristics for Nukon are listed in Table 3.c.1-1.

A baseline analysis of Nukon low density fiberglass (LDFG) includes a size distribution with two categories—60 percent small fines and 40 percent large pieces per NEI 04-07 (Reference 18 p. Section 3.4.3.3.1). The debris generation calculation uses a four-category size distribution based on the guidance in NEI 04-07 Volume 2 (Reference 19 pp. Appendix II and Appendix VI, p. VI-14). This guidance provides an approach for determining a size distribution for LDFG using the air jet impact test (AJIT) data, with conservatism added due to the potentially higher level of destruction from a two-phase jet. Within the 17.0D ZOI, the size distribution varies based on the distance of the insulation from the break (i.e., insulation debris generated near the break location consists of more small pieces than insulation debris generated near the edge of the ZOI).

Consequently, the following equations were developed to determine the fraction of fines (individual fibers), small pieces (less than 6 inches), large pieces (greater than 6 inches), and intact blankets of Nukon LDFG as a function of the average distance between the break point and the centroid of the affected debris measured in units of break diameter (C).

$$F_{LDFG\,Fines}(C) = \begin{cases} 0.2 & \text{if } 0 < C \leq 4 \\ -0.01364 \cdot C + 0.2546 & \text{if } 4 < C \leq 15 \\ -0.025 \cdot C + 0.425 & \text{if } 15 < C \leq 17 \end{cases}$$

$$F_{LDFG\,Small}(C) = \begin{cases} 0.8 & \text{if } 0 < C \leq 4 \\ -0.0682 \cdot C + 1.0724 & \text{if } 4 < C \leq 15 \\ -0.025 \cdot C + 0.425 & \text{if } 15 < C \leq 17 \end{cases}$$

$$F_{LDFG\,Large}(C) = \begin{cases} 0 & \text{if } 0 < C \leq 4 \\ 0.0393 \cdot C - 0.157 & \text{if } 4 < C \leq 15 \\ -0.215 \cdot C + 3.655 & \text{if } 15 < C \leq 17 \end{cases}$$

$$F_{LDFG\,Intact}(C) = \begin{cases} 0 & \text{if } 0 < C \leq 4 \\ 0.0425 \cdot C - 0.170 & \text{if } 4 < C \leq 15 \\ 0.265 \cdot C - 3.505 & \text{if } 15 < C \leq 17 \end{cases}$$

3.c.2 Provide bulk densities (i.e., including voids between the fibers/particles) and material densities (i.e., the density of the microscopic fibers/particles themselves) for fibrous and particulate debris.

Response to 3.c.2:

See the response to Section 3.c.1 for the material and bulk densities of the various types of debris.

3.c.3 Provide assumed specific surface areas for fibrous and particulate debris.

Response to 3.c.3:

Specific surface areas could be calculated for each debris type based on the characteristic diameter described in the response to Section 3.c.1. However, testing was used to determine strainer head loss and not an analytical method, so specific surface areas were not calculated or used for the head loss evaluations performed for Seabrook (see the response to Section 3.f).

3.c.4 Provide the technical basis for any debris characterization assumptions that deviate from NRC-approved guidance.

Response to 3.c.4:

The debris characterizations for all debris types follow NRC-approved guidance.

3.d Latent Debris

The objective of the latent debris evaluation process is to provide a reasonable approximation of the amount and types of latent debris existing within the containment and its potential impact on sump-screen head loss.

3.d.1 Provide the methodology used to estimate the quantity and composition of latent debris.

Response to 3.d.1:

Walkdowns have been completed for Seabrook specifically for the purpose of characterizing latent and miscellaneous debris. These walkdowns utilized the guidance in NEI 02-01 and the staff's SE of NEI 04-07.

The NRC's SE for NEI 04-07 (Reference 19, Section 3.5.2.2) recommended that walkdowns be performed to assess debris sources inside containment.

Samples were collected from eight surface types: floors, containment liner, ventilation ducts, cable trays, walls, equipment, piping, and grating. Where feasible, for each surface type a minimum of four samples were collected, bagged and weighed to determine the quantity of debris that was collected. A statistical approach was used to estimate an upper limit of the mean debris loading on each surface. The horizontal and vertical surface areas were conservatively estimated. The total latent debris mass for a surface type was calculated using the upper limit of the mean debris loading multiplied by the conservatively estimated area for that surface type. The total latent debris was calculated using the sum of the latent debris for each surface type.

Seabrook containment walkdowns were performed for the purpose of identifying and measuring plant labels, stickers, tape, tags, and other debris. Based on the walkdown data and the subsequent removal of cable tray adhesive labels, the quantity of miscellaneous debris in the Seabrook containment was estimated to be 39.8 ft^2. As discussed in the response to Section 3.b.5, a total surface area of 133 ft^2 of miscellaneous debris was conservatively assumed in the debris generation calculation performed for Seabrook.

3.d.2 Provide the basis for assumptions used in the evaluation.

Response to 3.d.2:

See the response to Section 3.d.3 for assumptions regarding material properties of latent debris.

3.d.3 Provide results of the latent debris evaluation, including amount of latent debris types and physical data for latent debris as requested for other debris under c. above.

Response to 3.d.3:

Latent debris includes dirt, dust, lint, paint chips, fines, and shards of loose thermal insulation fibers that could potentially transport to the sump strainers during recirculation. Latent debris can be introduced into containment several ways, including deterioration of items such as insulation and coatings, and by personnel tracking in particulate and fibers from outside containment. The quantity of latent debris is provided in the debris generation calculation. A walkdown at Seabrook was performed to measure quantities of latent debris, and the total quantity was calculated based on those samples. The total amount of latent debris calculated was 40.7 lbm, but 100 lbm was assumed in the debris generation calculation. This conservatively bounds the 40.7 lbm of actual latent debris with ample operating margin. Table 3.d.3-1 lists the assumed latent fiber and particulate constituents and their material characteristics.

Latent debris was assumed to consist of 15 percent fiber and 85 percent particulate by mass per NEI 04-07 Volume 2 (Reference 19 p. 50). Based on NEI 04-07 Volume 2 (Reference 19 pp. 50-52, V-11), the size and density of latent particulate were assumed to be 17.3 μm (specific surface area of 106,000 ft^{-1}) and 168.6 lbm/ft^3 (2.7 g/cm^3), respectively. Additionally, the bulk density and microscopic density of latent fiber were assumed to be 2.4 lbm/ft^3 and 93.6 lbm/ft^3 (1.5 g/cm^3), respectively.

Latent fiber was assumed to have a characteristic size of 5.5 μm. This is reasonably conservative, as it is the smallest fiber diameter listed in Table 3-2 of the general reference for LDFG found in NEI 04-07 (Reference 18, p 3-28).

Table 3.d.3-1: Latent Fiber and Particulate Constituents

	Latent Debris (lbm)	Bulk Density (lbm/ft^3)	Microscopic Density (lbm/ft^3)	Characteristic Size (μm)
Particulate (85%)	85	-	168.6	17.3
Fiber (15%)	15	2.4	93.6	5.5
Total	100			

3.d.4 Provide amount of sacrificial strainer surface area allotted to miscellaneous latent debris.

Response to 3.d.4:

As discussed in the response to Section 3.b.5, a total surface area of 133 ft^2 of miscellaneous debris was conservatively assumed. This surface area would result in a 100 ft^2 reduction in strainer area (75% of 133 ft^2) (Reference 19 p. 49).

3.e Debris Transport

The objective of the debris transport evaluation process is to estimate the fraction of debris that would be transported from debris sources within containment to the sump suction strainers.

3.e.1 Describe the methodology used to analyze debris transport during blowdown, washdown, pool-fill-up, and recirculation phases of an accident.

Response to 3.e.1:

The methodology used in the transport analysis is based on the NEI 04-07 guidance and the associated NRC SE (Reference 19) for refined analyses, as well as the refined methodologies suggested by the SE in Appendices III, IV, and VI (Reference 19). The specific effect of each of the four modes of transport was analyzed in the debris transport calculation for each type of debris generated. These modes of transport are:

1. Blowdown Transport – the transport of debris in all directions to all areas of containment caused by the break jet
2. Washdown Transport – the transport of debris from higher to lower portions of containment, caused by flow from the containment sprays
3. Pool Fill-Up Transport – the transport of debris as the break and spray flows initially reach the containment floor and fill the sump pool
4. Recirculation Transport – the transport of debris from active regions in the recirculation pool to the sump strainers, driven by the flow through the sump strainers

The logic tree approach was applied for each type of debris determined from the debris generation calculation. The logic tree shown in Figure 3.e.1-1 is slightly different from the baseline. This departure was made to account for certain non-conservative assumptions identified by the NRC SE (Reference 19) including the transport of large pieces, erosion of small and large pieces, the potential for washdown debris to enter the pool after inactive areas have been filled, and the direct transport of debris to the sump screens during pool fill-up.

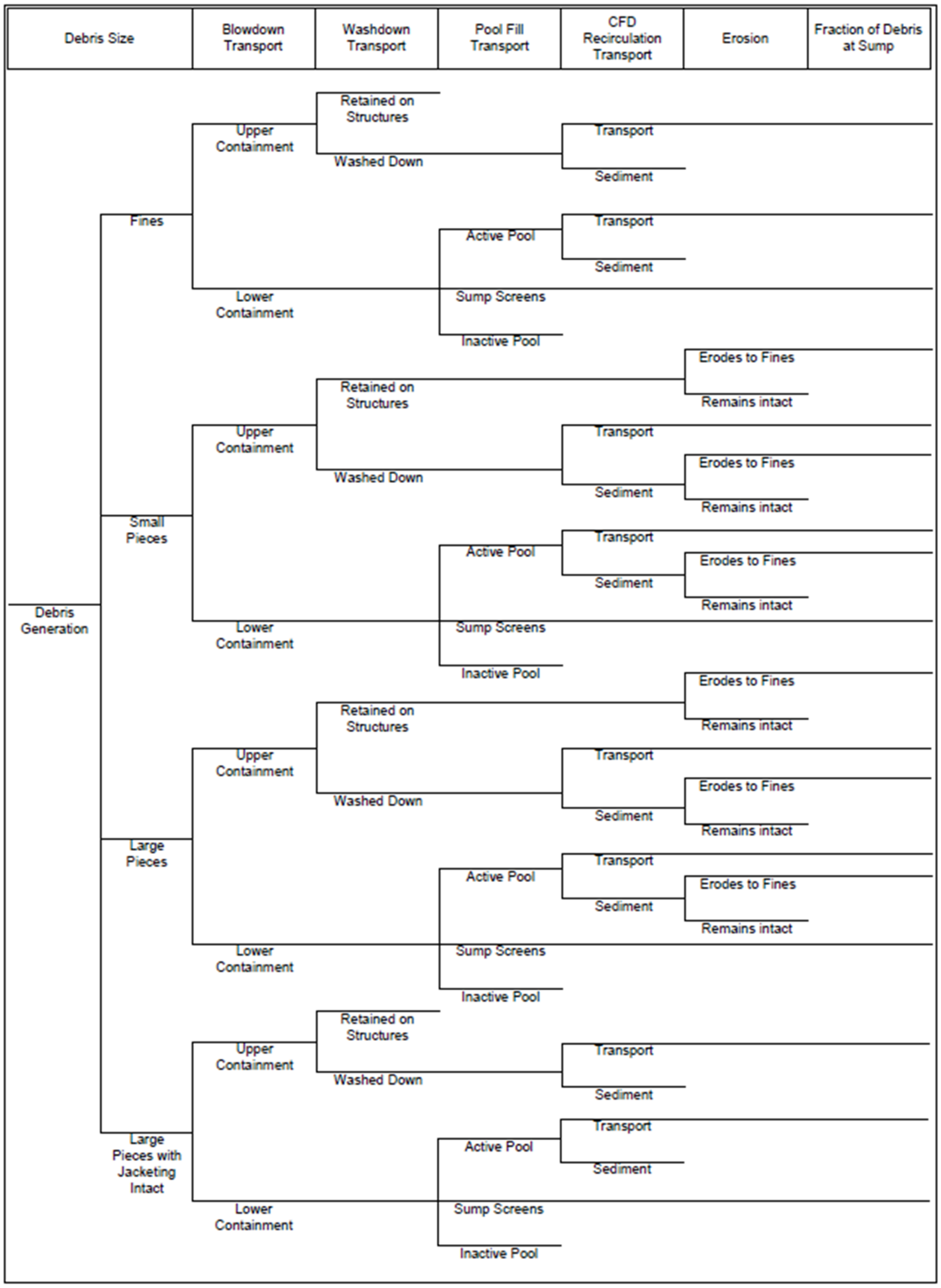

Figure 3.e.1-1: Generic Debris Transport Logic Tree

The basic methodology for the transport analysis is summarized below.

1. The CAD model was provided as input to determine break locations and sizes.
2. The debris generation calculation was provided as input for debris types and sizes.
3. Potential upstream blockage points were qualitatively addressed.
4. The fraction of debris blown into upper containment and lower containment was determined based on the volumes of upper and lower containment.
5. The fraction of debris washed down by containment spray flow was determined along with the locations where the debris would be washed down.
6. The quantity of debris transported to inactive areas or directly to the sump strainers was calculated based on the volume of the inactive and sump cavities proportional to the water volume at the time these cavities are filled.
7. The location of each type/size of debris at the beginning of recirculation was determined based on the break location.
8. A CFD model was developed to simulate the flow patterns that would develop during recirculation.
9. A graphical determination of the transport fraction of each type of debris was made using the velocity and turbulent kinetic energy (TKE) profiles from the CFD model output, along with the determined initial distribution of debris.
10. The initial recirculation transport fractions from the CFD analysis were gathered to determine the final recirculation transport fractions for input into the logic trees.
11. The quantity of debris that could experience erosion due to the break flow or spray flow was determined.
12. The overall transport fraction for each type/size of debris was determined by combining each of the previous steps into logic trees.

<u>Potential Upstream Blockage Points</u>

Potential upstream blockage points were qualitatively addressed in the debris transport calculation and will not prevent recirculation flow from reaching the sump strainers. Upstream effects are discussed in the response to Section 3.l.

<u>CFD Model of Containment Recirculation Pool</u>

A diagram showing the significant parts of the CFD model is shown in Figure 3.e.1-2. The strainer module mass sinks, break location mass sources, and the various direct and washdown spray regions are highlighted.

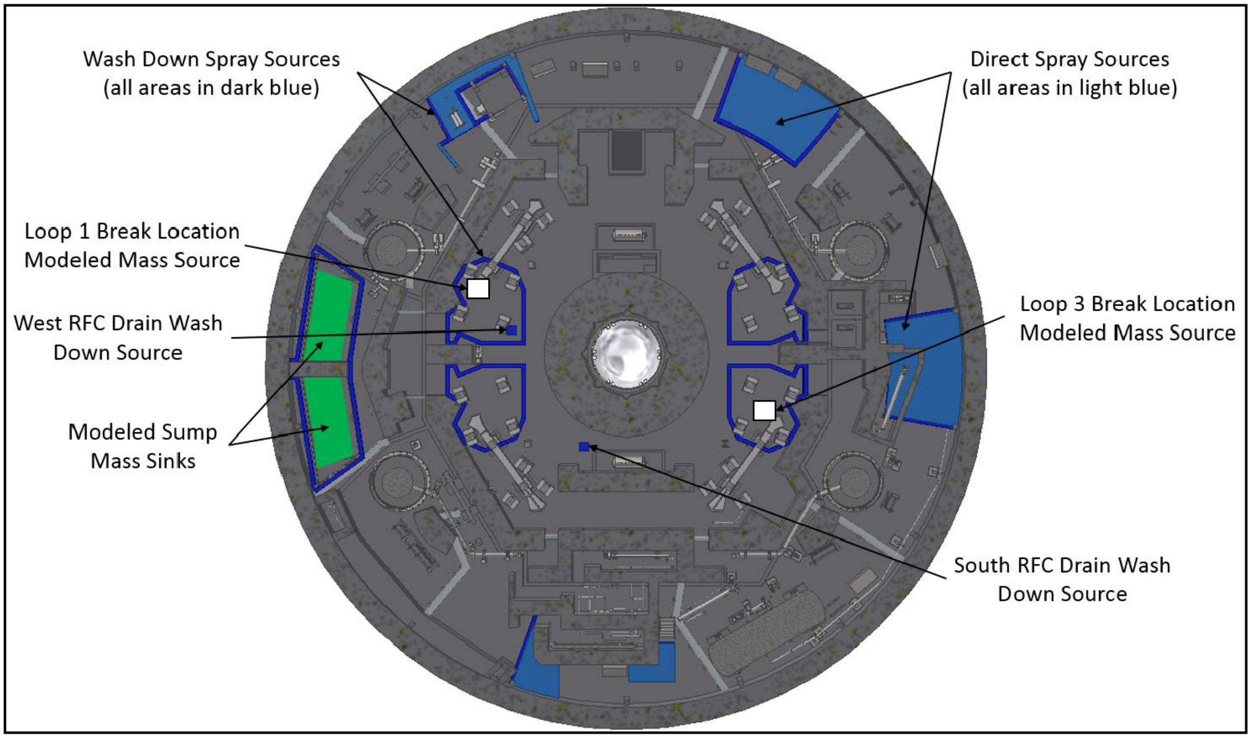

Figure 3.e.1-2: Significant Features in CFD Model

The key CFD modeling attributes/considerations included the following:

<u>Computational Mesh</u>

A rectangular mesh was defined in the CFD model that was fine enough to resolve important features, but not so fine that the simulation would take excessively long to run. A 6-inch cell length was chosen as the largest cell size that could reasonably resolve the concrete structures in the Seabrook containment. For the cells right above the containment floor, the mesh was set to 3 inches tall in order to closely resolve the vicinity of settled debris. The total cell count in the model was 4,000,000.

<u>Modeling of Containment Spray Flows</u>

Various plan and section drawings, as well as the containment building CAD model, were considered when determining the spray flow path to the pool. Spray water would drain to the pool through many pathways. Some of these pathways include the steam generator compartments through the open area above the steam generators, through the annulus via the various sections of grating, and through the refueling canal drains. The sprays were defined as regions and populated with discrete mass source particles. The appropriate flow rate and velocity was set for the sprays in each region.

Some spray flow will wash down into the refueling canal and through the refueling canal drains into the sump pool inside the bioshield (see Figure 3.e.1-2). A modification is planned to ensure that the refueling canal drains will not be blocked by debris. The modification installs a strainer on each of the drains, adds a new drain line, and enlarges the existing drain piping to four inches.

The strainers have a rectangular box shape. The top and bottom surfaces are approximately 24” x 24” or 30” x 30” with 1-inch square openings. The four sides of the strainer have 0.5-inch diameter openings. The strainers are installed approximately 4 inches above the refueling canal floor over a segment of perforated drainpipe and are configured to maintain at least the top surface unobstructed. Small pieces and fine debris that transports into the refueling canal is assumed to wash down the drains with the spray flow. Large debris is retained in the refueling canal by the strainers and is subject to erosion. The total holdup inside the refueling canal and drain lines was calculated and accounted for when determining the sump water level (see the response to Section 3.g.8).

Modeling of Break Flow

The water falling from the postulated break would introduce momentum into the containment pool that influences the flow dynamics. This break stream momentum was accounted for by introducing the break flow to the pool at the velocity a freefalling object would have if it fell the vertical distance from the location of the break to the surface of the pool.

Modeling of the Sump Strainers

The emergency sump at Seabrook consists of two cavities with a dividing wall between them. Both sump cavities are enclosed within a steel curb. The mass sinks used to pull flow from the CFD model were defined at the top of the sump cavities. Note that the specific details of the sump strainers were not modeled. Therefore, the model accurately predicts pool flows up to the sump curbs, but does not accurately predict flow in the sump itself. A negative flow rate was set for the sump module, which tells the CFD model to draw the specified amount of water from the pool over the entire exposed surface area of the module obstacle.

Turbulence Modeling

Several different turbulence-modeling approaches can be selected for a Flow-3D calculation. The approaches (ranging from least to most sophisticated) are:

1. Prandtl mixing length
2. Turbulent energy model
3. Two-equation k-ε model

4. Renormalized group theory (RNG) model
5. Large eddy simulation model

The RNG turbulence model was determined to be the most appropriate for this CFD analysis. The RNG model has a large spectrum of length scales that would likely exist in a containment pool during emergency recirculation. The RNG approach applies statistical methods in a derivation of the averaged equations for turbulence quantities (such as TKE and its dissipation rate). RNG-based turbulence schemes rely less on empirical constants while setting a framework for the derivation of a range of models at different scales.

<u>Steady-State Metrics</u>

The CFD model was started from a stagnant state at a defined pool depth and run long enough for steady-state conditions to develop. A plot of mean kinetic energy was used to determine when steady-state conditions were reached. Checks were also made of the velocity and turbulent energy patterns in the pool to verify that steady-state conditions were reached.

<u>Debris Transport Metrics</u>

The metrics for predicting debris transport during recirculation are the TKE necessary to keep debris suspended, and the flow velocity necessary to tumble sunken debris along the floor or lift it over a curb. Debris transport metrics have been derived or adopted from data. The metrics utilized in the transport analysis performed for Seabrook originate from the sources below.

1. NUREG/CR-6772 Table 3.1 (Reference 24 p. 16)
2. NUREG/CR-6808 Figure 5.2 and Table 5-3 (Reference 25, pp. 5-14 and 5-33)

<u>Graphical Determination of Debris Transport Fractions for Recirculation</u>

The following steps were taken to determine what percentage of a particular type of debris could be expected to transport through the containment pool to the emergency sump screens. Detailed explanations of each bullet are provided in the paragraphs below.

1. Colored contour velocity and TKE maps were generated from the Flow-3D results in the form of bitmap files indicating regions of the pool through which a particular type of debris could be expected to transport.
2. The bitmap images were overlaid on the initial debris distribution plots and imported into AutoCAD with the appropriate scaling factor to convert the length scale of the color maps to feet.

3. Closed polylines were drawn around the contiguous areas where velocity and TKE were high enough that debris could be carried in suspension or tumbled along the floor to the sump strainers for uniformly distributed debris.
4. The areas within the closed polylines were determined using an AutoCAD querying feature.
5. The combined area within the polylines was compared to the initial debris distribution area.
6. The percentage of a particular debris type that would transport to the sump strainers was determined based on the above comparison.

Plots showing the TKE and the velocity magnitude in the pool were generated for each case to determine areas where specific types of debris would be transported. The limits on the plots were set according to the minimum TKE or velocity metrics necessary to move each type of debris. The overlying yellow areas represent regions where the debris would be suspended, and the red areas represent regions where the debris would be tumbled along the floor (see Figure 3.e.1-4). The yellow TKE portion of the plots is a three-dimensional representation of the TKE. Since the TKE is a three-dimensional representation, the plots do not show the TKE at any specific elevation. Rather, any debris that is shown to be present in this yellow area is assumed to transport, regardless of the elevation of TKE in the pool. The velocity portion of the plots represents the velocity magnitude just above the floor level (1.5 inches), where tumbling of sunken debris could occur. Directional flow vectors were also included in the plots to determine whether debris in certain areas would be transported to the sump strainers or transported to less active regions of the pool where it could settle to the floor (blue regions).

There are two exits from the refueling canal drain piping that discharge to the containment sump pool (see Figure 3.e.1-2). For the fines and small pieces of fibrous debris, the washdown split between the two exits is assumed to follow the flow split determined between the two flow paths. When determining the recirculation transport fractions, if a refueling canal drain discharge location is in an area deemed to be transportable for small pieces, then all of the small piece debris that washes down from the refueling canal drain piping to that drain location is assumed to transport.

The following figures and discussion are presented as an example of how the transport analysis was performed for small pieces of fiber that are blown into lower containment during blowdown. This same approach was used for other scenarios (e.g., small pieces washed down from upper containment) and debris types analyzed at Seabrook.

As shown in Figure 3.e.1-3, the small debris (depicted by green shading) was initially assumed to be distributed in the vicinity of the break location at the beginning of recirculation.

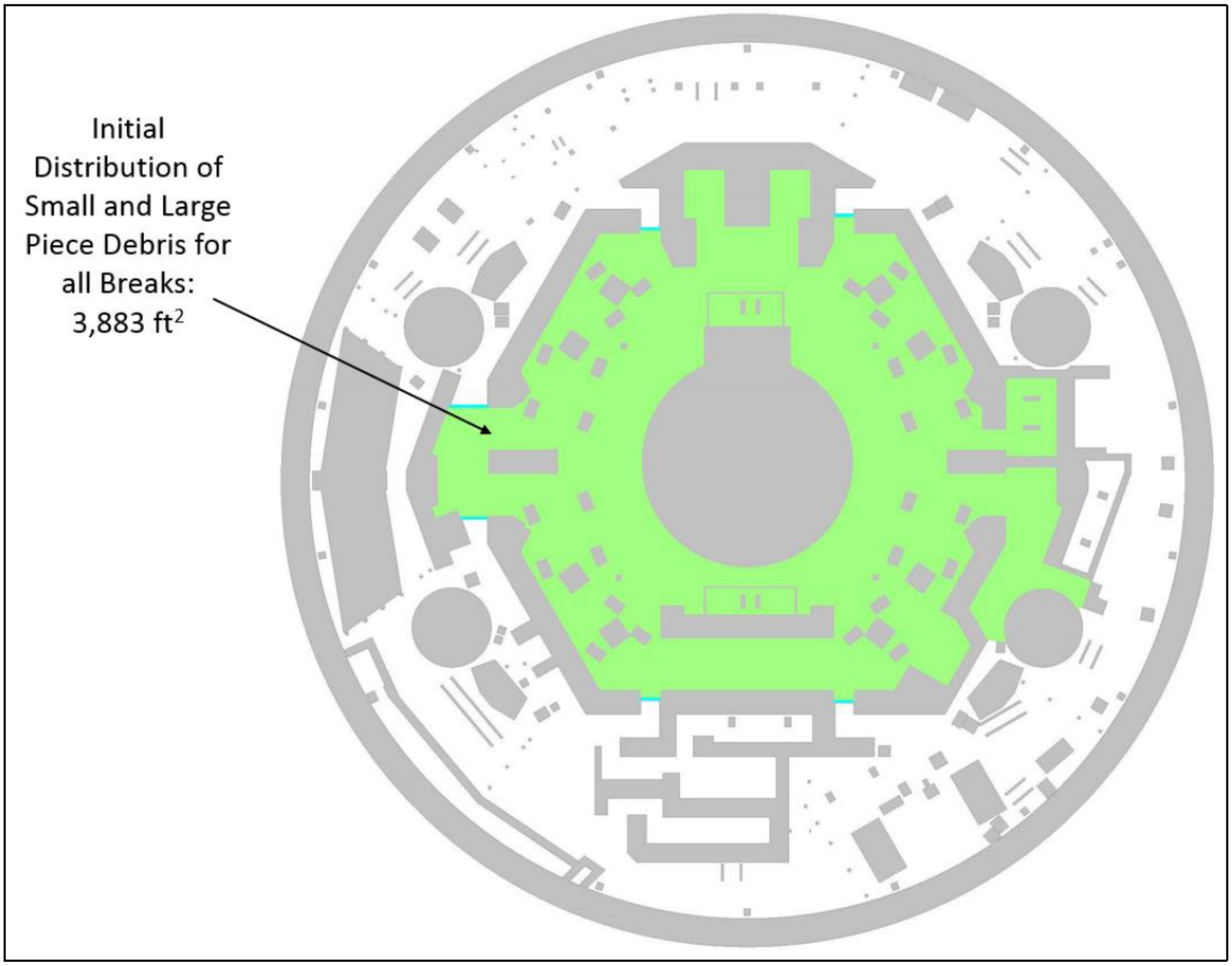

Figure 3.e.1-3: Distribution of Small Debris in Lower Containment

Figure 3.e.1-4 shows that the turbulence of the yellow regions and the velocity of the red regions in the pool are high enough to transport the small pieces of fiberglass due to the break flow to the sump strainers during recirculation. The blue regions do not have sufficiently high turbulence and velocity to transport small pieces of fiberglass. The initial distribution area (Figure 3.e.1-3) was overlaid on top of the plot showing tumbling velocity, TKE, and flow vectors (Figure 3.e.1-4) to determine the recirculation transport fraction, represented by the hatched portion (Figure 3.e.1-5).

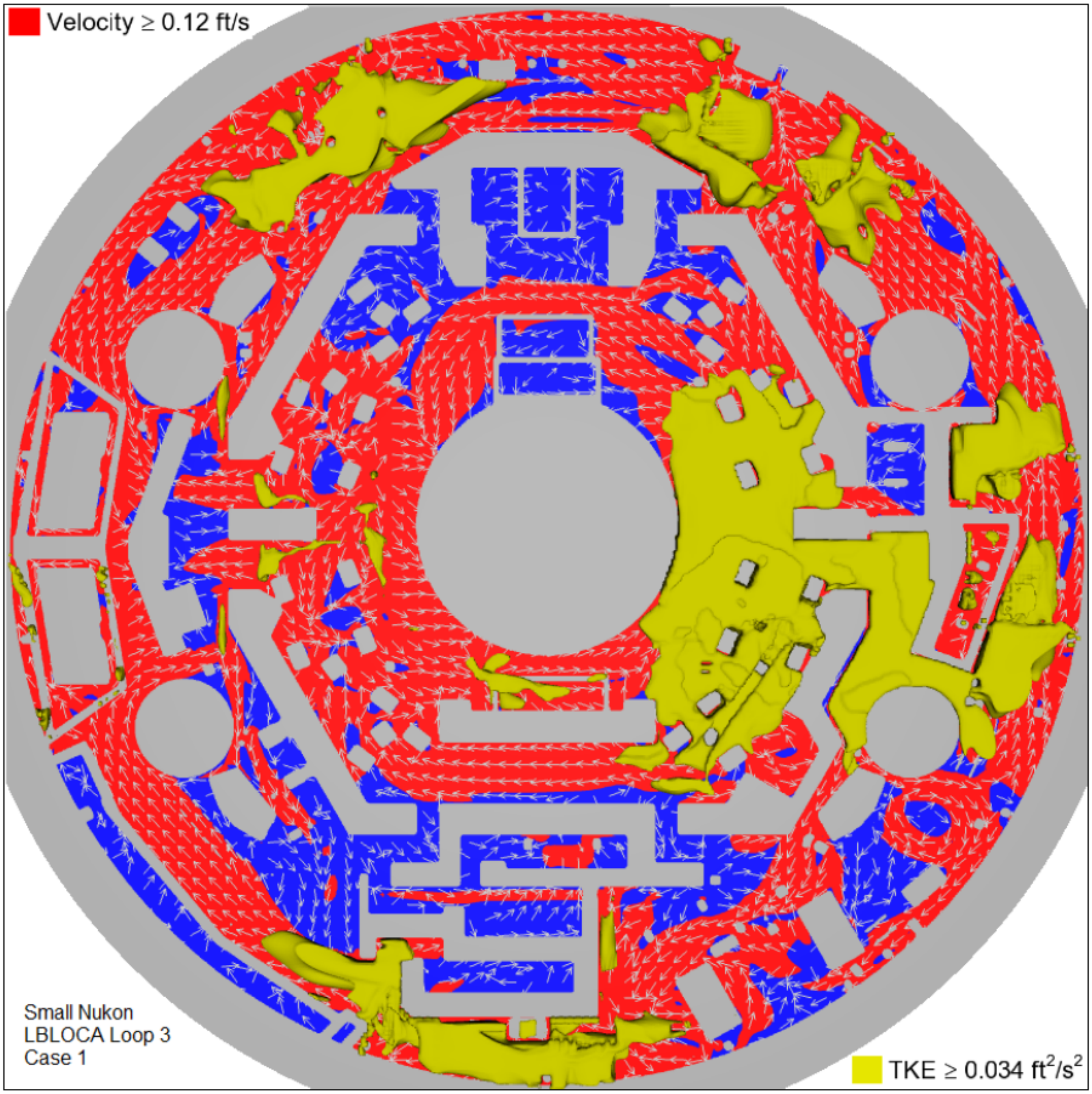

Figure 3.e.1-4: TKE and Velocity with Limits Set at Suspension/ Tumbling of Small Pieces of Fiberglass Debris

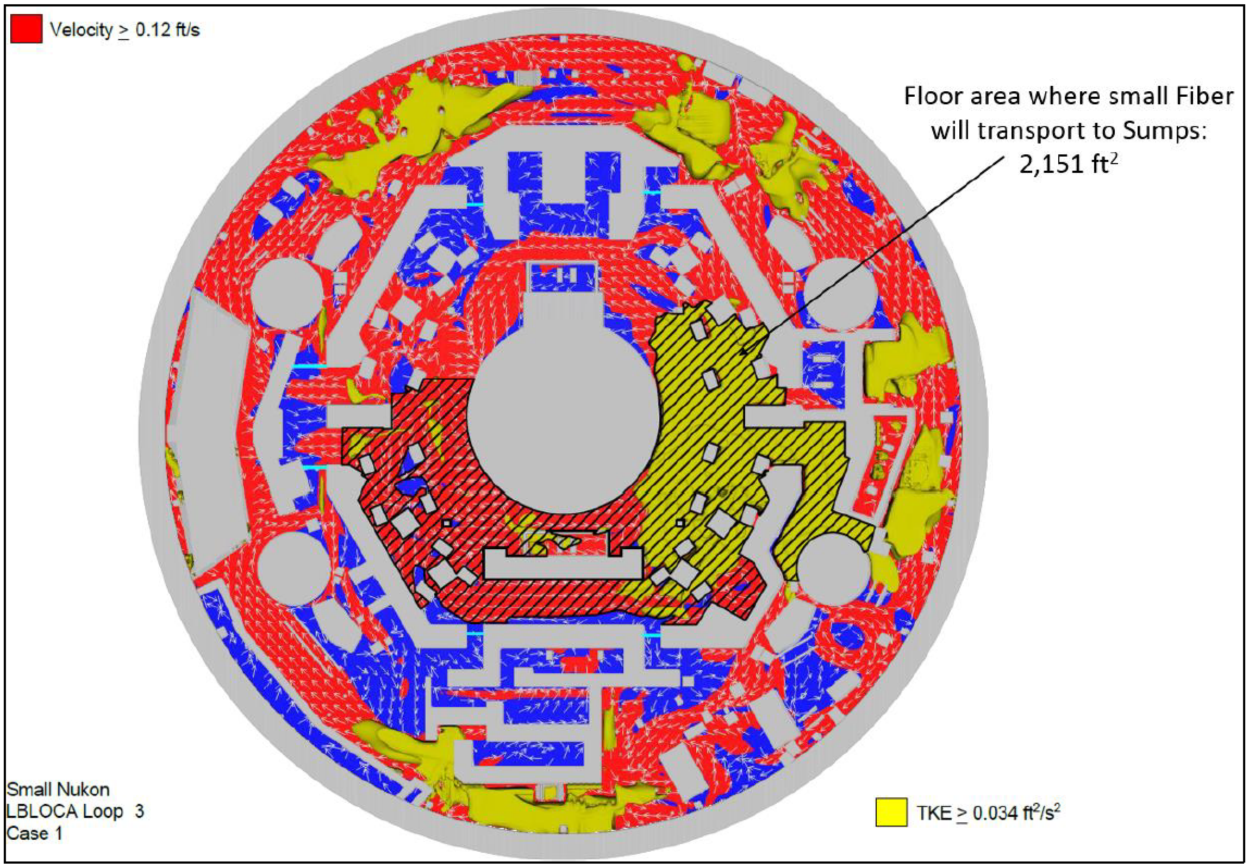

Figure 3.e.1-5: Floor Area where Small Pieces of Fiberglass Debris Would Transport to the Sump Strainers

This same analysis was applied for each type of debris at Seabrook. Recirculation-pool transport fractions were identified for each debris type associated with the location of its initial distribution. This includes a recirculation transport fraction for debris blown into lower containment, debris washed down inside the bioshield, debris washed down through the annulus, and debris washed down the refueling canal drains.

Erosion Discussion

Due to the turbulence in the recirculation pool and the force of break and spray flow, Nukon debris may erode into smaller pieces, making transport of this debris to the strainer more likely. To estimate erosion of trapped or non-transportable debris that would occur in the recirculation pool, 30-day erosion testing was performed. Based on a validation that the test results apply to Seabrook (ensuring that the flow rates and turbulence values are similar to what is expected in the recirculation pool), an erosion fraction of 10% was used for the small and large pieces of fiberglass debris in the pool. This fraction was applied to both transportable debris and settled debris present in the pool to maximize the amount of erosion. For pieces of debris held up on grating above the pool, an erosion fraction of 1% was used for fiberglass debris. For large fiberglass debris retained in the refueling canal by the refueling canal drain strainers, an erosion fraction of 10% was used.

3.e.2 Provide the technical basis for assumptions and methods used in the analysis that deviate from the approved guidance.

Response to 3.e.2:

The methodology used in the transport analysis is based on and does not deviate from the NRC approved NEI 04-07 guidance (Reference 18) and the associated NRC SE (Reference 19) for refined analyses, as well as the refined methodologies suggested by the SE in Appendices III, IV, and VI.

3.e.3 Identify any computational fluid dynamics codes used to compute debris transport fractions during recirculation and summarize the methodology, modeling assumptions, and results.

Response to 3.e.3:

To assist in the determination of recirculation transport fractions, several CFD simulations were performed using Flow-3D, a commercially available software package.

Three break cases form the basis for the debris transport analysis to determine the recirculation transport fractions. First, an LBLOCA in Loop 3 with two trains operational and an LBLOCA in Loop 3 with a single train failure were analyzed. Then an LBLOCA on Loop 1 with two trains operational was analyzed to confirm that a Loop 3 break is bounding and results in higher transport fractions than a Loop 1 break. Cases were chosen to represent and bound the different LOCA scenarios that could occur at Seabrook. All cases were run using a bounding minimum water level (2.8 ft), which is lower than the value for LBLOCAs discussed in the response to Section 3.g (see Table 3.g.1-1). This conservatively increases flow velocity and turbulence and is bounding in terms of debris transport.

The break cases modeled in CFD used a flow rate of 6,010 gpm/sump for 2 train operation and 7,400 gpm for single train operation. The total sump flow rate used in the 2 train CFD case (12,020 gpm) bounds the total sump flow rate used for the most limiting in-vessel analysis with the failure of one CBS pump (see the response to Section 3.n.1). The flow rate used for the single train CFD case is lower than the flow rate used for the limiting NPSH analysis of the RHR and CBS pumps (see the response to Section 3.g.16). This is acceptable because the only transport phase impacted by the sump flow rate is the recirculation transport, and increasing sump flow rates in the CFD model would not increase transport fractions for debris that is of consequence to the GSI-191/GL 2004-02 analysis, as stated below:

1. The recirculation transport fraction of fine debris, including fiber fines and particulate, is already 100% in the transport analysis (see Table 3.e.6-).
2. The erosion of the small and large pieces of fiber debris is accounted for and is independent of sump flow rates (see the response to Section 3.e.1).
3. The impact of fiber small pieces on strainer head loss was demonstrated in head loss testing. As stated in the response to Section 3.f.4, one test was performed with fiber small pieces included. The test did not add small pieces of fiber to the test tank until after all fiber fines and particulate had been introduced. Even with this conservative sequencing, the small pieces of fiber only had small impact on the conventional debris head loss. For a more realistic debris sequence (i.e., small pieces mixed together with other sizes and types of debris), the small pieces are expected to create more voids in the debris bed, resulting in even less impact on the conventional debris head loss. Additionally, comparison between the tests with and without addition of small pieces demonstrated that fiber smalls significantly inhibited the head loss impact of chemical debris.

The simulation results include a series of contour plots of velocity and TKE. These results have been combined with settling and tumbling velocities from the GSI-191/GL 2004-02 literature to determine the recirculation transport fractions for all debris types present in the Seabrook containment building. See the response to Section 3.e.1 for additional discussion of the CFD results.

3.e.4 Provide a summary of, and supporting basis for, any credit taken for debris interceptors.

Response to 3.e.4:

Debris interceptors at Seabrook are not credited for preventing any debris from reaching the sump strainers. In the CFD model, the annulus debris interceptors were not modeled. The bioshield debris interceptors were modeled as completely blocked, but no holdup of debris is credited. This is conservative because it forces all of the flow from inside the bioshield through the open passageway on the east side of the bioshield and into the annulus. This increases the flow velocity and turbulence in the annulus and results in higher recirculation transport fractions. Note that if the bioshield debris interceptors are assumed to be open, a portion of the flow inside the bioshield would travel through the bioshield debris interceptors, resulting in lower flow rates and velocities in the annulus.

This approach is similar to that adopted in the Indian Point debris transport analysis, which assumed that small and large pieces of debris would not pass through the debris barriers. The blocked debris barriers force all flow and debris from inside the crane wall to pass through the incore instrumentation tunnel in order to reach the sumps.

This methodology was accepted by the NRC staff during their audit of the Indian Point submittal (Reference 26).

Note that, while the debris interceptors are not credited for any debris retention, they provide a defense-in-depth measure for reducing the fiber that reaches the strainer. Debris within the bioshield would have to pass through or over four sets of annulus debris interceptors prior to reaching the strainers.

3.e.5 State whether fine debris was assumed to settle and provide basis for any settling credited.

Response to 3.e.5:

No credit was taken for settling of fine debris.

3.e.6 Provide the calculated debris transport fractions and the total quantities of each type of debris transported to the strainers.

Response to 3.e.6:

The following debris transport fractions are shown for blowdown, washdown, pool fill, and recirculation. Note that these fractions result in the bounding quantity of debris transported to the strainer. Cells with a dash in the tables of this subsection represent values that are not applicable (i.e., debris type not generated for a specific location, debris type not available for washdown/pool-fill, etc.).

<u>Blowdown Transport</u>

Table 3.e.6-1 shows the bounding blowdown transport fractions (the minimum amount of debris remaining in the compartment) as a function of break location and debris type. Note that only the limiting break locations with respect to the maximum overall debris transport fractions are listed in these tables. Also, RMI exists solely on the reactor vessel and would only become a source of debris for a break at a reactor nozzle. It was assumed that any RMI that is generated from a reactor nozzle break would fall to the reactor cavity floor and would not transport to the sump strainers. Hence, RMI is not listed in the tables in this section. Additionally, it was assumed that neither Microtherm nor Temp-Mat would become debris sources (see the response to Section 3.b.1). Unqualified coatings and latent debris are assumed to be uniformly distributed in the recirculation pool in lower containment (LC), so blowdown transport fractions are not applicable.

For small pieces of Nukon generated by steam generator compartment and reactor cavity breaks, two different blowdown transport fractions are given: one which maximizes transport to upper containment (UC) and one which minimizes transport to

UC. Both sets of blowdown fractions were analyzed in the logic tree for small pieces of Nukon at each break location. Depending on the status of containment spray for a particular break scenario, maximizing or minimizing blowdown transport to UC can result in higher overall transport fractions. The small Nukon blowdown transport fractions that result in higher overall transport fractions were used.

Table 3.e.6-1: Blowdown Transport Fractions

Break Location	Debris Type	Transport Fraction		
		To UC	To LC	Remaining in Compartment
Steam Generator Compartments	Fines/Particulate (all)	78%	22%	0%
	Nukon Small Pieces (minimum UC)	45%	55%	0%
	Nukon Small Pieces (maximum UC)	73%	27%	0%
	Nukon Large Pieces	20%	80%	0%
	Nukon Intact Blankets	0%	0%	100%
	Qualified Coatings	78%	22%	0%
	Unqualified Coatings	-	-	-
	Latent Debris	-	-	-
Reactor Cavity	Fines/Particulate (all)	78%	22%	0%
	Nukon Small Pieces (minimum UC)	45%	55%	0%
	Nukon Small Pieces (maximum UC)	73%	27%	0%
	Nukon Large Pieces	20%	80%	0%
	Nukon Intact Blankets	0%	0%	100%
	Qualified Coatings	78%	22%	0%
	Unqualified Coatings	-	-	-
	Latent Debris	-	-	-
Pressurizer Compartment	Fines/Particulate (all)	78%	22%	0%
	Nukon Small Pieces	76%	21%	3%
	Nukon Large Pieces	40%	15%	45%
	Nukon Intact Blankets	0%	0%	100%
	Qualified Coatings	78%	22%	0%
	Unqualified Coatings	-	-	-
	Latent Debris	-	-	-

Washdown Transport

Table 3.e.6-2 shows the bounding washdown transport fractions (maximum amount of debris washed to lower containment) as a function of debris type. Note that these transport fractions do not depend on the location of the break. Unqualified coatings and latent debris are assumed to be uniformly distributed in the recirculation pool in lower containment, so washdown transport fractions are not applicable.

Table 3.e.6-2: Washdown Transport Fractions

Debris Type	**Transport Fraction**		
	Washed Down in Annulus	Washed Down Through Steam Generator Comps	Washed Down through Refueling Canal Drains
Fines/Particulate (all)	81%	9%	10%
Small Nukon	70%	8%	10%
Large Nukon	0%	7%	0%*
Intact Nukon Blankets	-	-	-
Qualified Coatings	81%	9%	10%
Unqualified Coatings	-	-	-
Latent Debris	-	-	-

*10% of large Nukon is transported to the refueling canal, commensurate with the percentage of spray flow that goes to the refueling canal. The large pieces of Nukon are too large to transport through the refueling canal drain strainers, therefore it is retained in the refueling canal.

Pool-Fill Transport

The two recirculation sump cavities at Seabrook are on one side of containment next to the containment wall. A steel curb is located in front of the sump cavities and debris interceptors are installed on both sides. Due to the long, tortuous flow path from the break to the sump cavities and the large number of debris interceptors, a minimal quantity of debris would transport to these cavities during the pool fill-up phase. A 2% transport fraction of fine debris (excluding unqualified coatings) to the ECCS sump cavities was used for pool fill-up (1% to each sump). A pool fill-up transport fraction of 0% to the ECCS sump cavities was used for all other debris.

Once the ECCS sump cavity fills, the water level would have to rise to a level of 2’-6” to the top of the curb surrounding the reactor cavity. The volume of the reactor cavity plus the 2’6” water level inside the curb and the pool volume at 2’-6” were first calculated. Of the remaining 98% of debris (100% minus 2% transport to the sump cavities), the transport fraction to the inactive reactor cavity during pool fill-up was calculated to be 37%. However, the pool-fill transport fraction used is limited to 15% per guidance in Section 3.6.3 of the SER (Reference 19).

For cases of single train failure, the inactive sump would be an inactive cavity. The pool-fill transport to the active sump would be 1% and the transport to inactive cavities would be limited to 15%, as limited by Section 3.6.3 of the SER (Reference 19).

Table 3.e.6-3 shows the bounding (minimum) pool fill transport fractions as a function of debris type for two train operation and Table 3.e.6-4 for one train operation.

Table 3.e.6-3: Pool fill Transport Fractions (Two Trains Operational)

Debris Type	Pool Fill Transport Fraction	
	Per Active Sump	Reactor Cavity
Fines/Particulate (all)	1%	15%
Small Nukon	0%	0%
Large Nukon	0%	0%
Qualified Coatings	1%	15%
Unqualified Coatings	0%	0%
Latent Debris	1%	15%

Table 3.e.6-4: Pool fill Transport Fractions (One Train Operational)

Debris Type	Pool Fill Transport Fraction	
	Active Sump	Inactive Cavities (Inactive Sump & Reactor Cavity)
Fines/Particulate (all)	1%	15%
Small Nukon	0%	0%
Large Nukon	0%	0%
Qualified Coatings	1%	15%
Unqualified Coatings	0%	0%
Latent Debris	1%	15%

<u>Recirculation Transport</u>

For the recirculation transport fractions, three different break cases form the basis for the debris transport analysis, and were evaluated for Seabrook:

1. Case 1: LBLOCA in SG Compartment Loop 3, Two Trains Operational
2. Case 2: LBLOCA in SG Compartment Loop 3, One Train Operational
3. Case 3: LBLOCA in SG Compartment Loop 1, Two Trains Operational

It was assumed that for any breaks that could occur in the reactor cavity or in the pressurizer compartment, the recirculation transport fractions for a break inside the bioshield could be applied since the path to the sump strainers for these break locations is the same.

The bounding (maximum) recirculation transport fractions for Nukon small and large debris as a function of evaluation case are shown in Table 3.e.6-5. No credit was taken for the settling of fine debris, so the recirculation transport fraction for fine Nukon, qualified coatings, unqualified coatings, and latent debris are 100% transport during recirculation for all cases. See the response to Section 3.e.1 for the methodology used for recirculation transport. Note that only results from Cases 1 and 2 are given in Table 3.e.6-5. As discussed in the response to Section 3.e.3, Case 3 was only used to confirm the Loop 3 break location used in Cases 1 and 2 is bounding.

Table 3.e.6-5: Recirculation Transport Fractions

	Fine Fiber and Particulate Debris	Nukon Small Pieces				Nukon Large Pieces
		Blown into lower containment	Washed down from upper containment			
			Inside bioshield	Inside annulus	Through refueling canal drain	
Loop 3 Two Train (Case 1)	100%	55%	68%	96%	100%	0%
Loop 3 Single Train (Case 2)	100%	56%	63%	68%	100%	0%

<u>Overall Debris Transport</u>

Transport logic trees were developed for each size and type of debris generated. These trees were used to determine the total fraction of debris that would reach the sump strainers in each of the postulated cases. The overall transport fractions are provided in Table 3.e.6-6 through Table 3.e.6-8. Note that the two train fractions are per active sump (maximum of 50% transport to each sump).

Table 3.e.6-6: Overall Transport Fractions per Active Sump for a Break inside the Bioshield

Debris Type	1 Train		2 Train	
	CBS On	CBS Off	CBS On	CBS Off
Fine Debris	97%	42%	48%	21%
Small Nukon by Erosion to Fines	9%	6%	5%	3%
Small Nukon Transport as Smalls	55%	28%	34%	14%
Large Nukon by Erosion to Fines	9%	8%	4%	4%
Large Nukon Transport as Larges	0%	0%	0%	0%
Intact Nukon Blankets	0%	0%	0%	0%
Qualified Epoxy	97%	42%	48%	21%
Unqualified Coatings	100%	100%	50%	50%
Latent Debris	85%	85%	43%	43%

Table 3.e.6-7: Overall Transport Fractions per Active Sump for a Reactor Cavity Break

Debris Type	1 Train		2 Train	
	CBS On	CBS Off	CBS On	CBS Off
Fine Debris	100%	45%	50%	23%
Small Nukon by Erosion to Fines	9%	6%	5%	3%
Small Nukon Transport as Smalls	55%	28%	34%	14%
Large Nukon by Erosion to Fines	9%	8%	4%	4%
Large Nukon Transport as Larges	0%	0%	0%	0%
Intact Nukon Blankets	0%	0%	0%	0%
Qualified Epoxy	100%	45%	50%	23%
Unqualified Coatings	100%	100%	50%	50%
Latent Debris	100%	100%	50%	50%

Table 3.e.6-8: Overall Transport Fractions per Active Sump for a Pressurizer Compartment Break

Debris Type	1 Train		2 Train	
	CBS On	CBS Off	CBS On	CBS Off
Fine Debris	97%	42%	48%	21%
Small Nukon by Erosion to Fines	9%	2%	5%	1%
Small Nukon Transport as Smalls	53%	11%	34%	5%
Large Nukon by Erosion to Fines	3%	2%	1%	1%
Large Nukon Transport as Larges	0%	0%	0%	0%
Intact Nukon Blankets	0%	0%	0%	0%
Qualified Epoxy	97%	42%	48%	21%
Unqualified Coatings	100%	100%	50%	50%
Latent Debris	85%	85%	43%	43%

The transported debris quantities for the most limiting break cases identified in the response to Section 3.b.4 are presented below. Since all the bounding breaks are DEGBs in the steam generator compartments, overall debris transport fractions from Table 3.e.6-6 were used to determine the bounding transported debris quantities.

Table 3.e.6-9 shows the quantities of debris transported for the worst-case fiber breaks for two train and single train operation. Note that the transported debris quantities given are per active sump for each scenario. For example, for break RC-0007-01-03 for two train operation 847.72 lbm of Nukon smalls transports to each sump for a total quantity of 1695.44 lbm of Nukon smalls transported.

Table 3.e.6-9: Transported Debris per Active Sump for the Worst-Case Fiber Breaks

	1-Train	2-Train	1-Train	2-Train
Break Location	RC-0007-01-03		RC-0001-01-03	
Location Description	Loop 3 Hot Leg at SG Nozzle		Loop 1 Hot Leg at SG Nozzle	
Break Size	31"		31"	
Break Type	DEGB		DEGB	
Nukon Fines (lbm)	716.33	354.47	736.00	364.21
Nukon Fines Due to Erosion of Small and Large Pieces (lbm)	343.08	177.41	337.82	176.63
Nukon Smalls (lbm)	1371.31	847.72	1456.86	900.60
Nukon Larges (lbm)	0	0	0	0
Qualified Coatings excluding Westinghouse equipment and Support (ft^3)	1.503	0.744	0.954	0.472

Table 3.e.6-10 shows the quantities of debris transported for the worst-case particulate breaks for two train and single train operation. Note that the transported debris quantities given are per active sump for each scenario.

Table 3.e.6-10: Transported Debris per Active Sump for the Worst-Case Particulate Breaks

	1-Train	2-Train	1-Train	2-Train
Break Location	RC-0005-01-04		RC-0008-01-03	
Location Description	Loop 2 Crossover Leg		Loop 3 Crossover Leg	
Break Size	31"		31"	
Break Type	DEGB		DEGB	
Nukon Fines (lbm)	284.49	140.78	492.95	243.93
Nukon Fines Due to Erosion of Small and Large Pieces (lbm)	144.97	73.82	245.44	125.69
Nukon Smalls (lbm)	516.20	319.11	913.22	564.54
Nukon Larges (lbm)	0	0	0	0
Qualified Coatings excluding Westinghouse Equipment and Support (ft^3)	3.084	1.526	3.074	1.521

Unqualified coatings, latent debris, and miscellaneous debris quantities are non-break-specific, and the same transport quantities are applicable to all breaks. Table 3.e.6-11 presents the transported debris quantities per active sump for single train and two train operation.

Table 3.e.6-11: Transported Debris per Active Sump for Unqualified, Latent, and Miscellaneous Debris

Debris Type	Transported Quantity per Active Sump	
	1 Train	2 Train
Unqualified Epoxy (ft^3)	4.92	2.46
Unqualified IOZ (ft^3)	4.61	2.31
Latent Fiber (lbm)	12.75 for non-RX Breaks 15 for RX Breaks	6.45 for non-RX Breaks 7.5 for RX Breaks
Latent Particulate (lbm)	72.25 for non-RX Breaks 85 for RX Breaks	36.55 for non-RX Breaks 42.5 for RX Breaks
Miscellaneous Debris (ft^2)	133	66.5

Qualified coatings on Westinghouse equipment and supports were analyzed using a simplified approach. The resulting debris quantities depend on break size only. An overall transport fraction of 100% was applied to these coatings. Table 3.e.6-12 presents the transported quantities per active sump for single train and two train operation. See the response to Section 3.h for more discussion on coatings.

Table 3.e.6-12: Transported Quantities per Active Sump for Qualified Coatings on Westinghouse Equipment and Supports

Break Size	Transport per Active Sump			
	1 Train		2 Train	
	IOZ (ft^3)	Epoxy (ft^3)	IOZ (ft^3)	Epoxy (ft^3)
<=14”	2.71	0.53	1.35	0.27
17” – 20”	2.82	0.71	1.41	0.35
23” – 26”	2.94	0.89	1.47	0.44
27.5” – 31”	3.06	1.06	1.53	0.53

3.f Head Loss and Vortexing

The objectives of the head loss and vortexing evaluations are to calculate head loss across the sump strainer and to evaluate the susceptibility of the strainer to vortex formation.

3.f.1 Provide a schematic diagram of the emergency core cooling system (ECCS) and containment spray systems (CSS).

Response to 3.f.1:

See Figure 3.f.1-1 for the ECCS and CBS schematic of Seabrook.

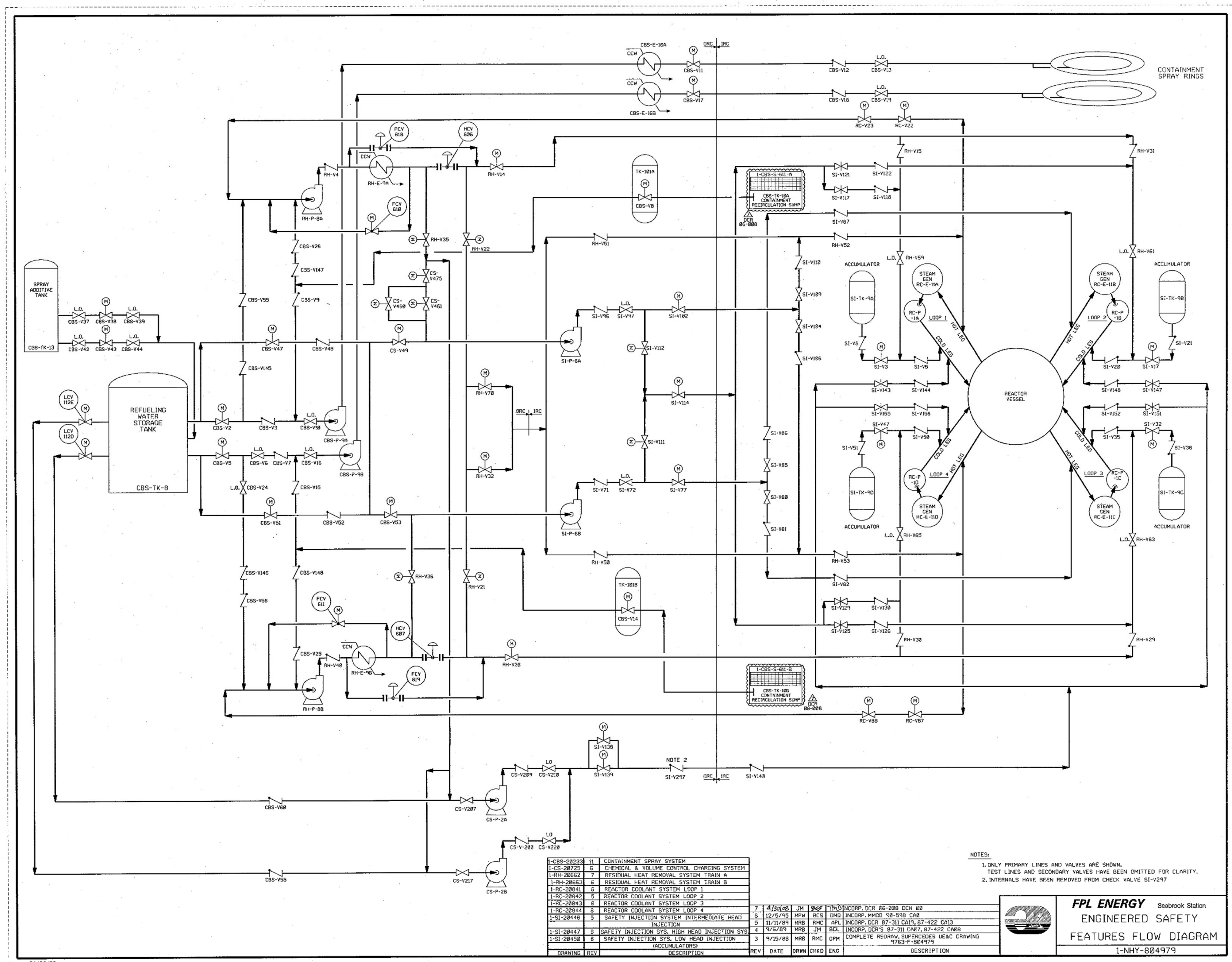

Figure 3.f.1-1: Seabrook Emergency Core Cooling System and Containment Building Spray System Schematic

3.f.2 Provide the minimum submergence of the strainer under small-break loss-of-coolant accident (SBLOCA) and large-break loss-of-coolant (LBLOCA) conditions.

Response to 3.f.2:

See the response to Section 3.g.1 for the minimum submergence of the strainers due to an SBLOCA and LBLOCA.

3.f.3 Provide a summary of the methodology, assumptions, and results of the vortexing evaluation. Provide bases for key assumptions.

Response to 3.f.3:

Observations from Seabrook strainer testing were used to assess the potential for vortexing during post-LOCA recirculation through the sump strainer.

The maximum flow rate through a Seabrook plant strainer is 7,907 gpm and occurs when the RHR pump on the opposite train is assumed to trip (see the response to Section 3.g.1). This strainer flow rate corresponds to an average approach velocity of 0.0075 ft/s for a total net strainer area of 2,345 ft^2. This total net strainer area was calculated by deducting 100 ft^2 from the unobstructed strainer surface area 2,445 ft^2 to account for the effect of miscellaneous debris (see the response to Section 3.d.4). Note that the total unobstructed strainer surface area used in this submittal includes the perforated plate surface area of the doghouse. As shown in the response to Section 3.g.1, the minimum sump water level results in a strainer submergence of 0.547 ft (or 6.6 inches) during recirculation.

Vortex testing was incorporated into the head loss test program described in the response to Section 3.f.4. The minimum test flow rate was 470.3 gpm and the test strainer screen area was 137.1 ft^2, which results in an average approach velocity of 0.0076 ft/s. This test approach velocity exceeds the expected plant strainer average approach velocity which is conservative for the vortexing evaluation. The test tank was designed such that the test strainer was situated in a pit like the plant strainer. As a result, debris-laden flow would approach the test strainer in a similar manner as the plant strainer.

Vortexing was not observed during head loss testing under plant strainer operating conditions. Vortex testing was performed at several points during the head loss testing. At clean screen conditions, submergence of the top of the discs was reduced to zero and no vortexing occurred. Similarly, no air-entraining vortices were observed during testing with the debris laden strainer until the strainer submergence was reduced to zero during post-testing draindown. Considering the testing observations and the hydraulic similarity of the plant strainer and test strainer described above, air-entraining vortices will not form at the Seabrook plant strainer during post-LOCA conditions.

3.f.4 Provide a summary of methodology, assumptions, and results of prototypical head loss testing for the strainer, including chemical effects. Provide bases for key assumptions.

Response to 3.f.4:

In 2019, NextEra performed new strainer head loss tests for Seabrook at Alden Research Laboratory (Alden) to measure the head losses caused by conventional debris (fiber and particulate) and chemical precipitate debris generated and transported to the sump strainers following a LOCA. The test program used a test strainer, debris quantities, and flow rates that were prototypical of plant conditions. Several tests were performed following the 2008 NRC Staff Review Guidance (Reference 5). Debris head losses from two of the tests were applied to derive strainer head loss. These two tests used debris loads and flow conditions that are the most representative of plant parameters and used the full debris load and thin-bed protocols.

Seabrook has two separate and independent containment sump recirculation strainers, one to support Train A of the ECCS and CBS systems and one to support Train B. As shown in Figure 3.f.4-1, each strainer is installed in a separate sump and features multiple disks installed vertically on top of a plenum box. A portion of each strainer extends above the containment floor. Each strainer also has one dog house assembly, which provides some filtering surface and connection to the suction piping. Refer to the response to Section 3.j.1 for additional details of the strainer.

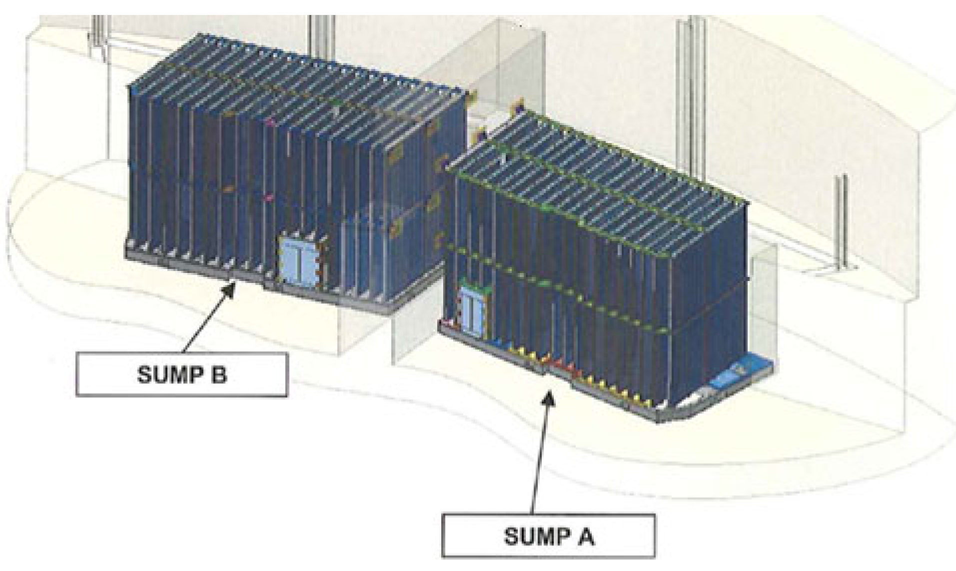

Figure 3.f.4-1: General Arrangement of the Seabrook Sump Strainer

<u>Test Loop Design</u>

The Seabrook strainer head loss test loop layout is shown in Figure 3.f.4-2. The main recirculation pump took suction from the test strainer doghouse. Downstream of the recirculation pump, filter housings with filter bags installed inside were used to clean the test loop before each test. During head loss testing, these filter housings were isolated and bypassed. The overall test loop flow rate was measured by orifice flowmeter "FM1" (see Figure 3.f.4-2), and a portion of the flow downstream of the flow meter can be diverted through a heat exchanger to maintain the test temperature. Afterwards, the flow was split between a debris hopper and the mixing lines. Flow to the debris hopper facilitated introduction of certain types of debris into the test tank. Flow through the mixing lines returns to the upstream portion of the test tank, providing turbulence to keep the introduced debris in suspension. The flow to the debris hopper was monitored by orifice flowmeter "FM2".

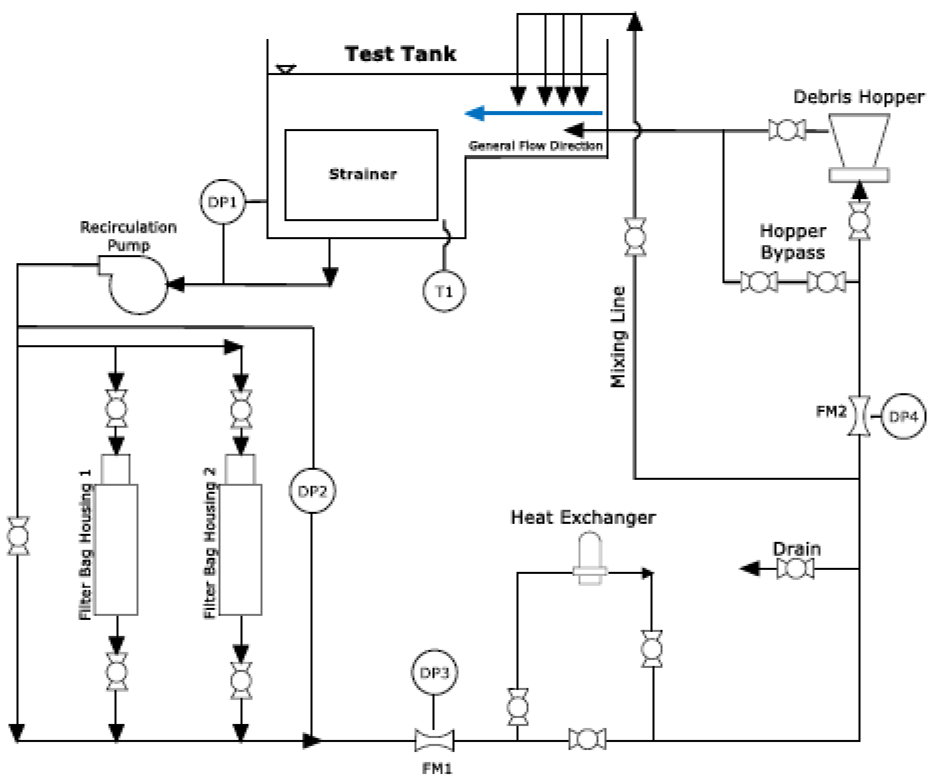

Figure 3.f.4-2: Piping Diagram of Head Loss Test Loop

<u>Test Tank</u>

The test tank, which is illustrated in Figure 3.f.4-3, included two regions: an upstream mixing region where debris was introduced into the tank and a downstream pit where the test strainer was installed. The pit geometry was configured to closely model the containment sump at Seabrook. The spacing between strainer disks and the pit wall was representative of the spacing at the plant. The depth of the downstream pit region relative to the upstream tank floor was selected such that the fraction of the test strainer disks above the upstream floor represented the configuration of the plant strainer. A 3” tall, ¼” thick curb was installed at the test tank pit entrance to model the toe kick prototypical to the SBK sump configuration. The installed curb was reduced from the actual curb height for conservatism.

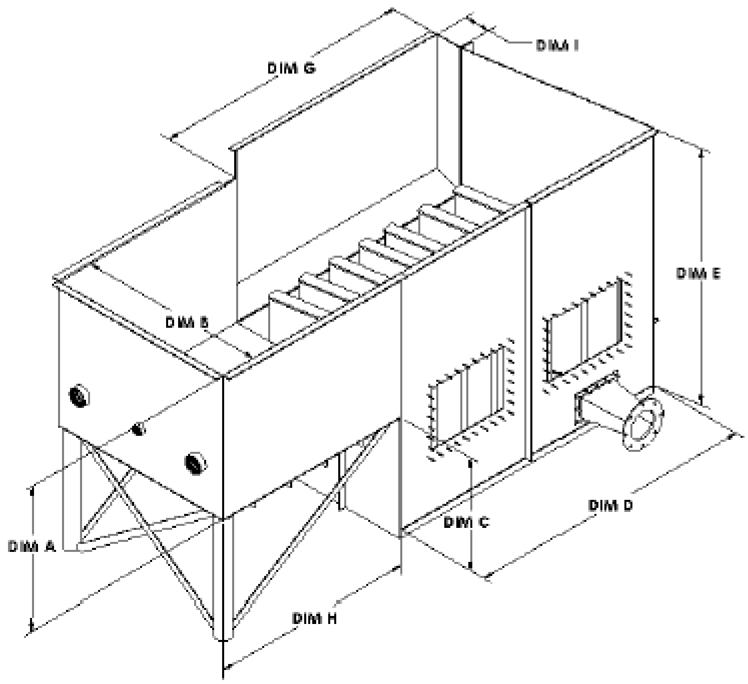

Figure 3.f.4-3: Seabrook Head Loss Test Tank

<u>Test Strainer</u>

The overall configuration of the test strainer (see Figure 3.f.4-4) is representative of the Seabrook plant strainers, with multiple vertical strainer disks installed on top of a plenum or doghouse. The heights of the plenum and doghouse of the test strainer were properly scaled down to maintain prototypical flow velocities inside and to avoid settling of any debris. The test strainer consisted of 6 disks that model the full-sized disks of the plant strainer and one shorter disk that models the disks on top of the doghouse for the plant strainer. The spacing between adjacent disks reflected the plant strainer condition. The key dimensions of the test strainer disk perforated plates and wire cloth matched those of the plant strainer. The disks of the test strainer were shorter than the plant strainer disks. However, the fraction of the disks extending above the floor of the upstream portion of the test tank was consistent with that of the plant strainer above the containment floor. The test strainer was also designed such that the distribution of approach velocity at clean conditions is consistent with that of the plant strainer. The test strainer has a total surface area of 137.1 ft^2.

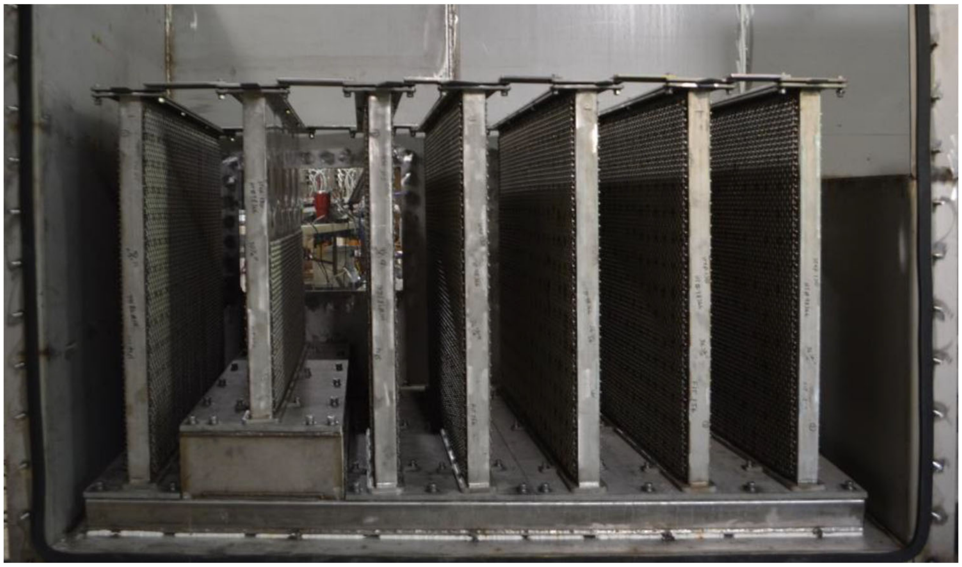

Figure 3.f.4-4: Seabrook Test Strainer inside Test Tank

Debris Materials and Preparation

Conventional debris consists of fiber and particulate debris from failed insulation and coatings, and latent materials that could be transported to the sump strainers following a LOCA. The conventional debris types that transport to the Seabrook sump strainers include Nukon fibrous insulation, qualified and unqualified coatings, and latent debris. For head loss testing, Nukon was used to simulate Nukon insulation and latent fiber, silica flour (Agsco 325) was used as a surrogate for coatings debris, and PCI Dirt/Dust mix was used as a surrogate for latent particulate debris.

Heat treated Nukon was procured and processed into fiber fines in accordance with the NEI protocol (Reference 27). The insulation was first cut into approximately 2 inch × 2 inch cubes (see Figure 3.f.4-5) and weighed out into required batches. The fiber was then placed in a preparation vessel that included a manifold with three high pressure nozzles. The debris was wetted with pre-heated test water until the base material was saturated and the pressure washer nozzles were submerged. The debris was then sprayed with test water pressurized to 1500 psi. The duration of the spray was controlled to provide consistent fiber slurry characteristics. The prepared fiber was predominantly Class 2 fibers as defined in NUREG/CR-6224 (Reference 28 pp. B-16), consisting mostly of individual fibers with lesser quantities of fiber shards and small entanglements. A backlit acrylic cylinder was used to photograph each prepared debris batch (see an example in Figure 3.f.4-5).

Figure 3.f.4-5: Nukon Insulation before (left) and after (right) Preparation

Small pieces of Nukon debris were only used in one test to assess their effects on strainer head loss. The test showed that adding small pieces to the test tank resulted in a small increase in conventional debris head loss but significantly reduced the impact on head loss by the chemical debris. Therefore, in the two head loss tests discussed in this submittal, no small pieces of Nukon debris were used.

To process the small pieces, Nukon sheets were first cut into pieces with dimensions of 1 inch × 3 inch, 1 inch × 6 inch, 2 inch × 2 inch, and 2 inch × 4 inch. Each batch of small pieces included four sub-batches of these sizes in equal proportions. Before preparation, the small pieces of different sizes were combined and placed in barrels. Afterwards, debris laden water was taken from the test tank and added to the mixed fibers until the fiber pieces were submerged. Fiber was then vigorously mixed with a paddle to break up the various fiber pieces.

Silica flour (Agsco 325) was used as a surrogate for coatings particulate debris on an equal volume basis. It has a density of 2.65 g/cm^3. The size distribution of the silica flour was characterized with the 10th, 50th and 90th percentile sizes of 5.4, 16.8 and 29.25 microns, respectively. Refer to the next sub-section for the introduction of silica flour debris during testing.

PCI Dirt/Dust mix was used as a surrogate for latent particulate debris and was introduced in its dry form directly into the upstream tank region for all head loss tests.

The chemical debris surrogate used for the head loss testing was aluminum oxyhydroxide (AlOOH). The chemical debris was prepared in accordance with WCAP-16530-NP-A (Reference 29) and met the settling requirements specified in WCAP-16530-NP-A.

<u>Debris Introduction</u>

During both tests, all conventional debris (i.e., Nukon, silica flour and PCI Dirt/Dust mix) were introduced to the test tank prior to chemical debris.

For the full debris load test described in this submittal, incremental batches of Nukon fines, silica flour, and PCI Dirt/Dust mix were introduced to the test tank. Prepared Nukon fines and silica flour were mixed before being introduced into the test tank through a debris hopper (Figure 3.f.4-6). PCI Dirt/Dust mix was sprinkled into the upstream tank region in its dry form. After each debris introduction, a minimum of three test tank pool turn-overs (PTOs) were allowed to elapse for debris to transport to the strainer prior to the next debris introduction.

For the thin bed test, silica flour and PCI Dirt/Dust mix were added to the test tank prior to the introduction of fibrous debris. Silica flour was added in dry form directly to the debris hopper and PCI Dirt/Dust mix was added to the upstream tank region directly. After introduction of particulate debris, incremental batches of Nukon fines were added. After each fibrous debris addition, a three PTO transport period elapsed before the next fiber introduction.

After conventional debris introduction and debris bed characterization (flow and temperature sweeps) were completed for each test, prepared chemical precipitate debris (AlOOH) was added to the test tank at a rate between 7 to 10 gpm.

Before each debris addition, the test tank and debris hopper were visually checked to verify that all debris of the previous batch had transported to the strainer. When using the debris hopper, debris was added to the hopper from the top opening (see Figure 3.f.4-6). The turbulence and mixing resulting from the hopper inflow was sufficient to prevent formation of debris agglomerations within the hopper. The flow with transported debris exited the hopper from its side opening into the test tank.

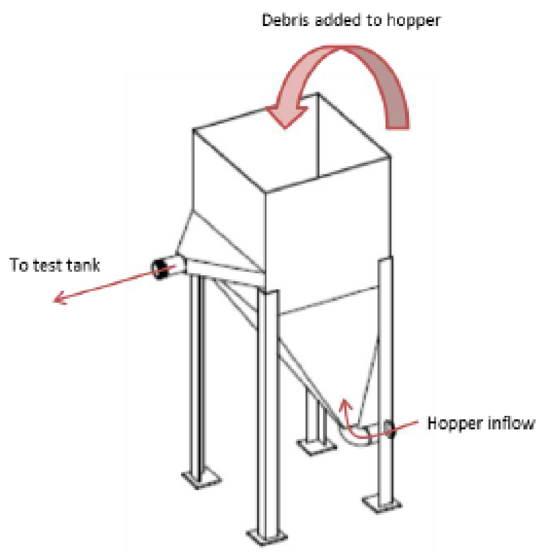

Figure 3.f.4-6: Debris Introduction Hopper

Test Parameters

The test debris quantities and test flow rate were scaled from plant values based on the ratio of the test strainer surface area (137.1 ft^2) to the plant strainer net surface area (2,345 ft^2). During testing, the test flow rate was maintained within -0%/+5% of 470.3 gpm for over 99% of the time.

Test water had a boric acid concentration of 0.249 mol/L and a sodium hydroxide (NaOH) concentration of 0.092 mol/L. This corresponds to the minimum Seabrook sump pool pH condition after an accident. Test water was prepared from deionized (DI) water with a conductivity below 5.0 µS/cm. A quantity of boric acid sufficient to provide the required boron concentration for the measured volume of water was weighed out. The water was continuously mixed while the boric acid was added. The solution was mixed until all the boric acid had dissolved before an initial pH reading was taken. A quantity of NaOH sufficient to provide the required concentration was then weighed out and added to the batch of test water, which was mixed until all the NaOH had dissolved. The final pH was approximately 8.95 at room temperature for all batches of test water generated.

During head loss testing, the water temperature was maintained at 120±5°F except when temperature sweeps were performed.

Test Debris Loads and Head Loss Response

Full Debris Load Test with Fiber Small Pieces

At the beginning of the test program, a Full Debris Load Test was first performed with fiber fines, particulate, fiber small pieces and chemical debris to assess how fiber small pieces impact strainer head loss response. During this test, fiber fines and particulate (i.e., coatings and latent debris surrogates) were batched into the test tank first, followed by batches with fiber small pieces only. After the head loss was stabilized, chemical debris was added to the test tank. The tested quantities of fiber fines, latent particulate, and chemical debris are similar to those of the later Full Debris Load Test described below while the coatings particulate debris load was higher.

The execution of this test was similar to the later Full Debris Load test described below except for the addition of fiber small pieces. The addition of the small pieces was conducted manually, not through the hopper. A 2-gallon bucket was used to lay the wetted small pieces, consisting of 2” squares, and 2” x 4”, 1” x 4” and 1” x 6” strips (in equal mass proportions), into the upstream portion of the test tank where the debris was subjected to tank mixing flows and hopper bypass flow to prevent agglomeration and enhance transport.

A few conclusions can be drawn from this test with fiber small pieces:

1. The test resulted in overall lower head losses for both the conventional debris and chemical debris, compared with the two tests discussed below.
2. It was observed that small pieces of fiber collected loosely on top of the test strainer, forming a debris “cap”. Although the spaces between strainer disks were bridged at the top by the small pieces, large open flow passages were observed between the debris cap and the more compact debris bed formed by the fiber fines and particulate.
3. The addition of fiber small pieces increased the conventional debris head loss by 0.2 psi at the test conditions (i.e., approximately 120°F and 475 gpm).
4. The head loss increase after adding the chemical debris was approximately 0.4 psi and was much less than those observed during the two tests discussed below (see Table 3.f.4-3).

It was suspected that a fraction of the chemical debris was caught in the loose debris cap formed by the fiber small pieces, resulting in less impact on the measured head loss by the chemical debris. As a result, for the later tests, fiber small pieces were not used.

Full Debris Load Test

The total conventional debris loads for the Seabrook Full Debris Load Test are scaled to equivalent plant debris load and summarized in Table 3.f.4-1.

Table 3.f.4-1: Conventional Debris Quantities for the Full Debris Load Test

Nukon Fines (lbm)	Silica Flour (ft^3)	PCI Dirt/Dust Mix (lbm)
1114.4	21.3	72.4

Figure 3.f.4-7 shows the head loss response to the conventional debris addition during the full debris load test. As shown in this figure, the debris bed was stabilized when a cumulative test debris load of interest was reached. Head loss was considered stable when head loss was neither increasing nor decreasing at a rate greater than 0.5% over at least 30 minutes (See Figure 3.f.4-8). The debris bed was also characterized via temperature and flow sweeps after the sixth debris addition. Afterwards, the remaining debris additions were completed, and head loss continued developing slowly for approximately 24 hours. A temperature sweep was then performed, which caused only a small decrease in head loss. Finally, a flow sweep was conducted. The overall test duration for the conventional debris head loss was over 50 hours.

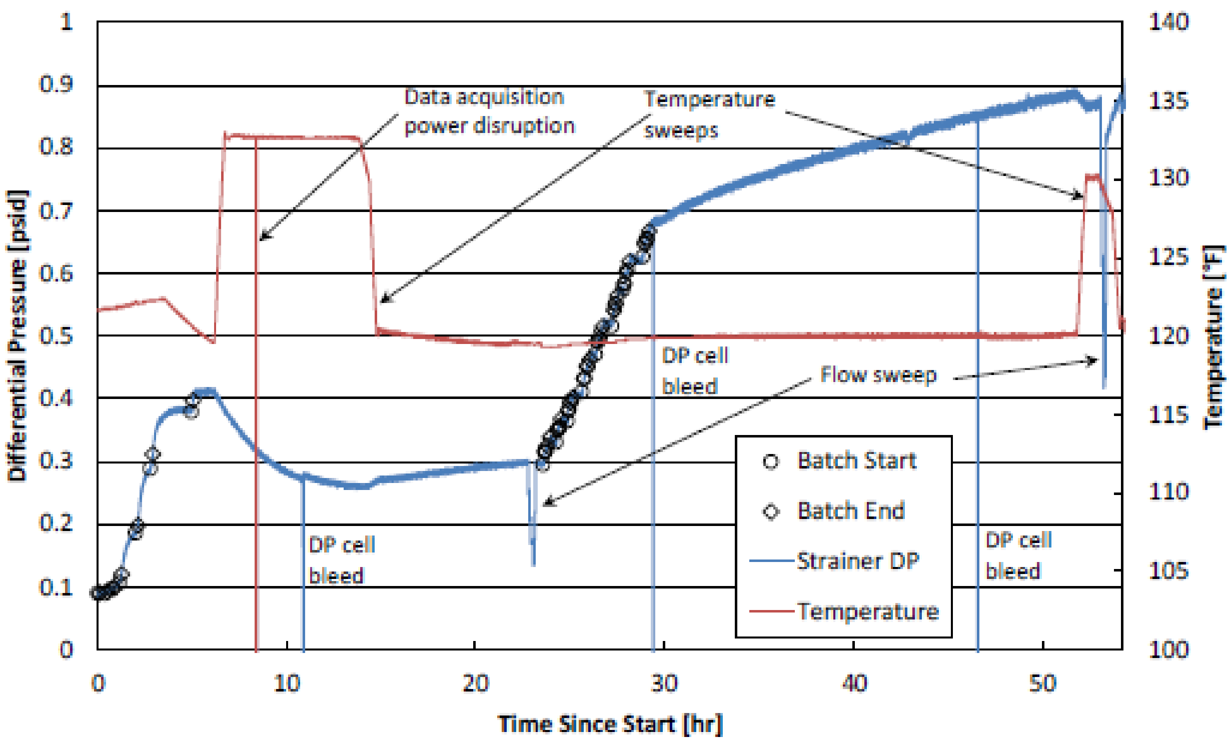

Figure 3.f.4-7: Head Loss Response to Conventional Debris in Full Debris Load Test

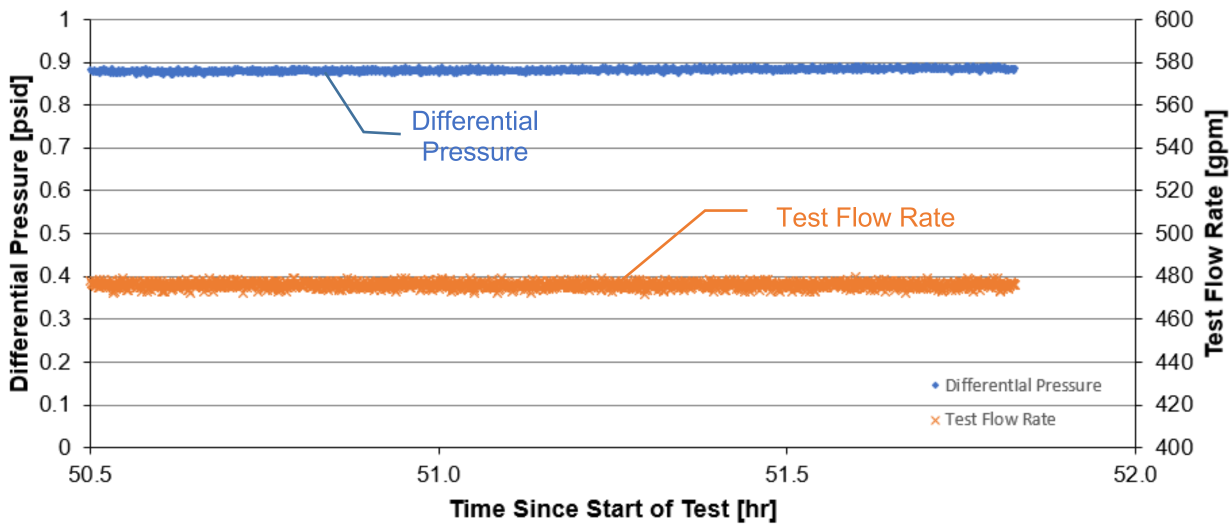

Figure 3.f.4-8: Head Loss Response after stabilization

After addition of all conventional debris, stabilization of head loss, and flow and temperature sweeps, chemical precipitation debris was added to the test tank. The addition was in two batches with the first one totaling 750 gallons and the second 500 gallons of prepared AlOOH. The total chemical debris load for the full debris load test corresponds to 182.1 kg of AlOOH at plant scale.

Figure 3.f.4-9 shows the head loss response to the two chemical debris batches. As shown in this figure, the head loss stabilized after each addition, and the second chemical debris addition caused a greater head loss increase than the first batch. It should be noted that a power disruption to the recirculation pump occurred after the head loss stabilized following addition of all chemical debris. As a result, no flow sweep was performed on the final debris bed.

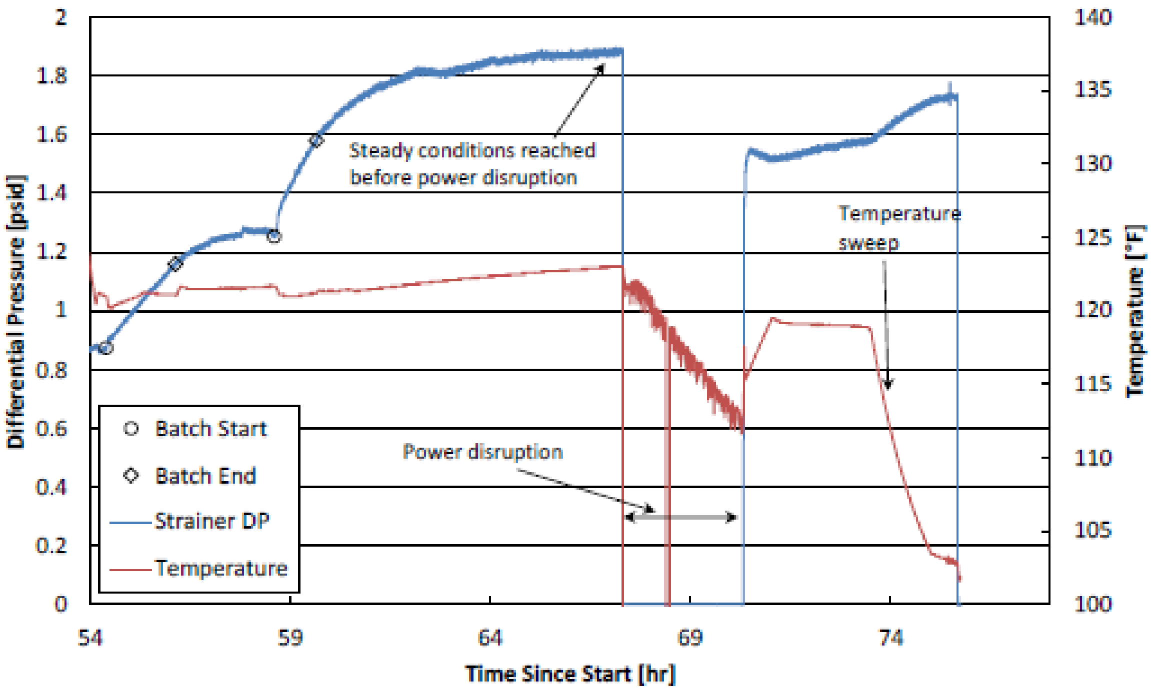

Figure 3.f.4-9: Head Loss Response to Chemical Debris Addition in Full Debris Load Test

Thin-Bed Test

The conventional debris loads for the thin-bed test are scaled to equivalent plant debris loads in Table 3.f.4-2.

Table 3.f.4-2: Conventional Debris Quantities for Thin Bed Test

Nukon Fines (lbm)	Silica Flour (ft^3)	PCI Dirt/Dust Mix (lbm)
1096.3	42.6	72.3

Figure 3.f.4-10 shows the head loss development as a result of the conventional debris additions during the thin bed test. Note that all particulate debris was introduced at the beginning of the test, followed by incremental batches of fibrous debris. Each batch of fiber debris resulted in new peaks in head loss and therefore debris addition continued until the largest plant debris load was introduced. Afterwards, head loss stabilized and relaxed significantly from its peak. Temperature and flow sweeps were then performed to characterize the debris bed.

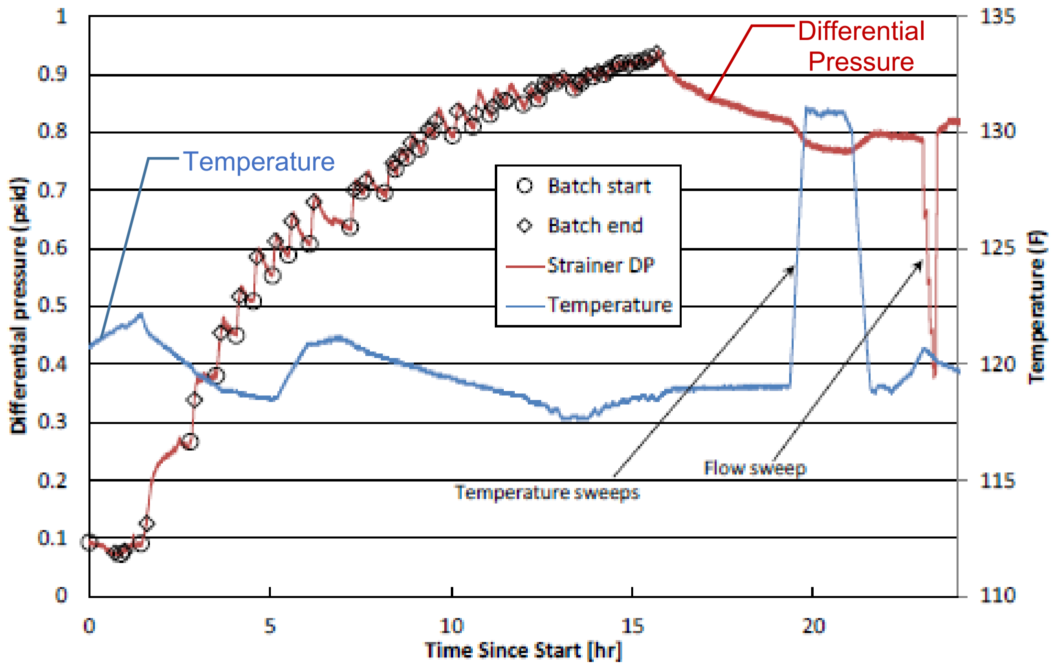

Figure 3.f.4-10: Head Loss Response to Conventional Debris for Thin Bed Test

After addition of all conventional debris, stabilization of head loss, and flow and temperature sweeps, chemical precipitation debris was added to the test tank in three batches. The total chemical debris load for the thin bed test corresponds to 182.1 kg of AlOOH at plant scale.

Figure 3.f.4-11 shows the head loss response to the chemical debris introduction. As shown in this figure, the head loss started to decrease after adding the first debris batch. The second batch resulted in a significant increase in head loss. The third chemical debris batch caused initially a modest head loss increase, followed by small fluctuations for approximately 9 hours. At the end of the test, flow sweeps were performed to characterize the debris bed.

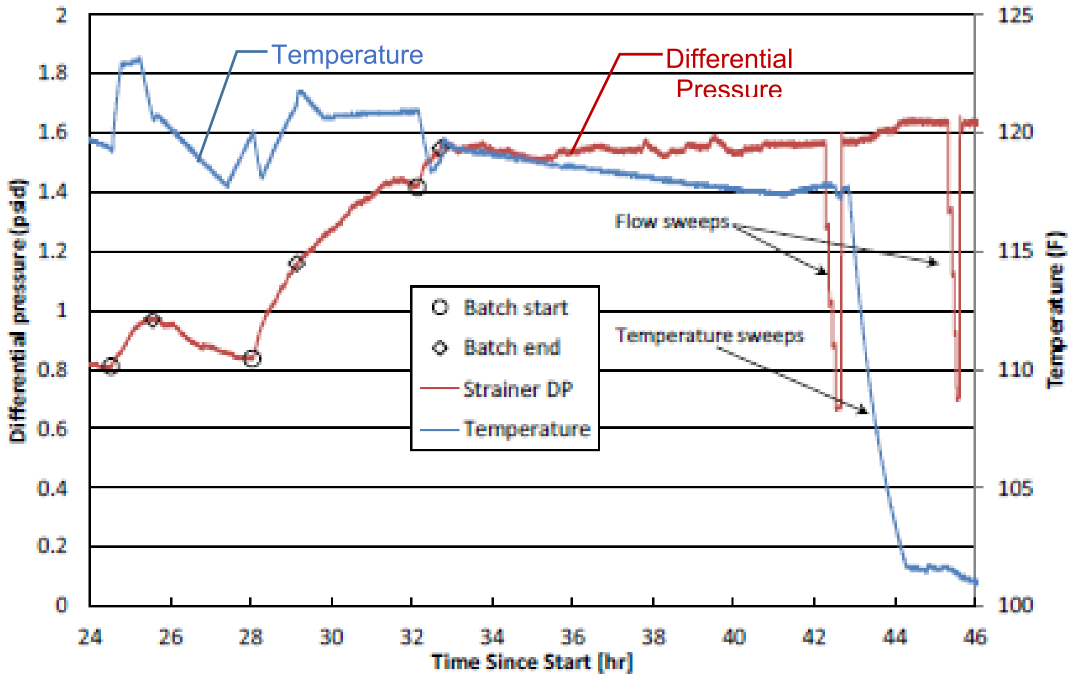

Figure 3.f.4-11: Head Loss Response to Chemical Debris for Thin Bed Test

<u>Summary of Head Loss Test Results</u>

A summary of the debris head loss results from the Seabrook tests at test conditions are provided in Table 3.f.4-3. The equivalent plant scale flow rates were determined using the ratio of the net plant strainer surface area to the test strainer surface area. The clean strainer head loss (CSHL) of the test strainer was subtracted from the measured overall head loss values to determine the debris head losses. The CSHL of the test strainer ranged from 0.079 psi to 0.087 psi for test flow rates ranging between 465 gpm and 482 gpm at a nominal temperature of 120°F.

Table 3.f.4-3: Summary of Raw Debris Head Loss Results from Seabrook Tests

Test Point	Debris Head Loss (psi)	Test Flow Rate (at Plant Scale) (gpm)	Temperature (°F)
Seabrook Full Debris Load Test			
Conventional Debris Max Head Loss	0.809	480 (8,210)	120.1
Conventional Debris Stable Head Loss	0.803	476 (8,142)	120.1
Chemical Debris Max Head Loss[1]	1.814	474 (8,107)	123.0
Chemical Debris Stable Head Loss[1]	0.743	481 (8,227)	128.4
Seabrook Thin-Bed Test			
Conventional Debris Max Head Loss	0.858	481 (8,227)	118.5
Conventional Debris Stable Head Loss	0.737	480 (8,210)	119.0
Chemical Debris Max Head Loss[1]	1.509	477 (8,159)	117.8
Chemical Debris Stable Head Loss[1]	1.481	475 (8,124)	117.7

[1] The chemical debris head loss here has contribution from the conventional and chemical debris.

3.f.5 Address the ability of the design to accommodate the maximum volume of debris that is predicted to arrive at the screen.

Response to 3.f.5:

As discussed in the response to Section 3.f.4, the head loss tests used test strainers that are prototypical to the plant strainer designs. Additionally, the test debris loads were scaled based on the ratio of the test strainer surface area and the plant net strainer surface area. The test strainer was designed to closely model the plant strainers with respect to key strainer disk dimensions and spacing between adjacent disks (see the response to Section 3.f.4). The arrangement of test strainer within the test tank reflected the pit style strainer at the plant. Finally, as discussed in the response to Section 3.f.7, the test debris loads bounded the maximum debris loads for the worst breaks postulated for Seabrook. With these considerations, the impact of debris on the plant strainer can be directly determined from the head loss test results.

3.f.6 Address the ability of the screen to resist the formation of a “thin bed” or to accommodate partial thin bed formation.

Response to 3.f.6:

The “thin-bed effect” is defined as the relatively high head losses across a thin bed of fibrous debris, which can sufficiently filter particulate debris to form a dense (or high particulate-to-fiber ratio) debris bed. As discussed in the response to Section 3.f.4 above, the thin bed test introduced the full particulate load into the test tank first, followed by fibrous debris batches. This batching schedule allowed the formation of a debris bed with a high particulate to fiber ratio. As shown in Table 3.f.7-1, the particulate debris loads used for the Seabrook thin bed test are much greater than the particulate debris loads at Seabrook. As a result, any thin-bed effects, should they occur, would be captured by the measured head losses.

3.f.7 Provide the basis for strainer design maximum head loss.

Response to 3.f.7:

<u>Comparison of Plant and Head Loss Test Flow Rates</u>

As discussed in the response to Section 3.g.1, the maximum strainer flow rate used for strainer head loss analysis is 7,907 gpm, which corresponds to an approach velocity of 0.0075 ft/s. During head loss testing, the test flow rates were maintained within -0%/+5% of 470.3 gpm (or between 470.3 gpm and 494 gpm) for over 99% of the time (see the response to Section 3.f.4). These test flow rates correspond to approach velocities of 0.0076 ft/s and 0.0080 ft/s, and both bound the plant condition.

Comparison of Plant and Head Loss Test Conventional Debris Loads

Table 3.f.7-1 compares the transported conventional debris loads of four Seabrook bounding breaks with those used in the head loss tests. The plant debris loads are described in the response to Section 3.e.6. The total coatings particulate debris loads shown in Table 3.f.7-1 were calculated by combining the volumes of qualified and unqualified coatings. The debris loads for Seabrook Full Debris Load Test and Thin-Bed Test were taken from Table 3.f.4-1 and Table 3.f.4-2, respectively.

As shown in Table 3.f.7-1, for the highest fiber and particulate breaks, the total fiber fines, total coatings particulate and latent particulate debris loads are all bounded by the full debris load test and thin bed test.

As shown in Table 3.f.4-3, a slightly higher conventional debris head loss was observed in the thin bed test than the full debris load test. However, the particulate debris load utilized for the thin bed test was more than 2.5 times the plant load (see Table 3.f.7-1). Therefore, the thin bed test is overly conservative as a representation of the Seabrook breaks, and the conventional debris head loss from the full debris load test (see Table 3.f.4-3) is used when evaluating strainer head losses.

Table 3.f.7-1: Comparison of Seabrook Test Conventional Debris Loads with Plant Debris Loads

	Highest Fiber Break		Highest Particulate Break		Seabrook Full Debris Load Test	Seabrook Thin-Bed Test
Break Location	RC-0007-01-03	RC-0001-01-03	RC-0005-01-04	RC-0008-01-03		
Location Description	Loop 3 Hot Leg at SG Nozzle	Loop 1 Hot Leg at SG Nozzle	Loop 2 Crossover Leg	Loop 3 Crossover Leg		
Break Size	31"	31"	31"	31"		
Break Type	DEGB	DEGB	DEGB	DEGB		
Nukon Fines (lbm)	716.33	736.00	284.49	492.95		
Nukon Fines Due to Erosion of Smalls and Larges (lbm)	343.08	337.82	144.97	245.44		
Latent Fiber (lbm)	12.75	12.75	12.75	12.75		
Total Fiber Fines (lbm)	**1072.16**	**1086.57**	**442.21**	**751.14**	**1114.4**	**1096.3**
Qualified Coatings excluding Westinghouse equipment (ft^3)	1.503	0.954	3.084	3.074		
Westinghouse Qualified Coatings (ft^3)	4.12	4.12	4.12	4.12		
Unqualified Coatings (ft^3)	9.53	9.53	9.53	9.53		
Total Coating Particulate (ft^3)	**15.153**	**14.604**	**16.734**	**16.724**	**21.3**	**42.6**
Latent Particulate (lbm)	**72.25**	**72.25**	**72.25**	**72.25**	**72.4**	**72.3**

Comparison of Plant and Head Loss Test Chemical Debris Loads

Table 3.f.7-2 compares the maximum chemical debris loads of Seabrook (see the response to Section 3.o.2.7.ii) with those used in the head loss tests (see the response to Section 3.f.4). As shown in the table, the total chemical debris loads used for the Seabrook tests exceed that predicted for the plant and therefore bound the plant conditions.

Table 3.f.7-2: Comparison of Plant and Test Chemical Debris Loads for Seabrook

	Plant Chemical Debris Load	Seabrook Full Debris Load	Seabrook Thin-Bed Test
Total Quantity of AlOOH (kg)	182	182.1	182.1

Based on the comparisons shown in this section, it is concluded that the Seabrook head loss tests bound and are therefore applicable for the plant conditions. The maximum conventional debris head loss and maximum chemical debris head loss from the full debris load test (see Table 3.f.4-3) will be adjusted from testing conditions to plant conditions before being used in the strainer head loss analysis (see the response to Section 3.f.10).

3.f.8 Describe significant margins and conservatisms used in head loss and vortexing calculations.

Response to 3.f.8:

Vortexing Testing

Testing was conducted to determine whether vortexing could occur. As discussed in the response to Section 3.f.3, the vortex tests were performed at both clean strainer and debris laden conditions.

The vortex test used strainer approach velocities exceeding 0.0076 ft/s for both the clean screen and conventional debris laden conditions, which is higher than the maximum approach velocity expected for the plant strainer of 0.0075 ft/s.

The clean strainer and debris laden vortex testing was performed at zero submergence, which is conservative when compared to the 6.6 inch minimum submergence from an SBLOCA (see the Responses to 3.f.3 and 3.g.1).

Strainer Head Loss

As shown in Table 3.f.7-1, the tested debris loads for both head loss tests are higher than the largest transported debris loads for the worst breaks postulated for Seabrook.

The head loss tests were performed at approach velocities higher than that of the plant strainer (see the response to Section 3.f.7).

As detailed in the response to Section 3.f.10, in the absence of flow sweep data for the chemical debris bed during the full debris load test, it was conservatively assumed that the flow through the debris bed is completely laminar when adjusting the measured chemical debris head loss from testing conditions to plant conditions. This results in a conservatively higher debris head loss.

As discussed in the response to Section 3.f.10, small conventional debris resulted in an increase in conventional debris head loss but decreased the head loss impact of chemical debris. Strainer head loss was evaluated by including the impact of smalls on conventional debris head loss but using chemical debris head loss data gathered without small debris. The head loss impact of small pieces was included in the conventional term by adding the unscaled small piece head loss measured in testing. Adding the unscaled value is conservative, because scaling the measured test head loss to plant conditions of interest for conventional debris head loss (i.e., from low temperature to high temperature) would result in a smaller head loss value.

3.f.9 Provide a summary of methodology, assumptions, bases for the assumptions, and results for the clean strainer head loss calculation.

Response to 3.f.9:

In order to pass through a Seabrook strainer, flow has to travel through debris interceptors and strainer disks, into a plenum below the disks, and into a doghouse where the flow from all the disks merges and exits the sump through the ECCS suction piping. The CSHL accounted for head losses along this flow path without a debris bed. As a result, the CSHL consisted of four components: the debris interceptor head loss, strainer disk head loss, plenum head loss, and doghouse head loss.

The debris interceptor head loss was calculated to be 0.04 ft at 8,050 gpm by modeling the debris interceptors as submerged weirs, only allowing flow over the top of the interceptors. This flow rate bounds the maximum strainer flow rate of 7,907 gpm.

The head loss of a strainer disk was based on previous head loss testing, where a single strainer disk was installed on top of a plenum. The measured head loss conservatively included losses due to flow through the disk, exiting the disk and expanding inside the plenum since the pressure was measured downstream of the disk exit. The measured head loss was 0.047 ft at an equivalent plant flow rate of 8200 gpm, which bounds the maximum strainer flow rate.

The plenum head loss includes losses due to flow merging from each strainer disk into the plenum. To calculate this head loss, it was conservatively assumed that the Seabrook strainer disks have a uniform flow distribution with the same approach velocity. This assumption increases the calculated flow rate through the strainer discs furthest from the plenum exit, thus increasing the calculated plenum head loss. The calculated plenum head loss is 0.251 ft based on a total strainer flow rate of 8,050 gpm.

The doghouse head loss includes losses due to flow merging inside the doghouse. This loss was modeled in two components: 1) head loss for flow merging from the plenum into the bottom opening of the doghouse and 2) head loss for flow merging inside the doghouse before exiting. The total doghouse head loss was calculated to be 0.289 ft at 8,050 gpm. Note that all flow merging inside the plenum and doghouse was modeled as tee or wye junctions using loss coefficients from a hydraulic handbook.

The total CSHL is determined to be 0.63 ft at 8,050 gpm by combining the head loss components discussed above.

3.f.10 Provide a summary of methodology, assumptions, bases for the assumptions, and results for the debris head loss analysis.

Response to 3.f.10:

The total strainer head loss was determined by combining the calculated plant strainer CSHL (see the response to Section 3.f.9) and the measured debris head losses (see the response to Section 3.f.4) scaled to plant conditions (e.g., temperature and strainer flow rate). The methodology for scaling measured debris head losses and CSHL from testing or analysis conditions to plant conditions is detailed in this section. As discussed in the response to Section 3.f.7, the maximum debris head losses from the full debris load test in Table 3.f.4-3 were used to determine the total strainer head loss. Depending on temperature, either the conventional or chemical debris head loss was used. The example application of this process on the conventional debris head loss is presented below.

The scaling was done using the following equation which relates the head losses through a debris bed (h_L) at two different flow rates (Q) and temperatures by a weighted average for the impact of flow, and water density (ρ) and viscosity (μ). The laminar and turbulent fractions (L_{Frac} and T_{Frac}) are weighting factors and can be determined from flow sweep data recorded during testing. In the equation, the variables with the subscript “1” represent testing conditions while those with subscript “2” are for plant conditions of interest. This equation was derived from Equation 6-4 in

NUREG/CR-6224 (Reference 28), which showed that head loss through a debris bed can be correlated to flow rate by a quadratic function.

$$h_{L,2} = \left[L_{Frac} \frac{\mu_2}{\mu_1} \frac{Q_2}{Q_1} + T_{Frac} \frac{\rho_2}{\rho_1} \left(\frac{Q_2}{Q_1} \right)^2 \right] h_{L,1}$$

To adjust the conventional debris head loss, the flow sweep data taken after adding the full conventional debris load during the full debris load test is plotted in the figure below and curve fit to a quadratic function of test flow rate.

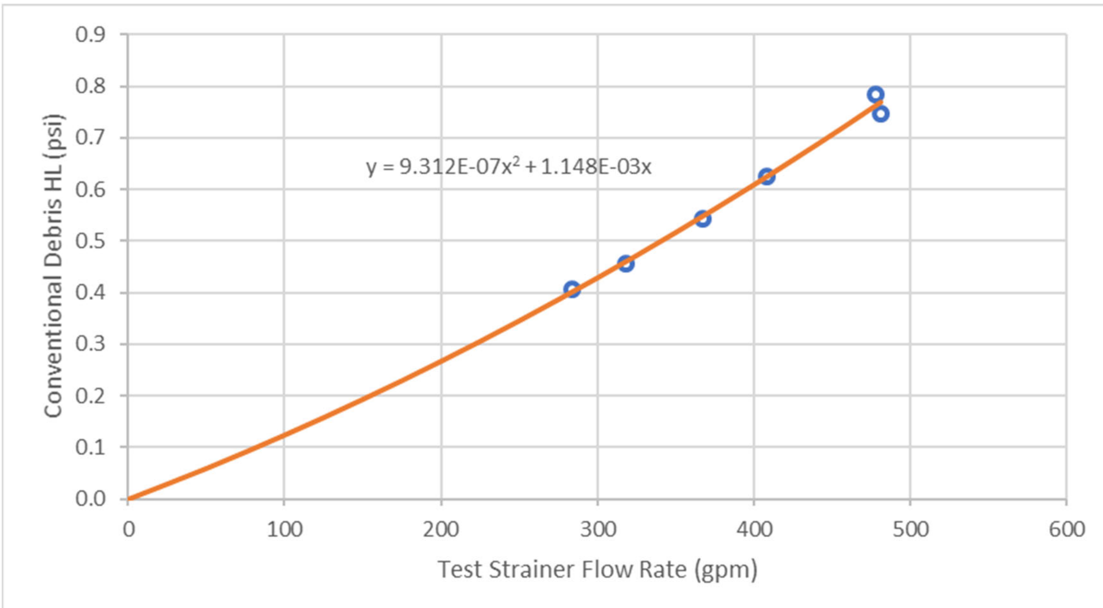

Figure 3.f.10-1: Conventional Debris Head Loss Flow Sweep Curve Fit

Using the curve-fit of the flow sweep data, the laminar and turbulent fractions for the flow through the conventional debris bed were calculated to be 72% and 28%, respectively, at the target test flow rate. These laminar and turbulent fractions were then substituted into the above equation, along with the maximum conventional debris head loss recorded during testing (0.81 psi at 8,210 gpm and 120.1°F, see Table 3.f.4-3) to determine the strainer conventional debris head loss at plant conditions.

As discussed previously, small pieces of Nukon debris were shown to have little impact on head loss, resulting in an increase of 0.2 psi. Although small pieces were not used in the full debris load test described in this submittal, the head loss impact of 0.2 psi was applied to the scaled conventional head loss. This approach is conservative since scaling the measured test head loss to plant conditions of interest for conventional debris head loss (i.e., from low temperature to high temperature) would result in a smaller head loss value.

As shown in the response to Section 3.o.2.9.i, for strainer chemical effects, chemical precipitation will not occur until the sump temperature decreases to 117.6°F. Therefore, for sump temperatures at or below 117.6°F, the chemical debris head loss must be used. The same methodology as described above was used to scale the maximum chemical debris head loss from testing (1.814 psi at 8,107 gpm and 123°F, see Table 3.f.4-3) to plant conditions.

As discussed in the response to Section 3.f.4, no flow sweep was performed at the end of the full debris load test due to power interruption. Therefore, the flow regime through the chemical debris bed was assumed to be 100% laminar (L_{Frac} = 100% and T_{Frac} = 0%). This approach conservatively increases the scaled debris head loss because the plant flow rate of interest (8010 gpm, which is rounded up from maximum plant strainer flow rate for margin) is less than the plant scale equivalent of the test flow rate (8,107 gpm). As a result, the ratio in flow rate Q_2/Q_1 is less than one in the above equation, and the flow ratio squared $(Q_2/Q_1)^2$ in the turbulent term is smaller than the flow ratio (Q_2/Q_1) in the laminar term. Since the density and viscosity ratios are both approximately 1 when scaling from the chemical head loss test temperature (123°F) to the chemical precipitation temperature (117.6°F), they have negligible impact on the result. Therefore, the scaled head loss is smaller when the turbulent term is included, compared to when only the laminar term is applied (i.e., a full laminar flow). The impact of small pieces of Nukon debris was not considered since small pieces were shown to reduce the head loss impact of chemical debris.

The same methodology was used to scale the plant strainer CSHL value (see the response to Section 3.f.9) to the plant conditions of interest. The flow sweep taken prior to the addition of any debris during testing is used to show that the flow through the clean strainer is fully turbulent (L_{Frac} = 0% and T_{Frac} = 100%).

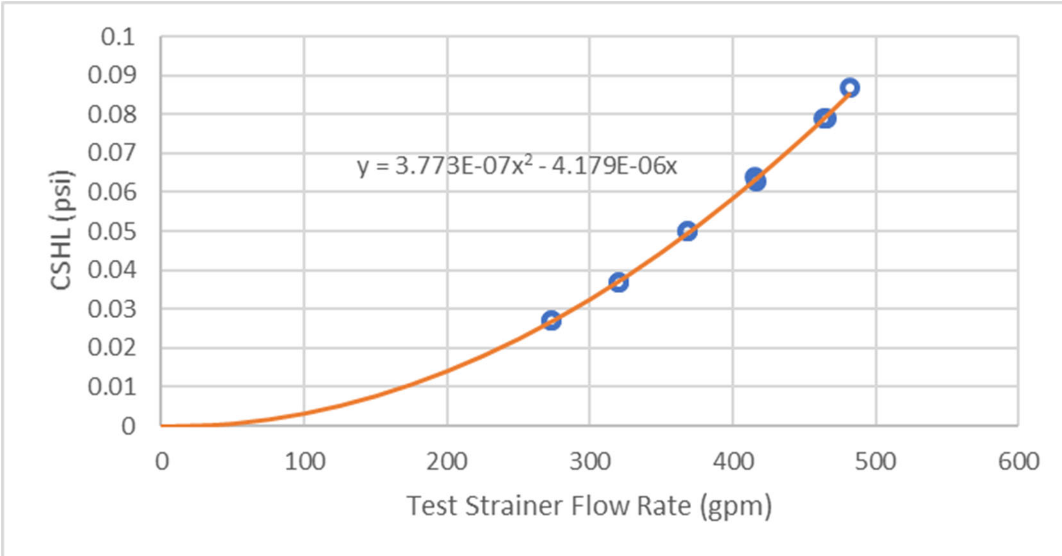

Figure 3.f.10-2: CSHL Flow Sweep Curve Fit

The scaled debris head losses and CSHL at a few different sump temperatures and a strainer flow rate of 8010 gpm are shown in Table 3.f.10-1, along with the total strainer head losses. For temperatures at or below 117.6°F, the total head loss was based on the chemical debris head loss.

Table 3.f.10-1: Seabrook Maximum Head Loss

T (°F)	Debris h_L (ft)	CSHL (ft)	Total Strainer Head Loss (ft)
211.27	1.680	0.624	2.304
117.6	4.398	0.644	5.042
35	12.95	0.651	13.60

3.f.11 State whether the sump is partially submerged or vented (i.e., lacks a complete water seal over its entire surface) for any accident scenarios and describe what failure criteria in addition to loss of net positive suction head (NPSH) margin were applied to address potential inability to pass the required flow through the strainer.

Response to 3.f.11:

As shown in Table 3.g.1-1, the Seabrook strainers remain fully submerged for all breaks under the minimum water level conditions. Therefore, no failure criteria other than loss of NPSH margin and strainer structural failure were considered.

3.f.12 State whether near-field settling was credited for the head-loss testing, and if so, provide a description of the scaling analysis used to justify near-field credit.

Response to 3.f.12:

No near-field settling was credited for head loss testing. Sufficient turbulence was maintained in the mixing section of the test tank to ensure that all debris had an opportunity to collect on the surfaces of the test strainer. The turbulence was created by configuring multiple inlet mixing nozzles in the upstream region of the test tank. The placement and size of the discharge piping was carefully chosen to achieve the desired level of turbulence in the test tank without disturbing the debris bed formed on the test strainer. Manual stirs were also applied as necessary. It was observed that a small amount of particulate debris, consisting of predominantly heavier components of the latent debris surrogate (coarse sand) settled behind the curb installed upstream of the pit.

3.f.13 State whether temperature/viscosity was used to scale the results of the head loss test to actual plant conditions. If scaling was used, provide the basis for concluding that boreholes or other differential-pressure induced effects did not affect the morphology of the test debris bed.

Response to 3.f.13:

As shown in the response to Section 3.f.10, the measured debris head losses were scaled for temperature and flow rate from test conditions to plant conditions. The scaling was done using flow regime information derived from Seabrook-specific flow sweep data collected during the latest head loss testing or conservatively assumed laminar and turbulent fractions. Therefore, any boreholes and other differential-pressure induced effects on bed morphology were captured and properly accounted for when scaling the head loss.

3.f.14 State whether containment accident pressure was credited in evaluating whether flashing would occur across the strainer surface, and if so, summarize the methodology used to determine the available containment pressure.

Response to 3.f.14:

<u>Flashing Analysis</u>

When the containment pressure is assumed to be equal to the vapor pressure at the sump temperature, 1 psi of containment accident pressure needs to be credited to prevent flashing downstream of the Seabrook strainer. The flashing analysis was performed at the top elevation of the strainer. The credited amount of containment accident pressure is very small, compared with the margin in the containment pressure for preventing flashing based on the safety analysis results.

Flashing would occur if the pressure downstream of the strainer was lower than the vapor pressure at the sump temperature. The minimum containment pressure that is required to prevent flashing is calculated by adding the strainer head loss to the vapor pressure at the sump temperature of interest and subtracting the strainer submergence. This methodology was applied to various post-accident containment and sump conditions to determine the minimum containment pressure required to prevent flashing. These pressures are then compared with the corresponding containment pressures from the containment analysis performed for Seabrook in the table below. As shown, the margins in containment pressure for preventing flashing are much larger than the 1 psi of accident pressure credited.

Table 3.f.14-1: Margin in Containment Pressure for Preventing Flashing

Time (s)	Sump Pool T (°F)	Vapor Pressure (psia)	Strainer Head Loss (psi)	Pressure due to Submergence (psi)	Min Containment P Req'd to Prevent Flashing (psia)	Containment Pressure from Containment Analysis (psia)	Margin (psi)
1,560	259.1	34.88	0.96	0.22	35.61	53.36	17.75
2,560	259.4	35.07	0.96	0.22	35.80	53.74	17.94
2,886	259.5	35.13	0.96	0.22	35.86	53.75	17.88
4,060	258.3	34.44	0.96	0.22	35.17	51.44	16.27
5,060	253.8	31.86	0.96	0.22	32.60	48.43	15.84
6,060	248.9	29.23	0.96	0.22	29.97	46.45	16.48
8,060	240.6	25.25	0.96	0.22	25.99	43.76	17.77
10,000	234.5	22.60	0.96	0.22	23.34	41.91	18.57
N/A*	117.6	1.58	2.16	0.22	3.52	14.6	11.08

*The containment analysis does not show at what time the sump pool reaches 117.6 °F or the associated containment pressure. It is therefore assumed that the containment pressure is equal to the minimum allowable containment pressure of 14.6 psia in the Seabrook Technical Specification.

The margins shown in the above table are also visualized in the figure below.

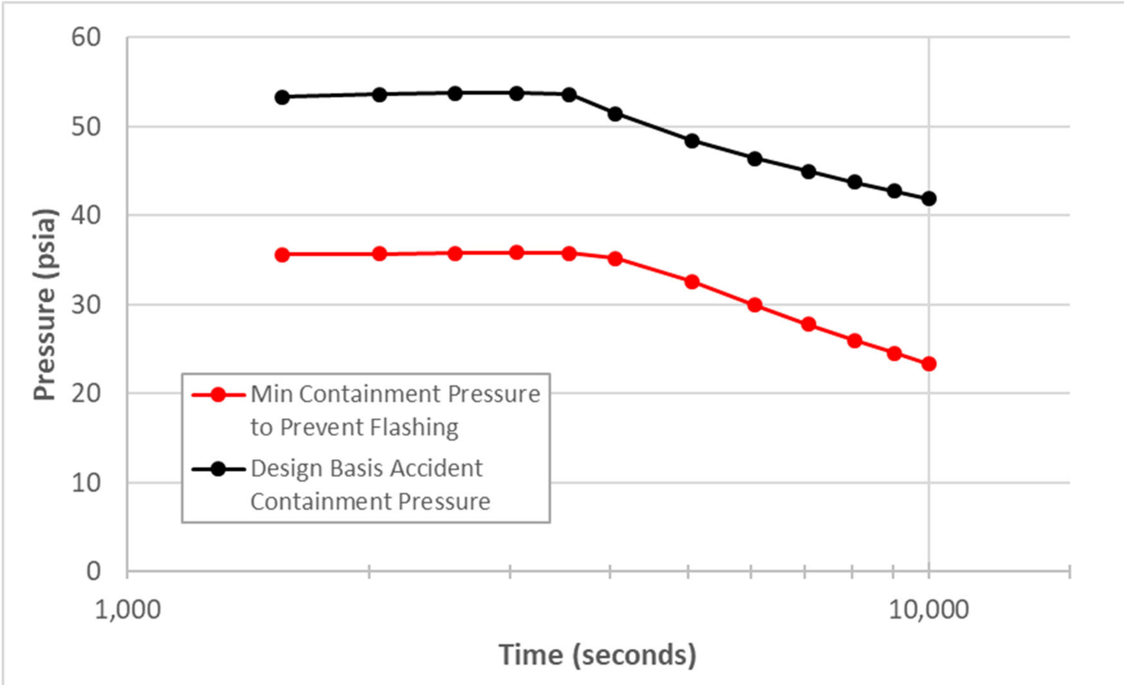

Figure 3.f.14-1: Margin in Containment Pressure for Preventing Flashing based on DBA Containment Pressure Curves

The above analysis of containment pressure margin for preventing flashing combined the following inputs. This approach was conservative as these input conditions cannot be physically concurrent.

- Debris head loss values which bound all possible breaks analyzed at Seabrook. Head loss of 0.96 psi at 211.27°F and 8010 gpm (see Table 3.f.10-1) was used in the analysis for all temperatures above 211.27°F. This is conservative as head loss decreases with increasing temperature. Chemical precipitation occurs at 117.6°F, and for this temperature a head loss of 2.16 psi at 117.6°F and 8010 gpm (see Table 3.f.10-1) was used. The flow rate at which these head losses were determined bounds the maximum sump strainer flow rate of 7907 gpm (see Section 3.f.3).
- Post-LOCA sump temperature curve resulting in the maximum sump temperature, and the containment pressure curve resulting in the lowest containment pressure.
- A strainer submergence based on the minimum SBLOCA sump water level: 0.547 ft (or 0.22 psi) from Table 3.g.1-1.

It is recognized that the margins shown in the above table are based on the temperature and pressure curves from the LBLOCA containment analysis, which biased inputs to maximize the containment pressure. However, should more realistic inputs for smaller breaks be used in the containment analysis, both the sump temperature and containment pressure would decrease, and the margins are expected to be similar. This is demonstrated in the Vogtle submittal, which analyzed the margins in the containment pressure for preventing flashing using both the design basis and best estimate containment analysis results, and showed similar margin values. More details can be found in Figures 3.f.14-1, 3.f.14-2 and 3.f.14-3 of the July 2018 Vogtle GL 2004-02 submittal to the NRC (Reference 2). This is due mainly to the lower sump temperatures when best estimate conditions are used. Seabrook has the same nuclear steam supply system design as Vogtle (Westinghouse 4-loop) and therefore a similar comparison in containment pressure is expected, should NextEra reperform Seabrook containment analysis using best estimate inputs.

<u>Degasification Analysis</u>

NextEra also performed a degasification analysis for Seabrook, which showed no voids will form at the mid-height of the strainer as flow travels through the debris bed and strainer at the maximum sump temperature of 260°F as well as 117.6°F, at which chemical precipitation is predicted to occur. The analysis was done by comparing air solubilities upstream and downstream of the strainer determined using Henry's law. The degasification evaluations were performed using a conservative combination of inputs that could not concurrently exist in reality (e.g., minimum SBLOCA water level, maximum LBLOCA strainer head loss). The resulting zero void fraction was due to the strainer submergence at its mid-height being greater than the total strainer head loss.

3.g Net Positive Suction Head

The objective of the NPSH section is to calculate the NPSH margin for the ECCS and CSS pumps that would exist during a LOCA, considering a spectrum of break sizes.

3.g.1 Provide applicable pump flow rates, the total recirculation sump flow rates, sump temperature(s), and minimum containment water level.

Response to 3.g.1:

Seabrook Pump/ Sump Flow Rates

Following an LBLOCA both trains of the RHR pumps, CCPs, SI pumps and CBS pumps would be automatically started. Operation of the CBS pumps is initiated by high containment pressure. Operation of the other pumps is initiated by the safety injection signal. Recirculation is not initiated until at least 26 minutes after the LBLOCA. Recirculation is initiated by the RWST Lo-Lo level signal. Upon receipt of this signal, the RHR and CBS pumps are automatically re-aligned to take suction from the recirculation sumps. The CCPs and SI pumps are then re-aligned to take suction from the RHR pumps' discharge ("piggyback" mode). Approximately 5 to 6 hours after the accident, the SI and RHR pumps are aligned to hot leg recirculation supplying flow to the RCS hot legs. The CCPs continue to supply flow to the cold legs.

A hydraulic model of the ECCS and CBS systems was constructed to analyze the NPSH margin and the system flows. The modeled case with the minimum NPSH margin had the failure of the Train B RHR pump, resulting in a total flow rate of 7,907 gpm through the Train A sump during recirculation (3,327 gpm through the CBS pump and 4,580 gpm through the RHR pump). The Train A NPSH margin is less than and therefore bounds the Train B NPSH margin.

As noted, the CCPs and SI pumps operate in "piggyback" mode during recirculation, so flowrates for these pumps are already included in the total.

The ECCS and CBS flows and NPSH margins were calculated for both cold leg and hot leg recirculation conditions following an LBLOCA.

Seabrook Minimum Containment Water Level

The containment water level calculation evaluated bounding minimum sump pool volumes and levels. Table 3.g.1-1 summarizes the results of the containment water level calculation. Note that the SBLOCA water levels are for a break of a pressurizer spray line while the LBLOCA results are for a pressurizer surge line break.

The pool floor elevation is -26 ft, and the top surface of the top strainer disk is at an elevation of -24.05 ft.

The minimum water level elevations in Table 3.g.1-1 were calculated by adding the pool heights to the pool floor elevation. The submergence values in Table 3.g.1-1 were calculated by subtracting the top elevation of the strainers from the water level elevations.

Table 3.g.1-1: Minimum Sump Pool Water Levels

Break Case	Temperature	Minimum Water Level Elevation (ft)	Pool Height (ft)	Strainer Submergence (ft)
SBLOCA	160°F	-23.485	2.515	0.565
SBLOCA	260°F	-23.503	2.497	0.547
LBLOCA	212°F	-23.115	2.885	0.935
LBLOCA	260°F	-23.144	2.856	0.906

Seabrook Sump Temperature

Minimum water levels were determined at 260°F (maximum temperature), 212°F (design temperature), and 160°F (long-term temperature).

Strainer head loss testing was performed at approximately 120°F. NPSH margin was determined at 211.27°F and 117.6°F. Justification for the use of these temperatures is provided in the response to Section 3.g.14.

3.g.2 Describe the assumptions used in the calculations for the above parameters and the sources/bases of the assumptions.

Response to 3.g.2:

Seabrook Pump and Sump Flow Rates

A hydraulic model was constructed in Proto-Flo for the ECCS and CBS systems to analyze the NPSH margin and the system flows. The following assumptions were made in association with flow rates used to calculate the NPSH margin:

1. Spray header frictional and fitting losses were conservatively ignored for model simplification. This results in slightly lower system resistance and higher CBS pump flow rates.
2. Several globe/needle valves are partially throttled and locked in position per notes on their respective drawings. Since the exact position of each valve is unknown, they were assumed to be fully open and modeled with the fully open valve flow coefficient, resulting in higher flow rates.

3. Minor losses due to small bore (1” and smaller) branch lines with no flow (e.g. drains, vents, pressure taps, etc.) were considered negligible, and thus, these lines were not included in the model. Minor losses from thermowells were also considered negligible and excluded from the model.
4. It was assumed that no cooling is provided by the CBS and RHR heat exchangers. This maximizes the volumetric flow rate of recirculation flow, since higher temperature water is less dense and has a lower viscosity.
5. It was assumed that during recirculation following an LBLOCA, the RCS is completely depressurized, causing RCS pressure to be equal to the containment pressure, thus maximizing flow through the system.

Seabrook Minimum Containment Water Level

The significant assumptions used in the water volume calculation are listed as follows.

1. The water volume calculation does not assume any steam generator tube plugging. This is acceptable as the volume of plugged steam generator tubes that do not drain during a surge line break is offset by reactor head voiding.
2. It is assumed that the refueling canal drains will not be blocked. As stated in the response to Section 3.e.1, a modification is planned to install a strainer on each drain, add a new drain line, and enlarge the existing drain line to four inches. While the drain lines are assumed to be unblocked, the total hold-up in the refueling canal and drain lines was calculated and accounted for.

Seabrook Sump Temperature

The following assumptions were made in association with sump temperature during the calculation of NPSH margin:

1. Fluid properties such as density and viscosity were assumed to be at the saturation temperature of water at the minimum allowable containment pressure of 14.6 psia (i.e., 211.27°F).
2. The water temperature of 120°F for strainer head loss testing is conservative since at lower temperatures, higher fluid viscosity and density would result in higher head losses and more compression of the debris bed.

3.g.3 Provide the basis for the required NPSH values, e.g., 3 percent head drop or other criterion.

Response to 3.g.3:

The basis for the NPSH required (NPSHr) values used in calculating NPSH margin is the information provided from the original manufacturer's certified pump test curves at the flow rates predicted by the hydraulic model. The NPSHr curve is based on actual NPSH test results.

3.g.4 Describe how friction and other flow losses are accounted for.

Response to 3.g.4:

The hydraulic model, created using the safety-related Proto-Flo software, includes nominal RHR, SI, CCP, and CBS pump performance curves, industry standard system frictional and form losses, and vendor specific inputs (e.g., valve Cv and heat exchanger pressure drop). Steady-state boundary (operating) conditions were selected such that minimum NPSH margin would result. The hydraulic model accounted for all frictional and flow losses of the systems except the strainer head loss. The strainer head loss was subtracted from the NPSH margin calculated by the model in a hand calculation. The response to Section 3.f has the details on the evaluation of the strainer head losses.

3.g.5 Describe the system response scenarios for LBLOCA and SBLOCAs.

Response to 3.g.5:

See the response to Section 3.g.1.

3.g.6 Describe the operational status for each ECCS and CSS pump before and after the initiation of recirculation.

Response to 3.g.6:

<u>Pump Operational Status</u>

Prior to the initiating event, the ECCS and CBS pumps will be in a state of stand-by readiness. One CCP is operated during normal CVCS operations and will be automatically aligned for cold leg injection upon receipt of a safety injection signal.

Injection Phase

During the injection phase of ECCS operation, no manual actions are required, and all equipment is designed to operate automatically. Upon receipt of a safety injection signal, the RHR pumps, CCPs and SI pumps start automatically. The CBS pumps are initiated by high containment pressure. The RWST provides a suction source for the RHR pumps, CCPs, SI pumps, and CBS pumps operating in injection mode. The switchover from injection mode to recirculation mode occurs when two of the four RWST Lo-Lo level setpoints are reached in conjunction with a safety injection signal.

Switchover to Cold Leg Recirculation

The change from the injection phase to the recirculation phase is initiated automatically and completed by operator action. An RWST Lo-Lo level signal in conjunction with a safety injection signal shifts the ECCS from the injection phase to the recirculation phase of emergency core cooling. The containment recirculation valves automatically open and align to the RHR and CBS pump suctions. The RHR and CBS pumps continue to operate during the switchover. The RHR and CBS pumps take suction from both the containment sump and RWST until manual isolation of the RWST is performed once each sump isolation valve has reached the full open position.

The CCPs and SI pumps continue to take suction from the RWST until operator action is taken to align these pumps to take suction from the RHR pump discharge.

3.g.7 Describe the single failure assumptions relevant to pump operation and sump performance.

Response to 3.g.7:

The Train A RHR and CBS pumps, both take suction from a common sump, while the Train B RHR and CBS pumps take suction from a separate common sump during cold or hot leg recirculation. Both RHR pumps discharge to a common hydraulic network. Therefore, a maximum Train A RHR and CBS pump flow (the greatest challenge to required NPSH) occurs when the Train B RHR pump is inoperable. Therefore, for NPSH analysis, the limiting single failure is the failure of the opposite train RHR pump. All other ECCS pumps (SI pumps and CCPs) and valves are assumed operable to maximize the flow through the operating RHR pumpThis . also increases the head loss on the portion of the suction line shared by the RHR and CBS pumps.

Refer to the response to Section 3.n.1 for the single failure considered in the in-vessel downstream effects analysis.

3.g.8 Describe how the containment sump water level is determined.

Response to 3.g.8:

The water volume calculation used the methodology described below to calculate the minimum containment sump water level:

1. A correlation was first established for the relationship between the containment water level and the water volume at the -26'-0" elevation.
2. The quantity of water added to containment from the RWST, accumulators, spray additive tank (SAT), and RCS volume above the break elevation was calculated.
3. The quantity of water that is diverted from the containment sump by the following effects was evaluated:
   - Water held up in the RCS.
   - Water held up in the reactor cavity.
   - Water held up on containment surfaces due to condensation.
   - Water held up as steam in the containment atmosphere.
   - Water held up as containment spray droplets.
   - Water required to fill up the containment building spray piping.
   - Water held up in the refueling canal and drain lines.
4. Given the net mass of water added to the containment floor based on Items 2 and 3 listed above, the post-LOCA containment water level was calculated using the correlation established in Item 1.

The calculation determined bounding minimum containment water levels for LBLOCA and SBLOCA using break size-specific injection volumes and holdup volumes.

3.g.9 Provide assumptions that are included in the analysis to ensure a minimum (conservative) water level in determining NPSH margin.

Response to 3.g.9:

To minimize the sump pool water level and volume of water added to the pool, the minimum volumes from the following sources were used: RWST, accumulators, and spray additive tank (see the response to Section 3.g.12). Additionally, various hold-up volumes that divert water away from the pool were considered (see the response to Section 3.g.8). The inputs for calculating the hold-up volumes are biased to increase the volumes. For example, the maximum containment free volume was used when calculating steam hold-up, and was not reduced for the sump pool.

3.g.10 Describe whether and how the following volumes have been accounted for in pool level calculations: empty spray pipe, water droplets, condensation, and holdup on horizontal and vertical surfaces. If any are not accounted for, explain why.

Response to 3.g.10:

As described in the response to Section 3.g.8, the following volumes were accounted for within the water volume calculation as hold-up volumes that remove water from the containment pool:

1. Water required to fill the containment building spray piping
2. Water droplets in transit from the containment spray nozzles
3. Water hold-up on containment surfaces due to condensation
4. Steam hold-up in the containment atmosphere

3.g.11 Provide assumptions (and their bases) as to what equipment will displace water resulting in higher pool level.

Response to 3.g.11:

The pieces of equipment and supports credited when evaluating the sump pool water level are summarized below:

1. Pads for pressure relief tanks, excess letdown heat exchanger, reactor coolant drain tanks and reactor coolant drain tank heat exchangers
2. Supports for the steam generators, reactor coolant pumps, and cross-over legs
3. In-core instrumentation hatches
4. Concrete walls, concrete columns, and secondary shield wall
5. Sump strainer and debris interceptors

The dimensions of the equipment and supports from plant design drawings were used to calculate their cross-sectional areas. No assumptions were made.

Displacement of water by the sloped containment floor at the -26 ft elevation was credited. For drainage, the containment floor has a 4-inch slope from the high point at the containment liner (at Elevation -25.67 ft) to the containment trench in the annulus area (at Elevation -26 ft). There is a similar slope from the high point at the primary shield wall (at Elevation -25.67 ft) to the trench. The displacement of water by the sloped floor was considered when calculating the water level and was conservatively evaluated by biasing the inputs to reduce the credited volume.

3.g.12 Provide assumptions (and their bases) as to what water sources provide pool volume and how much volume is from each source.

Response to 3.g.12:

The following design inputs provided the basis for water sources and their volumes to determine the minimum containment water level:

1. The RWST minimum deliverable volume is 350,000 gal.
2. Each of four SI accumulators has a minimum water volume of 6,121 gal (24,484 gal total).
3. The minimum mass of water provided by the SAT is 72,200 lbm (equivalent to 8,690 gal at 85°F).
4. The mass of water provided by the RCS for an LBLOCA is 29,742 lbm (equivalent to 3,802 gal) at 260°F.

3.g.13 If credit is taken for containment accident pressure in determining available NPSH, provide description of the calculation of containment accident pressure used in determining the available NPSH.

Response to 3.g.13:

No credit was taken for containment accident pressure when evaluating NPSH at Seabrook. See the response to Section 3.g.14.

3.g.14 Provide assumptions made which minimize the containment accident pressure and maximize the sump water temperature.

Response to 3.g.14:

<u>Seabrook Containment Accident Pressure</u>

Containment accident pressure was not credited in determining available NPSH. The TS minimum containment pressure is 14.6 psia. The temperature at which the vapor pressure of water is equal to the minimum containment pressure is 211.27°F. For sump temperatures at or above 211.27°F, the containment pressure is assumed to be equal to the water vapor pressure at the corresponding sump temperature. For sump temperatures below 211.27°F, the containment pressure is assumed to be the TS minimum allowable containment pressure of 14.6 psia. This approach did not credit any containment accident pressure, conservatively neglecting the pre-accident air partial pressure and the increase in the air partial pressure due to heat up of the containment atmosphere following the accident.

<u>Seabrook Sump Temperature</u>

As indicated in the response to Section 3.g.1, pump NPSH margin was evaluated at sump temperatures of 211.27°F (the saturation temperature at the minimum TS containment pressure of 14.6 psia) and 117.6°F (the highest temperature that chemical precipitation could occur inside containment; see the response to Section 3.o.2.7.ii).

As will be shown in the response to Section 3.g.16, the minimum pump NPSH margins occur at 211.27°F due to the conservative containment pressure assumed in the analysis, as discussed above.

1. For sump temperatures at or above 211.27°F, the containment pressure was assumed to be equal to the vapor pressure at the corresponding sump temperature. As a result, the containment pressure and vapor pressure cancel out and the NPSH margin depends primarily on the strainer head loss, which is the highest at the lower end of this temperature range (211.27°F).
2. For sump temperatures below 211.27°F, the containment pressure was assumed to stay at 14.6 psia. However, water vapor pressure is now lower than 14.6 psia. The difference between the two results in greater pump NPSH margin, compared with that evaluated at 211.27°F. This is demonstrated by the much higher NPSH margins at 117.6°F.

The NPSH available (NPSHa) at 211.27°F was calculated in the Proto-Flo model by combining the containment pressure and elevation difference between the minimum sump water level and pump suction before subtracting the total flow head loss inside the piping between the strainer and pump suction and vapor pressure at 211.27°F. The NPSHr was determined in the Proto-Flo model by linearly interpolating the vendor curve based on pump flow rate. The NPSH margin is calculated as the difference between NPSHa and NPSHr. The strainer head loss, which includes CSHL and conventional debris head loss, was then subtracted from the NPSH margin in a hand calculation. Refer to the response to Section 3.f.10 for details on the strainer head loss.

The pump NPSH margin was also determined at a sump temperature of 117.6°F, when chemical precipitation is predicted to occur. At this temperature, the vapor pressure is less than the containment pressure of 14.6 psia, and the difference between the two increases the pump NPSHa and NPSH margin. For the analysis at 117.6°F, the strainer head loss used includes CSHL and debris head loss with contribution from both the conventional and chemical precipitation debris.

3.g.15 Specify whether the containment accident pressure is set at the vapor pressure corresponding to the sump liquid temperature.

Response to 3.g.15:

As discussed in the response to Section 3.g.14, for sump temperatures at or above 211.17°F, the containment pressure was set equal to the vapor pressure at the corresponding sump temperature. For sump temperatures below 211.27°F, the containment pressure was set at the TS minimum allowable containment pressure of 14.6 psia.

3.g.16 Provide the NPSH margin results for pumps taking suction from the sump in recirculation mode.

Response to 3.g.16:

Table 3.g.16-1 shows the minimum NPSH margins for the RHR and CBS pumps in recirculation mode. The most limiting NPSH margin occurs for the Train A CBS pump at a sump temperature of 211.27°F. The case presented in the table has the single failure of the Train B RHR pump, as described in the response to Section 3.g.7. These NPSH values are based on the minimum water level of a pressurizer surge line break and the maximum strainer head loss of the worst break.

Table 3.g.16-1: RHR and CBS Pumps NPSH Margin at 211.27°F

	Train A RHR Pump	Train A CBS Pump
Total Sump Flow Rate (gpm)	7907	
Pump Flow Rate (gpm)	4580	3327
NPSH Margin before Considering Strainer Head Loss (ft)	8.98	5.98
NPSH Margin after Considering Strainer Head Loss (ft)	6.686	3.676

Table 3.g.16-2 shows the pump NPSH margins calculated at 117.6°F. The strainer head loss at this temperature is 5.042 ft (see Table 3.f.10-1), which includes CSHL and head loss contribution from conventional and chemical debris. As stated in the response to Section 3.g.15, for sump temperatures below 211.27°F, the containment pressure was set at the TS minimum allowable containment pressure of 14.6 psia. The difference between this containment pressure (14.6 psia) and vapor pressure at lower temperature increases the NPSHa and NPSH margin. At 117.6°F, the resulting NPSH margins are over 30 ft.

Table 3.g.16-2: RHR and CBS Pumps NPSH Margin at 117.6°F

	Train A RHR Pump	Train A CBS Pump
Total Sump A Flow Rate (gpm)	7907	
Pump Flow Rate (gpm)	4580	3327
NPSH Margin after Considering Strainer Head Loss (ft)	35.1	32.1

As shown in Table 3.g.16-1, the minimum NPSH margin is positive. Therefore, adequate NPSH margin is available for the Seabrook ECCS and CBS pumps to ensure their design functions after a LOCA. Note that there is no void fraction impact on NPSH margin, as discussed in the response to Section 3.f.14.

3.h Coatings Evaluation

The objective of the coatings evaluation section is to determine the plant-specific ZOI and debris characteristics for coatings for use in determining the eventual contribution of coatings to overall head loss at the sump screen.

3.h.1 Provide a summary of type(s) of coating systems used in containment, e.g., Carboline CZ 11 Inorganic Zinc primer, Ameron 90 epoxy finish coat.

Response to 3.h.1:

Qualified Coatings

The types of qualified coating systems used in containment are presented in Table 3.h.1-1. As shown in the table, Seabrook qualified coatings are broken into two categories according to whether the coating is on a Westinghouse component or support.

The qualified coatings on the following Westinghouse equipment were conservatively treated as unqualified coatings in the previous submittal (Reference 2), but justification has since been made for their treatment as qualified coatings.

1. Reactor coolant pump (RCP) and SG support legs, and crossover leg supports (coated with Ameron Dimetcote 6 IOZ Silicate)
2. Accumulators, RCP motors, RCP motor supports, and RCP motor air coolers (coated with Ameron Dimetcote E-Z II IOZ primer and Ameron Dimetcote 66 epoxy topcoat)

Westinghouse Technical Bulletin 06-15 identified that coatings applied to Westinghouse supplied equipment may not be fully qualified to ANSI N.101.2 requirements. To respond to this Technical Bulletin, Seabrook personnel obtained qualification reports for Westinghouse IOZ coating systems, performed ANSI N.101.2 qualification testing on Westinghouse coatings with a zinc primer and epoxy topcoat, and concluded that the 10.0D ZOI in the NEI 04-07 SER should be used.

Seabrook personnel also reviewed the procurement and application requirements for the coatings to be used for the Westinghouse supplied components and any repairs to be made to the coatings on these components. The review showed that the performance standard for original coating application and coating repairs is in accordance with Westinghouse Process Specification 597755, which requires Service Level 1 coatings to be applied per the requirements of ANSI N.101.2-1972 and ANSI N.5.12-1974. Adherence to these standards ensures that the coating systems have been qualified for nuclear service and have been applied on a correctly prepared substrate by qualified personnel. Additionally, quality control inspections are performed per the ANSI requirements and coating system manufacturer's requirements.

The qualified coatings on steel and concrete surfaces other than the specified Westinghouse components are also included in Table 3.h.1-1.

Table 3.h.1-1: Seabrook Qualified Coatings Systems Used in Debris Generation Analyses

Substrate		Layer	Type	DFT (mil)	Density (lbm/ft³)
Westinghouse Equipment and Support	RCP and SG support legs, crossover support legs	1st Coat	Ameron Dimetcote 6 IOZ Silicate	12	208
	Accumulators, RCP motors, RCP motor supports and RCP motor air coolers	1st Coat	Ameron Dimetcote E-Z II IOZ Primer	6	208
		2nd Coat	Ameron Dimetcote 66 Epoxy	9	94
			Total	15	--
Other	Steel Surfaces	1st Coat	Keeler and Long (K&L) #6548 - Epoxy	8	141
		2nd Coat	K&L #D-1 / K&L E-1 – Epoxy	6	111
			Total	14	--
	Concrete Surfaces	1st Coat	K&L #4000 – Epoxy Primer/Surfacer	50	116
		2nd Coat	K&L #D-1 – Epoxy	6	111
			Total	56	--

Unqualified Coatings

Unqualified coatings are those that fail under design basis accident conditions and create debris that could be transported to the containment recirculation strainers. Unqualified coatings are applied over numerous substrates within containment. The quantity and properties of these unqualified coatings at Seabrook are shown in Table 3.h.1-2.

Table 3.h.1-2: Seabrook Unqualified Coatings Properties and Quantities Used in Debris Generation Analyses

Coating Type	Volume (ft^3)	Density (lb/ft^3)	Characteristic Size (µm)
Unqualified Epoxy	4.92	94	10
Unqualified IOZ	4.61	208	10

3.h.2 Describe and provide bases for assumptions made in post-LOCA paint debris transport analysis.

Response to 3.h.2:

The following assumptions related to coatings were made in the debris transport analysis performed for Seabrook:

1. It was conservatively assumed that all unqualified coatings are located in lower containment. This is conservative since it results in 100% of unqualified coatings being present in the pool at the start of recirculation.
2. It was assumed that no settling of particulate debris (insulation, dirt/dust, and coatings) occurs in the debris transport analysis.
3. It was assumed that the unqualified coatings debris would be uniformly distributed in the recirculation pool. This is a reasonable assumption since these coatings are scattered around containment in small quantities.
4. Unqualified coatings were assumed to fail after pool fill-up has occurred and therefore none of the unqualified coatings would transport to inactive cavities during pool fill-up. Together with the first assumption listed, this results in 100% transport of the unqualified coatings.

3.h.3 Discuss suction strainer head loss testing performed as it relates to both qualified and unqualified coatings. Identify surrogate material and what surrogate material was used to simulate coatings debris.

Response to 3.h.3:

Agsco 325 silica flour was used as a surrogate for the qualified and unqualified coatings for head loss testing. Agsco 325 silica flour has a density of 2.65 g/cm^3 (165.4 lbm/ft^3) and a particle size between 5 µm and 40 µm. See the response to Section 3.f.4 for additional discussion on treatment of coatings in head loss testing.

3.h.4 Provide bases for the choice of surrogates.

Response to 3.h.4:

See the response to Section 3.f.4.

3.h.5 Describe and provide bases for coatings debris generation assumptions. For example, describe how the quantity of paint debris was determined based on ZOI size for qualified and unqualified coatings.

Response to 3.h.5:

The following assumptions related to coatings were made in the debris generation calculation:

1. The debris size distribution for qualified coatings are not well known, and were therefore assumed to be 100% 10 μm particulate as recommended by the Guidance Report (Reference 18 pp. 3-30).
2. The size and density of all epoxy unqualified coatings were assumed to be 10 μm and 94 lb/ft^3, as recommended by NEI 04-07. All unqualified IOZ was assumed to have a particulate size of 10 μm and a density of 208 lb/ft^3. This density corresponds to Carbozinc 11 – a typical IOZ used in nuclear power plants.
3. It was assumed that the accumulators, RCP motors, RCP motor supports, and RCP motor air coolers (all Westinghouse equipment) have a total coating thickness of 15 mil, which consists of an IOZ primer and epoxy topcoat. Based on the Carbozinc 11 application recommendations, it was assumed that this is split into 6 mil IOZ and 9 mil epoxy. The densities of the IOZ primer and epoxy topcoat are assumed to be 208 lbm/ft^3 and 94 lbm/ft^3, respectively.

The unqualified coatings in containment were quantified based on detailed logs that are regularly updated, and the resulting quantities are shown in Table 3.h.1-2. The quantities apply to all breaks, regardless of size or location.

Different methodologies were used to determine the generated quantity of qualified coatings on specific Westinghouse equipment and non-Westinghouse substrates (e.g., steel and concrete surfaces).

<u>Analysis of Qualified Coatings on Westinghouse Equipment and Support</u>

The qualified coatings on the Westinghouse equipment that could become debris was analyzed in a hand calculation using the 10.0D ZOI. As discussed in the response to Section 3.h.1, the qualified coatings on the RCP, RCP motors, motor supports and motor air coolers, SG support legs, and crossover leg supports are of concern. The total volume of qualified coatings on these Westinghouse components and supports were first determined using the surface area of the components, taken from the Seabrook CAD model, and the coating dry-film thicknesses (DFTs).

To determine the amount of debris that could be generated from these coatings, a 10.0D ZOI for various break sizes and locations on the RCS loops was overlaid on a plan view drawing of the containment. It was then determined what equipment was within the ZOI, and the qualified coatings quantity for the enveloped equipment was quantified. Since the accumulators are outside of the bioshield wall, they are not affected by breaks inside the bioshield.

This approach is demonstrated in Figure 3.h.5-1 and Figure 3.h.5-2 for 27.5” to 31” DEGBs. Figure 3.h.5-1 shows representative 10.0D ZOIs for 29” and 31” DEGBs as red and gold circles, respectively. The 29” ZOI is centered on the hot leg, and the 31” ZOI is centered on the crossover leg. As shown in the figure, the worst-case break locations would destroy the coatings on one RCS loop plus a fraction of the coatings on the SG and crossover leg supports of the adjacent loop. Figure 3.h.5-2 shows the ZOIs of another 31” DEGB centered on the opposite end of the crossover leg and a 27.5” DEGB centered on the cold leg. It shows that these ZOIs could impact coatings on one RCS loop but would not impact coatings on the adjacent loops. Based on these two figures, it is conservatively estimated that, for the 27.5” to 31” breaks, the generated debris would include Westinghouse qualified coatings from one RCP motor/ motor support/ air cooler and coatings on the RCP/ SG /crossover leg supports of one whole loop and half of another loop.

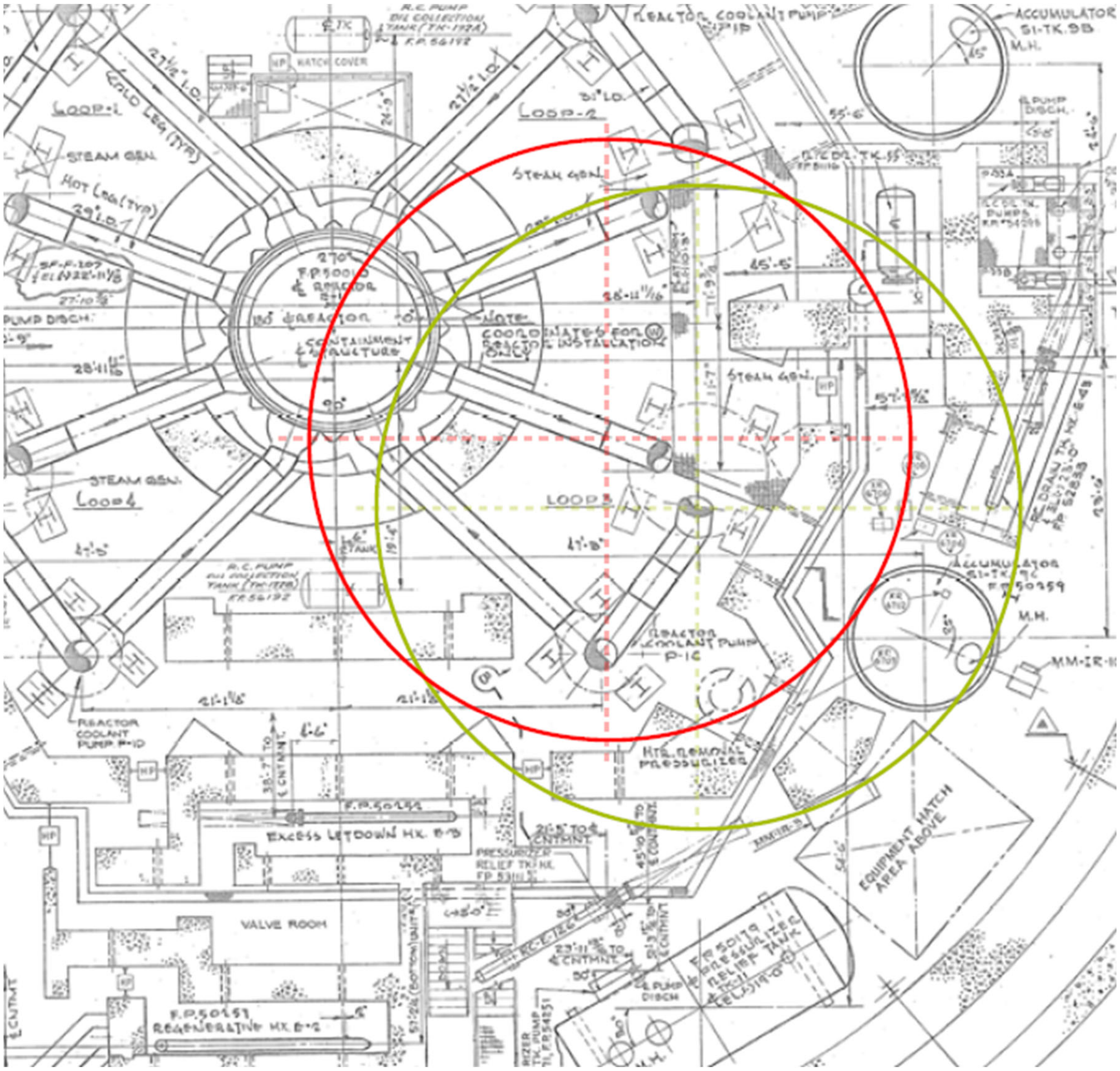

Figure 3.h.5-1: Westinghouse Qualified Coatings ZOI Evaluation for 29" (red) and 31" (gold) DEGBs

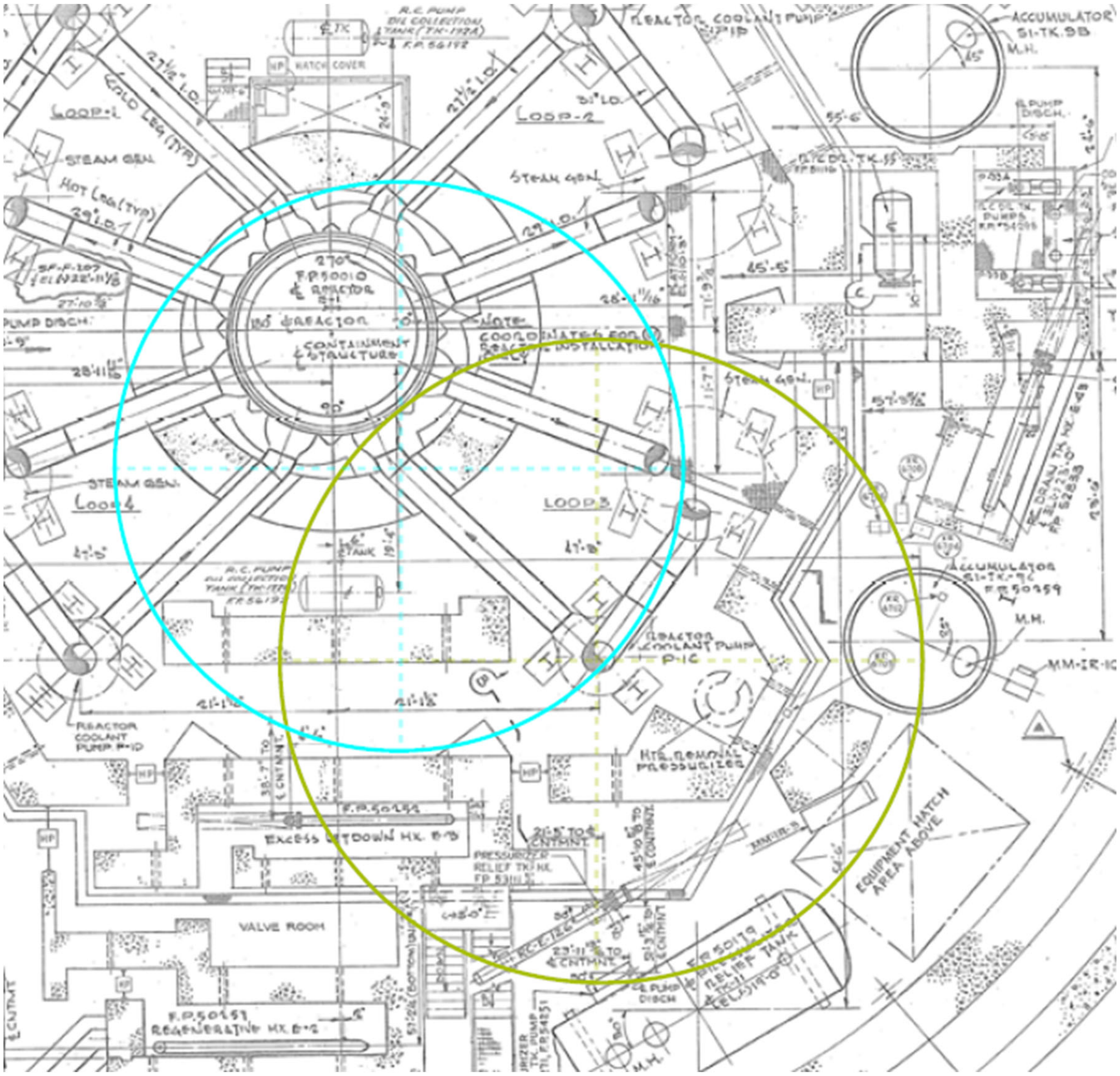

Figure 3.h.5-2: Westinghouse Qualified Coatings ZOI Evaluation for 27.5" (blue) and 31" (gold) DEGBs

A similar approach was used to determine the generated quantities of qualified coatings on Westinghouse equipment and supports for smaller DEGBs and partial breaks. As discussed in the response to Section 3.b.1, the ZOI for partial breaks is represented by hemispheres of eight different orientations. In the figures below, the ZOI for each partial break is shown as a full circle to help visualize the hemispherical ZOIs of different orientations. Shading is used to demonstrate a worst-case ZOI orientation for generation of qualified coatings on Westinghouse equipment. Note that the ZOI orientations considered for the Westinghouse coatings were conservatively selected to maximize coatings generation and were not limited to the standard orientations considered for other partial breaks.

Figure 3.h.5-3 shows that for breaks of 14” and smaller can be conservatively estimated to include coatings on one RCP motor/motor support/air cooler and 75% of coatings on the RCP/SG/crossover leg supports of one loop.

Figure 3.h.5-4 shows that 17” and 20” breaks can be conservatively estimated to include coatings on one RCP motor/motor support/air cooler and coatings on the RCP/SG/crossover leg supports of one loop.

Figure 3.h.5-5 shows that 23” and 26” breaks can be conservatively estimated to include coatings on one RCP motor/motor support/air cooler and coatings on the RCP/SG/crossover leg supports of one whole loop and 25% of another loop.

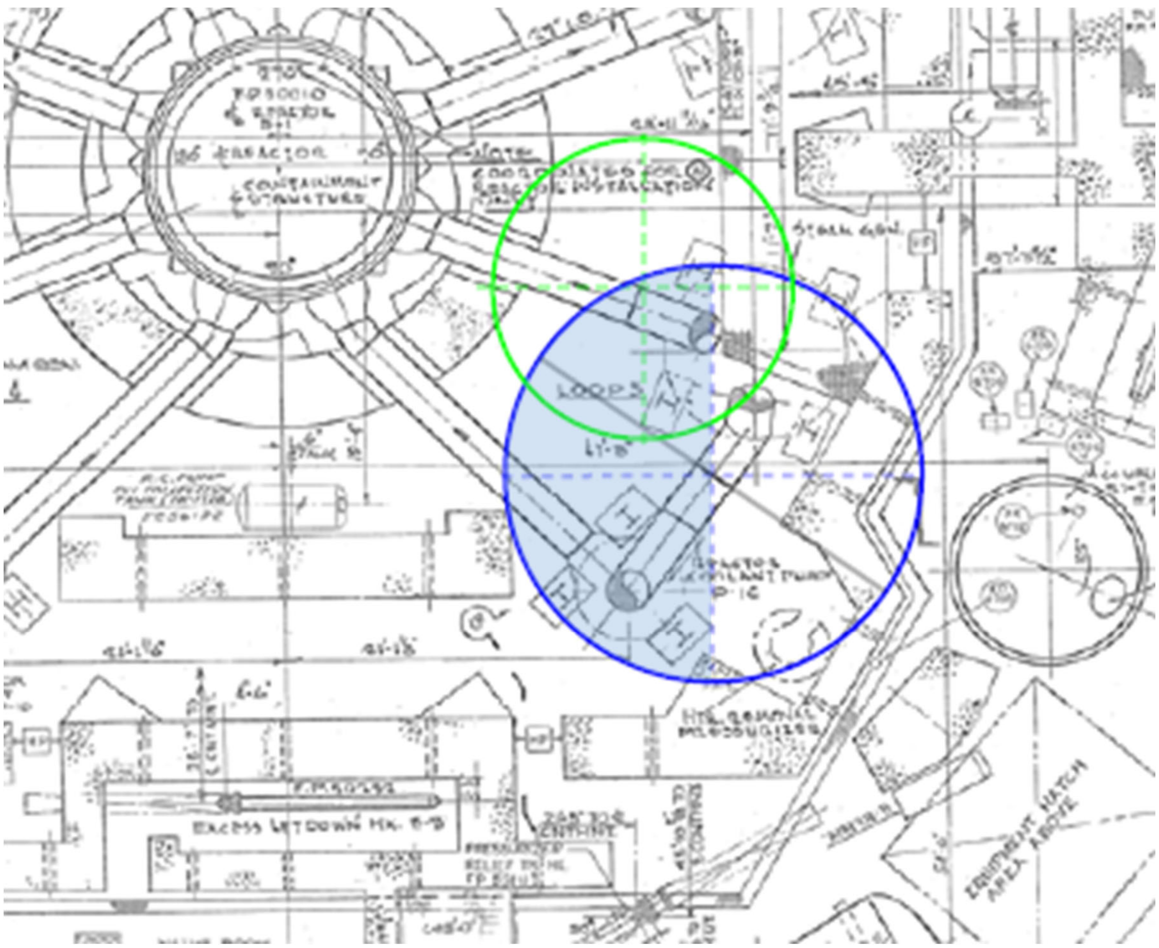

Figure 3.h.5-3: Break ZOI for 11.188” DEGB (green) and 14” Partial Break (blue)

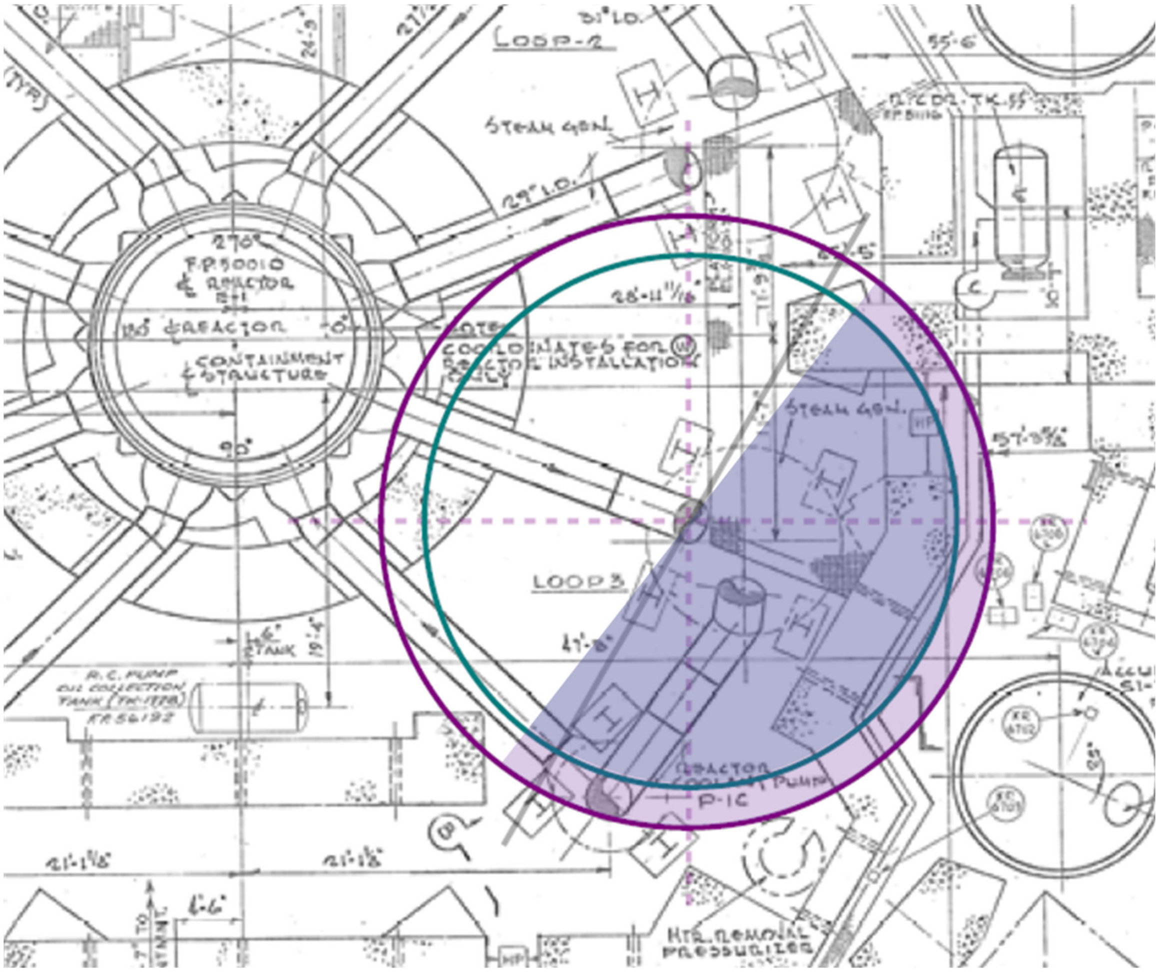

Figure 3.h.5-4: Break ZOI for 17" (teal) and 20" (purple) Partial Breaks

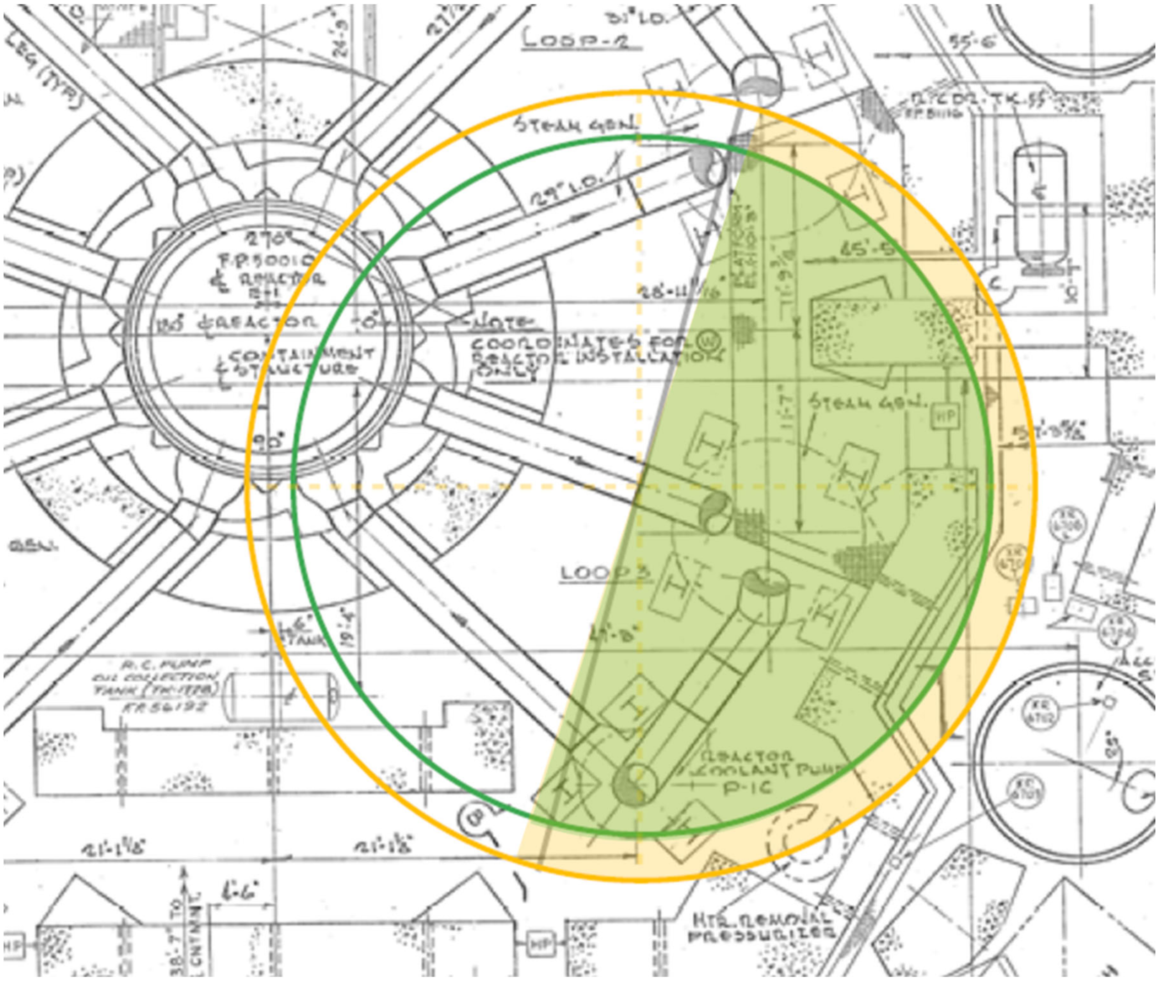

Figure 3.h.5-5: Break ZOI for 23” (green) and 26” (yellow) Partial Breaks

Table 3.h.5-1 summarizes the generated debris quantities from the qualified coatings on the Westinghouse equipment and supports for different break sizes.

Table 3.h.5-1: Summary of Debris Generated for Qualified Coatings on Westinghouse Equipment and Supports

Break Size	IOZ (ft^3)	Epoxy (ft^3)	Total (ft^3)
<=14”	2.71	0.53	3.24
17” – 20”	2.82	0.71	3.53
23” – 26”	2.94	0.89	3.83
27.5” – 31”	3.06	1.06	4.12

Analysis of Non-Westinghouse Qualified Coatings

Qualified coatings on substrates other than the specified Westinghouse components and supports were analyzed in BADGER using a 4.0D ZOI.

For reactor nozzle breaks, the ANSI 58.2-1988 jet model methodology was implemented to evaluate the ZOI length of a nozzle break subjected to partial separation of the two pipe ends. See the response to Section 3.b.1 for additional information.

The generated quantities of qualified coatings (not on the Westinghouse components and supports) for the four worst-case DEGBs are shown in Table 3.b.4-1.

3.h.6 Describe what debris characteristics were assumed, i.e., chips, particulate, size distribution and provide bases for the assumptions.

Response to 3.h.6:

In accordance with the guidance provided in NEI 04-07 (Reference 18 pp. 3-12, 3-13) and the associated NRC SE (Reference 19 p. 22), all coating debris was treated as 10-micron particulate. See the Responses to 3.h.1, 3.h.2, and 3.h.5 for additional debris characteristics description.

3.h.7 Describe any ongoing containment coating conditions assessment program.

Response to 3.h.7:

The current program for controlling the quantity of unqualified/ degraded coatings includes two separate inspections by qualified personnel during each refueling outage, and notification of plant management prior to restart if the volume of unqualified/ degraded coatings approaches pre-established limits.

The first inspection takes place at the beginning of every refueling outage, when areas and components from which peeling coatings have the potential for falling into the reactor cavity are inspected by the NextEra coating supervisor and NextEra design engineering coating specialist. The second inspection takes place at the end of every refueling outage when the condition of containment coatings is assessed by a team using guidance from EPRI. Accessible coated areas of the containment and equipment are included in the second inspection. Plant management is notified prior to restart if the volume of unqualified/ degraded coatings approaches pre-established limits.

The initial coating inspection process is a visual inspection. The acceptability of visual inspection as the first step in monitoring of containment building coatings is validated by EPRI. Following identification of degraded coatings, the degraded coatings are repaired per procedure if required. For degraded coatings that are not repaired, areas of coatings determined to have inadequate adhesion are removed, and the nuclear coatings specialist assesses the remaining coating to determine if it is acceptable for use. The assessment is by means of additional nondestructive and destructive examinations as appropriate (Reference 21 p. 25).

3.i Debris Source Term

The objective of the debris source term section is to identify any significant design and operational measures taken to control or reduce the plant debris source term to prevent potential adverse effects on the ECCS and CSS recirculation functions.

Provide the information requested in GL 2004-02 Requested Information Item 2(f) regarding programmatic controls taken to limit debris sources in containment.

> *GL 2004-02 Requested Information Item 2(f)*
> *A description of the existing or planned programmatic controls that will ensure that potential sources of debris introduced into containment (e.g., insulations, signs, coatings, and foreign materials) will be assessed for potential adverse effects on the ECCS and CSS recirculation functions. Addressees may reference their responses to GL 98-04, "Potential for Degradation of the Emergency Core Cooling System and the Containment Spray System after a Loss-of-Coolant Accident Because of Construction and Protective Coating Deficiencies and Foreign Material in Containment," to the extent that their responses address these specific foreign material control issues.*

In responding to GL2004-02 Requested Information Item 2(f), provide the following:

3.i.1 A summary of the containment housekeeping programmatic controls in place to control or reduce the latent debris burden. Specifically for RMI/low-fiber plants, provide a description of programmatic controls to maintain the latent debris fiber source term into the future to ensure assumptions and conclusions regarding inability to form a thin bed of fibrous debris remain valid.

Response to 3.i.1:

NextEra has procedural controls in place for Seabrook to reduce and control the amount of loose debris and fibrous materials in containment. The Containment and Containment Spray Recirculation Sump Surveillance procedure requires inspection of all accessible areas to verify that no loose debris, fibrous materials that could degrade into loose debris, or bubbling/chipping paint is present prior to setting containment integrity.

The maintenance director has been placed in charge of maintaining the general housekeeping of containment which includes tracking the overall cleanliness of containment and promptly correcting identified deficiencies.

3.i.2 A summary of the foreign material exclusion programmatic controls in place to control the introduction of foreign material into the containment.

Response to 3.i.2:

Foreign material exclusion programmatic controls are in place at Seabrook. This ensures that proper work control is specified for debris-generating activities within the containment building in order to prevent introduction of foreign material into the containment sump or strainers. Additionally, the foreign material exclusion program requires that engineering be consulted anytime foreign material covers are placed or modifications are performed on the containment sump strainers.

Furthermore, the containment entry procedure provides additional controls to evaluate foreign materials to be brought into containment and ensure they are removed. The procedure requires tracking of all non-bulk items brought into containment. Procedural controls are also in place to evaluate aluminum or zinc prior to being taken into containment.

3.i.3 A description of how permanent plant changes inside containment are programmatically controlled so as to not change the analytical assumptions and numerical inputs of the licensee analyses supporting the conclusion that the reactor plant remains in compliance with 10 CFR 50.46 and related regulatory requirements.

Response to 3.i.3:

NextEra engineering change processes and procedures ensure that temporary or permanent modifications that may affect the ECCS, including sump performance, are evaluated for GL 2004-02 compliance. During engineering change preparation, the process requires affected critical attributes to be listed, evaluated, and documented when affected. This includes the introduction of materials into containment that could affect sump performance or lead to equipment degradation. It also includes repair, replacement, and installation of coatings inside containment, including installing coated equipment.

NextEra implemented the industry's standard design change process including the industry procedure IP-ENG-001. The standard process and tools are intended to facilitate sharing of information, solutions, and design changes throughout the industry. This process requires activities that affect UFSAR described SSC design functions to be evaluated as a design change in accordance with NextEra's 10 CFR 50 Appendix B program. This includes modifications that would impact the containment sump. Design changes require a final impact review meeting (i.e., final design workshop) and assessment in accordance with 10 CFR 50.59. Additional meetings may be required based on complexity and risk of the change. A failure modes and effects analysis is required if the design change introduces any new failure modes or changes failure modes for the affected SSCs.

3.i.4 A description of how maintenance activities including associated temporary changes are assessed and managed in accordance with the Maintenance Rule, 10 CFR 50.65.

Response to 3.i.4:

Seabrook maintenance activities (including temporary changes or temporary system alterations) are controlled by plant procedure, including having all temporary modifications developed though the plant modification procedure. This process maintains configuration control for non-permanent changes to plant systems, structures, and components while ensuring the applicable technical reviews and administrative reviews and approvals are obtained. The risk associated with temporary modifications is assessed and managed per the Maintenance Rule 10 CFR50.65(a)(4). If, during at-power operation conditions, the temporary alteration associated with maintenance is expected to be in effect for greater than 90 days, the temporary alteration is subject to the requirements of 10 CFR 50.59 prior to implementation.

NextEra has established a procedure for identifying, planning and executing critical online maintenance activities. Implementation of the methodology ensures all aspects for the development and successful completion of a critical maintenance work window are identified, and organizational ownership and accountabilities are assigned. The methodology is designed to align a station's resources to effectively assess the risk associated with on-line critical maintenance and to plan and execute the work in a safe and efficient manner.

NextEra has also established a procedure to identify, evaluate and appropriately manage the overall risk associated with online and outage work activities. All high-risk work has a risk management plan developed which provides a format to break down an activity into component steps, for which risks must be assessed and managed. NextEra uses a graded approach for scheduling to ensure accountability and ownership of the schedule. An online schedule tool is used to implement site maintenance and testing activities. The schedule reflects activities that have an impact on site operation and maintenance resources. When time-critical support is required for risk significant activities, the activities will be placed on the schedule and logically tied to ensure timely completion.

3.i.5 If any of the following suggested design and operational refinements given in the guidance report (guidance report, Section 5) and SE (SE, Section 5.1) were used, summarize the application of the refinements.

a. Recent or planned insulation change-outs in the containment which will reduce the debris burden at the sump strainers.

Response to 3.i.5.a:

There have not been any recent or planned insulation change-outs in containment to reduce the debris burden at the sump strainer.

b. Any actions taken to modify existing insulation (e.g., jacketing or banding) to reduce the debris burden at the sump strainer.

Response to 3.i.5.b:

There have not been any recent or planned insulation jacketing or banding modifications to reduce the debris burden at the sump strainer.

c. Modifications to equipment or systems conducted to reduce the debris burden at the sump strainers.

Response to 3.i.5.c:

Four types of debris interceptors are installed at Seabrook and are described in the response to Section 3.j.1. As shown in the response to Section 3.e.4, the debris interceptors are not credited for any debris retention. They provide a defense-in-depth measure for reducing the fiber that reaches the strainer. Debris within the bioshield pool would pass through four sets of annulus debris interceptors prior to reaching the strainers. Testing of prototypical debris interceptors at velocities expected during a LOCA showed effective retention of debris that was not readily suspended in the test water.

Additionally, accessible cable tray, raceway and node junction adhesive labels inside containment were removed to reduce the debris transported to the strainer.

d. Actions taken to modify or improve the containment coatings program.

Response to 3.i.5.d:

The programmatic controls related to coatings are provided in the response to Section 3.h.7.

3.j Screen Modification Package

The objective of the screen modification package section is to provide a basic description of the sump screen modification.

3.j.1 Provide a description of the major features of the sump screen design modification.

Response to 3.j.1:

The original sump screens were replaced with new strainer modules during outage OR12 (Spring 2008). The new strainers are passive (i.e., there are no active components and the strainers do not utilize backflushing).

The new strainer system uses the GE disk strainers. Each installed strainer has an unobstructed surface area of 2,445 ft^2. The strainer perforations are nominal 1/16-inch diameter round holes (0.0625-inch diameter openings). The strainer modules use an arrangement of parallel, rectangular strainer disks that have exterior debris capturing surfaces of perforated plate covered with woven wire mesh. The wire mesh decreases the head loss across the strainer plates by breaking up debris beds. Each strainer disk, constructed of two plates, has an open interior to channel disk flow downward to the strainer plenum. The disks are mounted on the discharge plenum, which channels disk flow to the suction piping. All strainers are fabricated from stainless steel.

Each strainer module interfaces with its associated ECCS inlet pipe. The ECCS inlet pipe is located inside a strainer “dog house” which is directly open to the strainer plenum. The “dog house” interface seals the “dog house” against the wall to preclude fibers passing into the ECCS lines. The roof of the “dog house” is equipped with cover plates similar to those used in the rest of the plenum.

The volume of debris at the screen is discussed in the response to Section 3.e. The capability to provide the required NPSH with the debris volume is discussed in the response to Section 3.g. The capability to structurally withstand the effects of the maximum debris volume is discussed in the response to Section 3.k.

Four types of debris interceptors are installed in the Seabrook containment. However, as discussed in the response to Section 3.e.4, the debris interceptors are no longer credited for debris holdup, although they do provide a defense-in-depth measure for reducing the amount of fiber that reaches the strainer. The debris interceptors are briefly described below for information.

<u>Bioshield Debris Interceptors</u>

Bioshield debris interceptors are installed in the passageways in the bioshield wall except for the eastern-most door. (This is to ensure that there is at least one unobstructed passageway for water from the break to the annulus). They are approximately 6-feet tall and have hinged gates (doors) where needed to allow for personnel and equipment access.

Annulus Debris Interceptors

Annulus debris interceptors are located radially around the containment building in the outer annulus area between the bioshield wall and the containment wall. The locations are shown in Figure 3.j.1-1. They have a hinged gate at each location to allow for personnel and equipment access. Most annulus debris interceptors also have an 18-inch wide horizontally oriented debris interceptor panel mounted on top.

Accumulator Skirt Debris Interceptors

Where an annulus debris interceptor adjoins the support structure for an accumulator (accumulator skirt), the skirt serves as part of the debris interceptor span. Debris interceptor panels are installed on the accumulator skirt openings.

Bioshield Scupper Debris Interceptors

Bioshield scupper debris interceptors have been installed on one end of 18 scuppers in the bioshield wall to prevent debris bypassing the annulus debris interceptors via the scuppers. The scuppers are small passageways (approximately 4-inches square) through the bioshield wall that allow water leaking inside the bioshield to pass through the wall to the floor drains located outside the bioshield. Installing debris interceptors on the scupper openings prevents potential fiber bypass around the annulus debris interceptors.

Figures 3.j.1-1 and 3.j.1-2 provide an overview of the strainer layout and configuration within containment. Figures 3.j.1-3 through 3.j.1-5 provide details on the strainer assembly and disk assemblies.

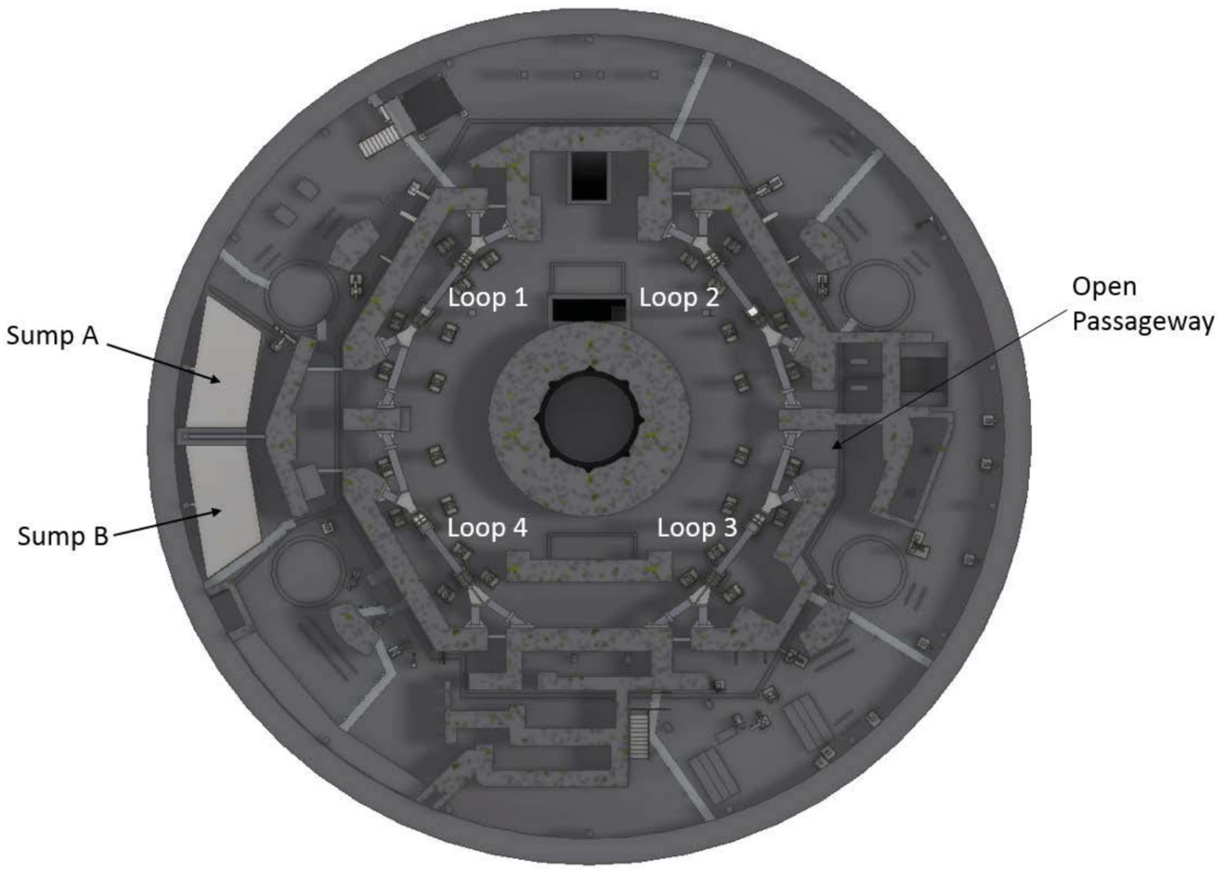

Figure 3.j.1-1: Plan View of Seabrook Lower Containment

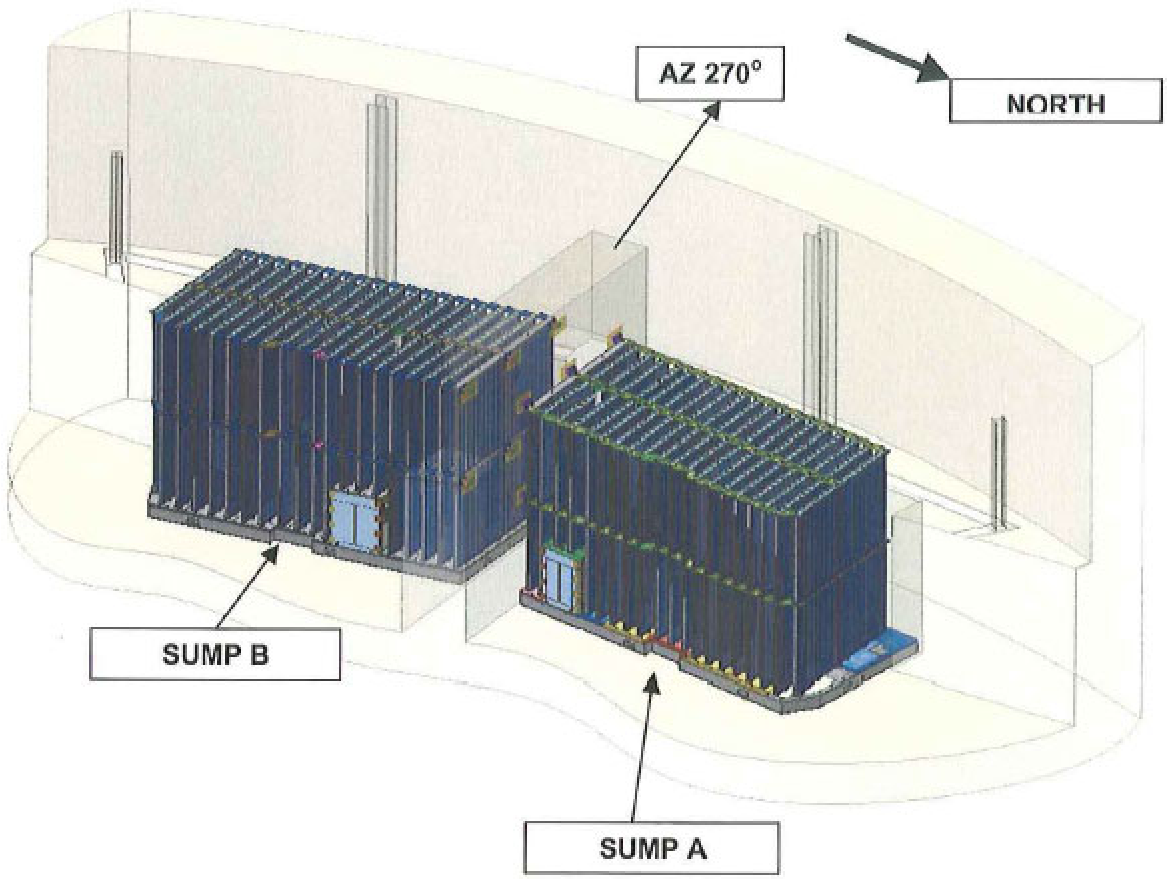

Figure 3.j.1-2: Seabrook Station Unit 1 Containment Sump Strainer System General Arrangement

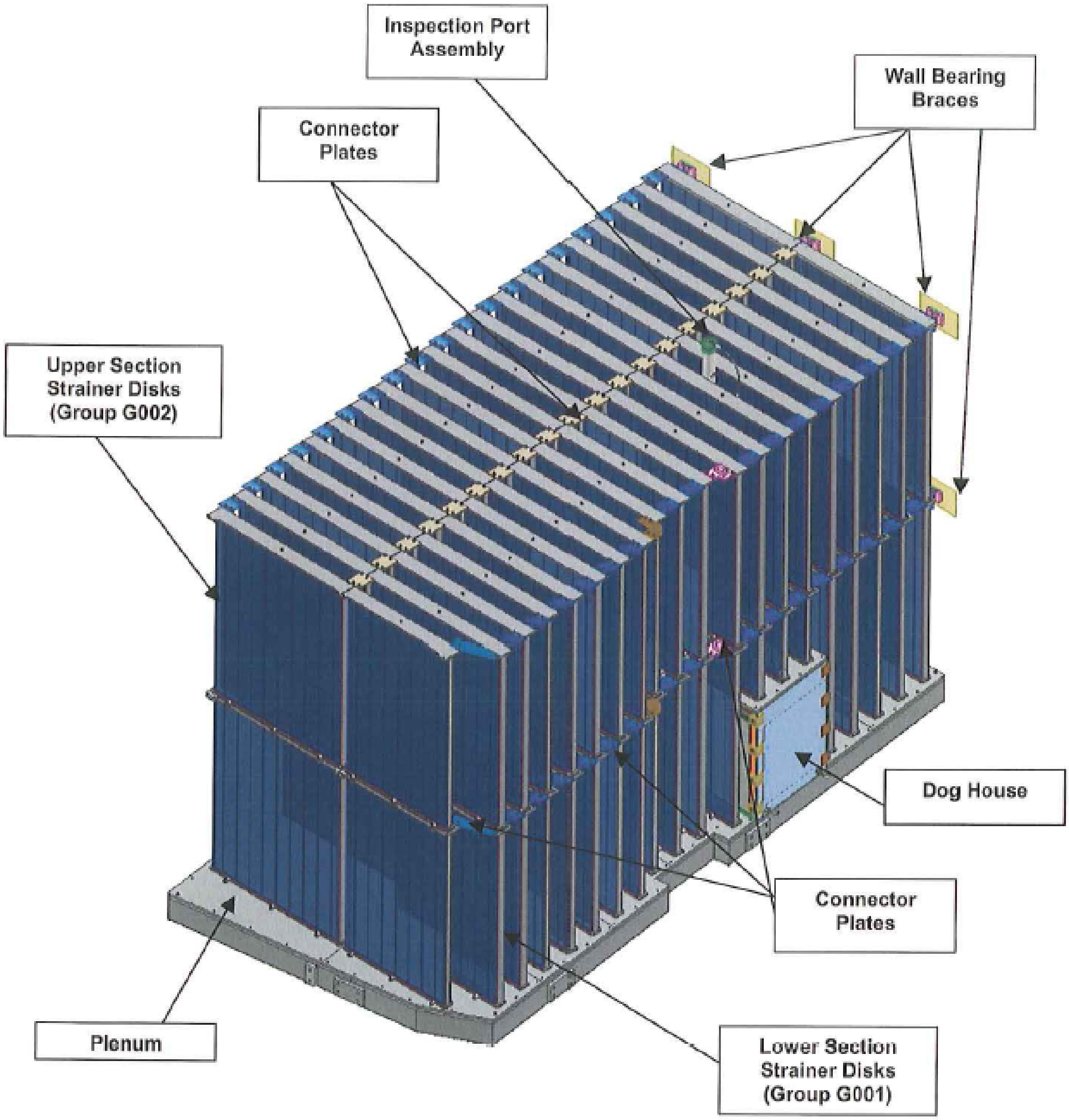

Figure 3.j.1-3: Sump B Assembly

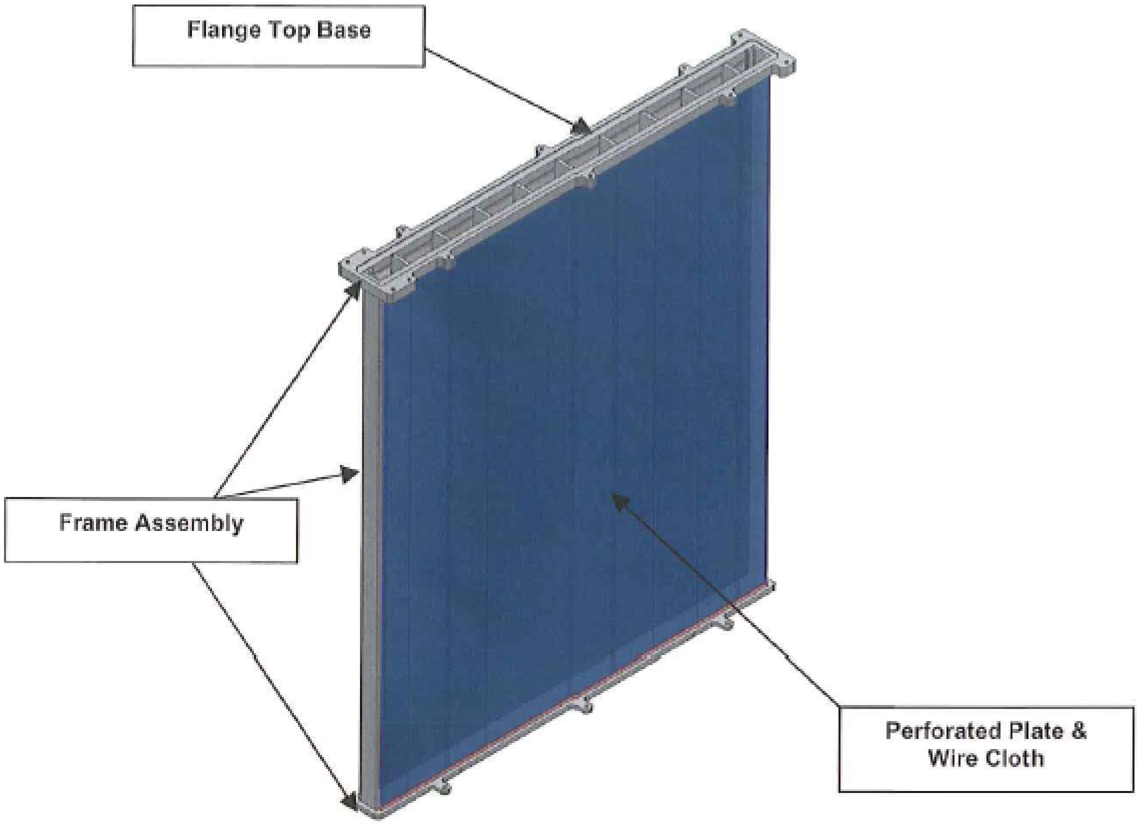

Figure 3.j.1-4: Lower Section – Strainer Disk Assembly (Typical)

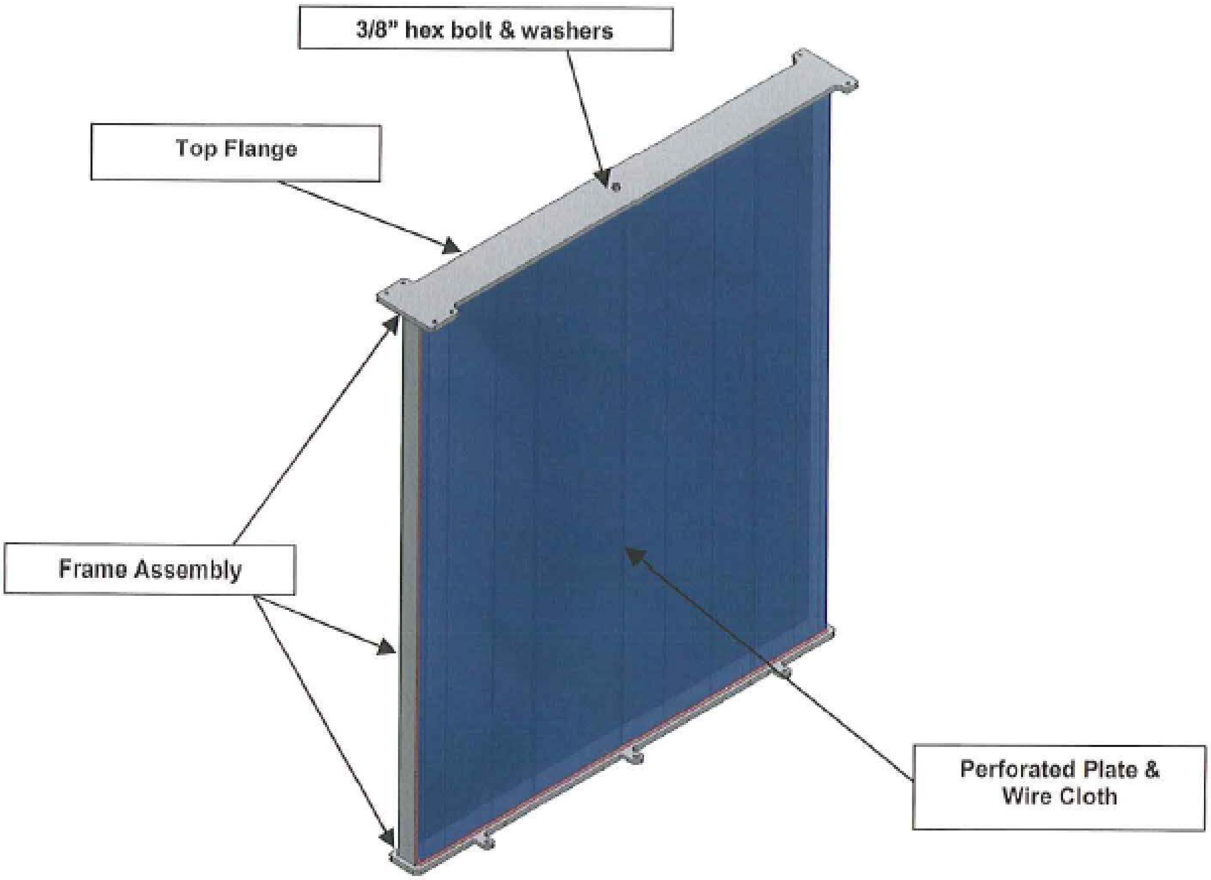

Figure 3.j.1-5: Upper Section – Strainer Disk Assembly (Typical)

3.j.2 Provide a list of any modifications, such as reroute of piping and other components, relocation of supports, addition of whip restraints and missile shields, etc., necessitated by the sump strainer modifications.

Response to 3.j.2:

Containment spray drain tubing downstream of the drain valves required reroute to facilitate installation of the new sump strainers. Tubing was rerouted and supported from the top of the “B” sump platform.

3.k Sump Structural Analysis

The objective of the sump structural analysis section is to verify the structural adequacy of the sump strainer including seismic loads and loads due to differential pressure, missiles, and jet forces.

Provide the information requested in GL2004-02 Requested Information Item 2(d)(vii).

GL 2004-02 Requested Information Item 2(d)(vii)
Verification that the strength of the trash racks is adequate to protect the debris screens from missiles and other large debris. The submittal should also provide verification that the trash racks and sump screens are capable of withstanding the loads imposed by expanding jets, missiles, the accumulation of debris, and pressure differentials caused by post-LOCA blockage under flow conditions.

3.k.1 Summarize the design inputs, design codes, loads, and load combinations utilized for the sump strainer structural analysis.

Response to 3.k.1:

Seabrook Sump Structural Analysis

The previous sump strainers have been completely replaced by new strainer modules and debris interceptors. As shown in the response to Section 3.e.4, debris interceptors are no longer credited for debris holdup. Therefore, the discussion on the structural qualification of the debris interceptors has been removed from this section.

The Seabrook containment has two independent sumps. Each sump has its own strainer module consisting of 20 strainer disk sets. Each disk set is composed of four individual strainer disks with two side by side and an additional two mounted above the lower disks. The disks are bolted vertically to each other and to a bottom plenum by means of flanged connections. The disk sets are bolted to those in adjoining vertical planes by means of connector plates attached to the flanges. All strainer components are fabricated from stainless steel and the anchorage details are designed to accommodate thermal expansion. Therefore, there are no internal component thermal stresses.

The strainers and their components were analyzed using a detailed ANSYS structural analysis model. The strainers and their supports were designed and analyzed using the ASME BP&V Code, Section III, Subsection NC, Class 2 (for the components) and Subsection NF (for the supports) as a guide. The capability of the strainer perforated plate disks as structural members is based on an equivalent plate approach similar to that presented in ASME III, Appendix A, Article A-8000. ASME Service Level B allowables are used as a guide for the stress evaluation of both normal and accident conditions. Thus, ASME III Subsection NF paragraph NF-3251.2 was used for Class

2 plate and shell type components and NF-3350 for Class 2 linear type supports. For bolts, the stress limits of NF-3324.6, increased by values provided in Table NF-3225.2- 1, were used. Welds were evaluated per paragraph NF-3324.5. Expansion anchors were evaluated using the ultimate capacity values with a safety factor of four.

The structural load symbols are provided in Table 3.k.1-1. The strainer structural loads and load combinations are summarized in Table 3.k.1-2. The interaction ratios for the components in the models are provided in Table 3.k.2-1. The results of the calculation indicate the interaction ratios for the strainer assembly components are less than or equal to 1.0, and the strainers meet the acceptance criteria for all applicable loadings.

Table 3.k.1-1: Structural Load Symbols

Symbol	Load Definition
D	Dead Load, in air
D'	Dead Load Debris Weight plus Hydrodynamic Mass (Submerged)
L	Live Load
T_o	Normal Operating Thermal Load
T_a	Accident Thermal Load
E_{o1}	Earthquake Load, OBE in air
E_{o2}	Earthquake Load, OBE in water
E_{ss1}	Earthquake Load, SSE in air
E_{ss2}	Earthquake Load, SSE in water
P_{CR}	Differential (Crush) Pressure

Table 3.k.1-2: Strainer Loads and Load Combinations

Load	Strainer Load Combination
1	$D + L + E_{o1}$
2	$D + L + T_o + E_{o1}$
3	$D + L + T_o + E_{ss1}$
4	$D' + L + T_a + E_{o2} + P_{CR}$
5	$D' + L + T_a + E_{ss2} + P_{CR}$

Note: The RH pipe is not directly connected to the strainer so there are no reaction loads transmitted to the strainer.

3.k.2 Summarize the structural qualification results and design margins for the various components of the sump strainer structural assembly.

Response to 3.k.2:

The structural qualification results and margins for the sump strainer structural assembly are presented in the tables below.

Table 3.k.2-1: Strainer Module Stress Ratio Results

Component	Stress/Load Value	Allowable	Ratio to Allowable
Disk			
Perforated Plate	28.6 ksi	31.0 ksi (2S)	0.92
Wire Cloth	25.8 ksi	31.0 ksi (2S)	0.83
Frame/Rib	8.5 ksi	12.3 ksi (1.33 x $0.4S_y$)	0.69
Weld of Perf to End Channels	5.2 ksi	12.3 ksi (1.33 x $0.4S_y$)	0.42
Weld of Perf to Flanges	4.8 ksi	12.3 ksi (1.33 x $0.4S_y$)	0.39
Resistance Weld of Wire Cloth	36 lbs	750 lbs	0.05
Weld of Ribs to Frame	8 ksi	12.3 ksi (1.33 x $0.4S_y$)	0.65
Disk to Disk Bolting	9.3 ksi	23.3 ksi ($0.345S_U$)	0.40
Disk to Plenum Bolting	3.3 ksi	23.3 ksi ($0.345S_U$)	0.14
Disk Connector Plates	10.2 ksi	23.05 ksi (1.33 x $0.75S_y$)	0.44
Connector Plate Bolting (max single shear)	19.96 ksi	19.96 ksi ($0.1426S_U$)	1.00
Connector Plate Bolting (max double shear)	14.6 ksi	19.96 ksi ($0.1426S_U$)	0.73
Separator Wall Anchorage Detail			
Weld/bolt of Disk Flange to Intermediate Plate	17.3 ksi	23.3 ksi ($0.345S_U$)	0.74
Intermediate Plate	3.7 ksi	23.1 ksi	0.16
1-1/8" Diameter Stud	91.2 ksi	102.8 ksi	0.89
Clip Brackets	14.5 ksi	23.1 ksi	0.63
Weld of Brackets to Base Plate	3.5 ksi	12.3 ksi (1.33 x $0.4S_y$)	0.29
Hilti Base Plate	13.7 ksi	23.1 ksi	0.59
Hilti Expansion Anchors-Tension	2.8 kips	3.1 kips	0.91
Supporting Base Frame and Plenum Roof			
Frame Tubing	14.6 ksi	31.0 ksi (2S)	0.47
Tube Splice Connection	7.8 ksi	9.63 ksi ($0.1426S_U$)	0.81

Component	**Stress/Load Value**	**Allowable**	**Ratio to Allowable**
Plenum Roof Plates	<19.3 ksi	31.0 ksi (2S)	<0.62
Plenum Roof Bolts	15.3 ksi	19.96 ksi ($0.1426S_U$)	0.77
Floor Anchorage Detail			
Weld Gusseted Bracket to Tube Member	2.7 ksi	12.3 ksi (1.33 x $0.4S_y$)	0.22
Shoulder Bolts – Tension/Shear Interaction	N/A	N/A	0.52
Hilti Base Plate	17.8 ksi	23.1 ksi	0.77
Hilti Expansion Anchors – Tension/Shear	N/A	N/A	0.96
“Dog House”			
Side Walls	See “Disks”	N/A	N/A
Eastern End Plate	30 ksi	31.0 ksi (2S)	0.97
Eastern End Plate Clip Connection	10.1 ksi	23.05 ksi (1.33 x $0.75S_y$)	0.44
East to West Section Bolted Connections	11.5 ksi	19.96 ksi ($0.1426S_U$)	0.58
Connections to Base Frame	15.6 ksi	19.96 ksi ($0.1426S_U$)	0.78
ECCS Wall Connections			
Interface Plate	15.9 ksi	31.0 ksi (2S)	0.51
Clamp Bolt	23.1 ksi	23.3 ksi ($0.345S_U$)	0.99
Hilti Expansion Anchors	2.1 kips	3.13 kips	0.66
Catch Basin Pan			
Hilti Expansion Anchors-Shear	107 lbs	1.26 kips	0.09

3.k.3 Summarize the evaluations performed for dynamic effects such as pipe whip, jet impingement, and missile impacts associated with high-energy line breaks (as applicable).

Response to 3.k.3:

The locations of the strainers have been assessed for susceptibility to missiles, jet impingement and pipe whip. The strainers are located outside of the bioshield wall, away from high-energy piping. Additionally, each strainer is located inside a pit, with the majority of the strainer area below the containment floor elevation. The strainers are not in the path of a postulated pipe whip or jet spray.

3.k.4 If a backflushing strategy is credited, provide a summary statement regarding the sump strainer structural analysis considering reverse flow.

Response to 3.k.4:

Each strainer assembly is a passive unit (i.e., there are no active components and the strainers do not utilize backflushing). They are described in the response to Section 3.j.

3.l Upstream Effects

The objective of the upstream effects assessment is to evaluate the flowpaths upstream of the containment sump for holdup of inventory, which could reduce flow to and possibly starve the sump.

Provide a summary of the upstream effects evaluation including the information requested in GL 2004-02 Requested Information Item 2(d)(iv).

> *GL 2004-02 Requested Information Item 2(d)(iv)*
> *The basis for concluding that the water inventory required to ensure adequate ECCS or CSS recirculation would not be held up or diverted by debris blockage at choke points in containment recirculation sump return flowpaths.*

3.l.1 Summarize the evaluation of the flowpaths from the postulated break locations and containment spray washdown to identify potential choke points in the flow field upstream of the sump.

Response to 3.l.1:

The following areas / items were considered as part of the evaluation to determine potential choke points for flow upstream of the sump:

1. Refueling Canal
2. Lower Containment
3. Containment Spray Washdown
4. Upstream Blockage Points Walkdown

Refueling Canal

The refueling canal at Seabrook is drained by three drains. One of these drains is located on the north side of the reactor cavity at the (-) 2’-11” elevation, and the other two are on the south side of the reactor at the (-) 12’-10½” and (-) 16’-4¼” elevations. Any containment spray flow falling directly into the refueling canal must flow through these drains. The pipes that comprise each drain exit are 4 inches in diameter, which currently converge into one 2-inch exit pipe. If these drains were to become blocked by debris blown into the refueling canal during washdown, it could cause a large volume of water to be held up.

An engineering change will be implemented to install a strainer for each drain, add a new drain line, and enlarge the existing drain line to prevent blockage of the drains by debris. As shown in the response to Section 3.e.1, the post-modification configuration of the refueling canal drain lines was analyzed in the debris transport analysis.

Lower Containment

The lower containment at Seabrook consists of two compartments – the containment area inside the bioshield wall, and the annulus outside the bioshield wall. Water travels from inner containment to the annulus by means of two doorways on the north side of containment, two doorways on the south side of containment, two passageways on the west side of containment, and one passageway on the east side of containment. With the exception of the passageway on the east side of containment, all doorways and passageways have debris interceptors installed that cover the space of each doorway/passageway. These debris interceptors are made of a wire mesh cloth with grate panels.

There are debris interceptors in the annulus as well. These interceptors vary in height from 14 inches to 18 inches, are comprised of wire mesh cloth and grating, and have a horizontal lip at the top. They were designed to have sufficient submergence to allow flow over the interceptors at the minimum water level.

It should be noted that, as discussed in the response to Section 3.e.4, the debris interceptors were not credited for debris holdup.

Containment Spray Washdown

Containment spray washdown has a clear path to the containment sump area. Large sections of the floor on each level in containment are covered with grating that allows the water to pass.

A complete evaluation of the containment CAD model, along with a review of the CFD model, indicated no significant areas that could become blocked by debris and hold up water during the sump recirculation phase.

Upstream Blockage Point Walkdown

A walkdown and analysis of the Seabrook containment was performed to assess potential chokepoints in the path from the RCS loops to the ECCS sump, including gates and screens. The walkdown confirmed that there are no potential chokepoints that would adversely affect operation of the ECCS and CBS in the recirculation mode or cause the sump water level to be less than the design basis values. The walkdown flow path survey included curbs, ledges, gates, tool boxes, etc., but because of the timing, did not cover the debris interceptors. Note that a separate walkdown specifically for the refueling canal drain lines was performed (see the response to Section 3.I.4).

3.I.2 Summarize measures taken to mitigate potential choke points.

Response to 3.I.2:

Per the response to Section 3.I.1, no measures were necessary to mitigate potential choke points for lower containment and containment spray washdown. However, measures to mitigate the potential choke point in the refueling canal will be implemented. See the response to Section 3.I.4 for more information.

3.I.3 Summarize the evaluation of water holdup at installed curbs and/or debris interceptors.

Response to 3.I.3:

The debris interceptor design and layout ensures that the debris interceptors do not create new choke points. The debris interceptors in the annulus are designed so that there are several inches of clearance between the top of the debris interceptor and the minimum water level. The passageway on the east side of containment does not have a debris interceptor to ensure that there is at least one completely unobstructed pathway for water to flow from the break to the outer annulus.

3.I.4 Describe how potential blockage of reactor cavity and refueling cavity drains has been evaluated, including likelihood of blockage and amount of expected holdup.

Response to 3.I.4:

The current Seabrook refueling canal drains and the associated drain lines have the potential to become clogged by debris following a LOCA. If the drains were to become blocked, the water held up in the refueling canal could significantly reduce the containment pool water level and sump strainer submergence. This would result in a reduction in allowable head loss across the strainer.

As described in the response to Section 3.e.1, an engineering change to the refueling canal drains will be implemented to ensure that the drains will not be clogged and there is an open flow path to the containment sump pool during post-accident sump recirculation.

3.m Downstream Effects – Components and Systems

The objective of the downstream effects, components and systems section is to evaluate the effect of debris carried downstream of the containment sump screen on the function of the ECCS and CSS in terms of potential wear of components and blockage of flow streams.

Provide the information requested in GL 2004-02 Requested Information Item 2(d)(v) and 2(d)(vi) regarding blockage, plugging, and wear at restrictions and close tolerance locations in the ECCS and CSS downstream of the sump.

> *GL 2004-02 Requested Information Item 2(d)(v)*
> *The basis for concluding that inadequate core or containment cooling would not result due to debris blockage at flow restrictions in the ECCS and CSS flowpaths downstream of the sump screen (e.g., a HPSI throttle valve, pump bearings and seals, fuel assembly inlet debris screen, or containment spray nozzles). The discussion should consider the adequacy of the sump screen's mesh spacing and state the basis for concluding that adverse gaps or breaches are not present on the screen surface.*
>
> *GL 2004-02 Requested Information Item 2(d)(vi)*
> *Verification that the close-tolerance subcomponents in pumps, valves and other ECCS and CSS components are not susceptible to plugging or excessive wear due to extended post-accident operation with debris-laden fluids.*

3.m.1 If NRC-approved methods were used (e.g., WCAP-16406-P-A with accompanying NRC SE), briefly summarize the application of the methods. Indicate where the approved methods were not used or where exceptions were taken, and summarize the evaluation of those areas.

Response to 3.m.1:

NextEra performed evaluations for Seabrook to address ex-vessel downstream effects in accordance with WCAP-16406-P-A and the associated NRC SER. The limitations and conditions provided in the NRC SER were addressed as part of the evaluations and it was shown that the WCAP-16406-P-A methodology was appropriate for use at Seabrook. All refinements or modifications that were applied to the WCAP-16406-P-A methodology are described below.

The following methodology was employed in the ex-vessel downstream effects evaluations.

Maximum Debris Ingestion Determination

Blockage and wear of the ECCS and CBS components and piping in the post-LOCA recirculation flowpaths downstream of the sump screen were addressed within the downstream effects evaluations. Seabrook has screens with a nominal hole diameter of 0.068 inches. The maximum spherical size particulate that is expected to pass through the strainer system and into the ECCS and CBS recirculation flowpaths is 0.068 inches. The adequacy of the sump screens' mesh spacing or strainer hole size was conservatively addressed by assuming that the maximum spherical size of particulate debris that can pass through the strainers is 0.1 inches.

Additionally, the maximum quantity of fines debris transported to the sump strainers for each debris type was assumed. Of these maximum quantities, 100% of fiber, qualified coatings, and latent debris that are generated and transported as fines were assumed to penetrate the strainer. For unqualified coatings, the size distribution presented in WCAP-16406-P-A was used to determine what percentage of debris was small enough to penetrate the strainer.

A surveillance procedure is in place to inspect the strainers and debris interceptors for visible evidence of structural distress or abnormal corrosion, that the inspection ports are capped and locked, and to confirm that there is no debris present on the strainers or debris interceptors.

Initial Debris Concentrations

Initial debris concentrations were developed using the assumptions and methodology described in Chapter 5 of WCAP-16406-P-A. The downstream effects evaluations were performed using conservative fiber and particulate debris concentrations: the total maximum initial debris concentration used in the evaluations was 4,557.65 ppm, with fiber debris contributing 3,004.00 ppm, and particulate debris contributing 1,553.65 ppm. The actual maximum initial debris concentration based on the latest debris loads is determined to be 1,587.89 ppm, approximately three times less than the concentration used in the downstream effects evaluations.

Flowpaths and Alignment Review

Both trains of the ECCS and CBS were reviewed to ensure all flowpaths and components impacted by the debris-laden recirculation flow were considered. Documents used for this effort included piping and instrumentation diagrams (P&IDs) and other plant design documents as applicable.

The components within the recirculation flowpaths were categorized as either "smaller", "further evaluation required", "larger", or "excluded" . The "smaller" category contains components with flow clearances known to be physically too small to pass the debris. The "further evaluation required" category includes components that are determined by industry guidance to have the potential to become plugged under debris loading. The “larger” category includes components with clearances sufficiently large enough to pass recirculation debris without causing blockage, and the “excluded” category contains components for which industry guidance suggests are not susceptible to debris blockage.

Component Blockage and Wear Evaluations Methodology

All component evaluations were performed based on WCAP-16406-P-A. Components addressed in the evaluations include pumps, heat exchangers, orifices, spray nozzles, instrumentation tubing, system piping, and valves required for the post-LOCA recirculation mode of operation of the ECCS and CBS. The evaluations included the following steps:

1. Identifying all components in the ECCS and CBS flowpaths (see Flowpaths and Alignment Review above).
2. Applying the appropriate wear models for pumps. Pumps experience erosive wear and abrasive wear due to debris ingestion. Two abrasive wear models were developed in WCAP-16406-P-A including the free flowing abrasive wear model and Archard abrasive wear model. Each model was used as appropriate in the evaluations.
3. Applying the appropriate erosive wear model for heat exchangers, orifices, spray nozzles, system piping, and valves.
4. Evaluating the potential for plugging of heat exchanger tubes, orifices, spray nozzles, system piping, and valves by comparing the maximum debris size expected to be ingested through the sump screen to the clearances within the components.
5. Evaluating the potential for debris sedimentation inside system piping, heat exchanger tubing, and valves that move or reposition during post-LOCA recirculation phase (and must go fully closed) by comparing operating line velocity to minimum line velocity required to avoid sedimentation (0.42 ft/s).
6. Evaluating the potential for debris collection in the instrument sensing lines.

3.m.2 Provide a summary and conclusions of downstream evaluations.

Response to 3.m.2:

The following is the summary of results and conclusions of the downstream effects evaluations:

ECCS/CBS Pumps

The evaluation for pumps addressed the effects of debris ingestion through the sump screen on three aspects of operability: hydraulic performance, mechanical-shaft seal assembly performance, and mechanical performance. The effect of recirculating sump debris on the hydraulic and mechanical performance of the ECCS and CBS pumps was determined to be acceptable. The mechanical shaft seal assembly performance evaluation found that no Seabrook ECCS or CBS pumps used cyclone separators in the seal piping arrangements. The RHR pumps have an API Plan 23 piping arrangement, which precludes the injection of debris laden post-LOCA fluids into the seal cavity chamber. The CBS pumps utilize an API Plan 21 seal cooling arrangement and the charging and safety injection pumps utilize an API Plan 01 seal cooling arrangement, both of which allow the injection of pump fluid for seal cooling. An evaluation of these arrangements concluded that the debris concentration in the seals will have no detrimental impact on the operation or integrity of the seals. The RHR and CBS pumps have backup bushings made of carbon material. An engineering evaluation was provided for the continued use of the RHR and CBS pumps' carbon backup bushings which determined that the backup bushings are "Acceptable As-Is". Additional analysis showed that, if wear and failure of the primary seals are assumed to occur, the disaster bushing would wear a negligible amount in 30 minutes, and that the leakage rate of the pump is kept to an acceptable limit until the leakage is isolated and another train of ECCS or CS could be started.

When evaluating pump wear as part of the hydraulic performance evaluation, a modification to the WCAP-16406-P-A methodology was used to refine the distribution of abrasive versus erosive particulate debris. WCAP-16406-P-A considers 50 microns to be the constant lower threshold size for abrasive debris (which is equal to 40% the wear ring gap of the hypothetical pump considered therein). The Seabrook analysis used 40% of the actual wear ring gap at any given time to define the threshold for abrasive-sized particulate. In other words, as the wear ring gap opens due to wear over time, the threshold size for abrasive debris increased and the amount of abrasive debris is reduced. However, the amount of abrasive debris that was reduced was assumed to contribute to erosive wear. As noted in the response to Section 3.m.1, the initial debris concentrations used for the downstream effects evaluations are conservative.

The evaluation for pumps determined that the effects of debris ingestion through the screen is not an issue with regard to hydraulic performance, mechanical-shaft seal assembly performance, and mechanical performance.

ECCS/CBS Valves

WCAP-16406-P-A provides the criteria for wear and plugging analysis for ECCS and CBS valves due to debris-laden fluid (Reference 31 pp. 8-27 and 8-28). The following tables are a summary of the criteria that would necessitate an evaluation. The valves that do not meet these criteria are not critically impacted by wear and plugging due to debris laden fluid.

Table 3.m.2-1: Valve Evaluation Blockage Criteria (Reference 31 pp. 8-28)

Valve Type	Size (inches)	Position During the Event
Gate	≤ 1	Open
Globe	< 1-1/2	Open
Globe	> 1 (Cage Guide)	Open
Check Valves/ Stop Check	≤ 1	Open
Butterfly	< 4	Throttled < 20°
Globe Valves	All	Throttled
Hermetically Sealed Valves	All	Open

Table 3.m.2-2: Valve Evaluation Erosive Criteria (Reference 31 pp. 8-27)

Valve Type	Size (inches)	Position During the Event
Globe	All	Throttled
Butterfly	All	Throttled

Valves were evaluated for blockage in the downstream effects evaluations. Valves that were determined to be “larger” or “excluded” did not warrant further evaluation, but those valves identified as “further evaluation required” received a more detailed evaluation. It was determined that all valves passed the acceptance criteria for the blockage evaluation.

Valves were evaluated for debris sedimentation. Valves identified as “larger” or “excluded” did not require additional analysis, but valves identified as “further evaluation required” were analyzed further. The line velocities for all valves analyzed was found to be greater than 0.42 ft/s, thus, debris sedimentation was not an issue.

Valves were screened to determine if an evaluation of the wear impact was required. All manually throttled valves in the post-LOCA recirculation flowpath were evaluated to determine the extent of erosion. The initial debris concentration provided above was used to calculate the initial wear rate, and then the large debris (all fiber, unqualified epoxy ≥ 675 μm, and unqualified IOZ ≥ 125 μm) was depleted over time using a depletion coefficient of $\lambda = 0.07$, as recommended by WCAP-16406-P-A. It was determined that all valves passed the acceptance criteria for the erosive wear evaluation, with the most limiting flow area increase being 2.878% for the sample purge throttle valve (SS-V208), below the 3% acceptance criteria provided by WCAP-16406-P-A.

ECCS/CBS Heat Exchangers, Flow Restrictions, and System Piping

Heat exchanger tubes, flow restrictions, and system piping were evaluated for the effects of erosive wear for the initial debris concentrations presented in the response to Section 3.m.1 over the mission time of 30 days. The erosive wear on these components was determined to be insufficient to affect system performance.

The smallest clearance found for Seabrook heat exchangers, orifices, spray nozzles, and system piping in the recirculation flowpaths that were not categorized as "excluded" is 0.375 inches, for the CBS spray nozzles. The maximum diameter of downstream debris was conservatively assumed to be 0.100 inches. Therefore, no blockage of the flowpaths is expected.

System piping and heat exchanger tubing was evaluated for plugging based on system flow and material settling velocities. For all piping, the minimum flow velocity was found to be greater than 0.42 ft/s, the minimum velocity required to prevent debris sedimentation. All system piping passed the acceptable criteria for plugging due to sedimentation.

ECCS/CBS Instrumentation Tubing

Instrumentation tubing (or sensing lines) was evaluated for debris settling from the process streams. According to WCAP-16406-P-A, Section 8.6.6, instrument tubing is designed to remain water solid without taking flow from the process stream. This prevents direct introduction of debris laden fluid into the instrument tubing. Settling of the debris is the only process by which the debris is introduced into the instrument tubing. Since the sensing lines are water solid and stagnant, the introduction of either fibrous or particulate debris by flow into the sensing lines is not possible. The terminal settling velocities of the debris sources in the process streams are small by comparison to the process fluid velocities; therefore, introduction of debris by settling into the instrument tubing is not expected. It was found that all instruments identified as required post-LOCA are located either on the top or side of the applicable headers. This excludes the possibility of debris settling in the subjected instrument tubing. Therefore, blockage and wear of ECCS or CBS instrument tubing due to debris laden fluid are not expected. An evaluation of the effects of debris laden recirculation fluid on the reactor vessel level monitoring system (RVLMS) was also performed, and it was determined that RVLMS is acceptable.

3.m.3 Provide a summary of design or operational changes made because of downstream evaluations.

Response to 3.m.3:

No plant design changes were made as a result of the downstream effects evaluations.

The only operational change made related to downstream effects is that surveillance requirements were updated for the new strainer system. A surveillance procedure is in place to inspect the strainers and debris interceptors for visible damage or corrosion, and to confirm that there is no debris present on the strainers or debris interceptors.

3.n Downstream Effects – Fuel and Vessel

The objective of the downstream effects, fuel and vessel section is to evaluate the effects that debris carried downstream of the containment sump screens and into the reactor vessel has on core cooling.

3.n.1 Show that the in-vessel effects evaluation is consistent with, or bounded by, the industry generic guidance (WCAP-16793-NP), as modified by NRC staff comments on that document. Briefly summarize the application of the methods. Indicate where the WCAP methods were not used or where exceptions were taken, and summarize the evaluation of those areas.

Response to 3.n.1:

In the January 2018 submittal, NextEra used the penetration data from the St. Lucie Unit 1 test to evaluate in-vessel downstream effects for Seabrook (Reference 2). Since then, NextEra performed new fiber bypass testing for Seabrook and applied the test results in the new in-vessel downstream effects analysis. The analysis followed the latest NRC staff review guidance (Reference 9) and pressurized water reactor owners group (PWROG) guidance (Reference 3), and used the methodology and acceptance criteria in WCAP-17788-P, Revision 1 (Reference 10; 32) for the resolution of in-vessel effects. A summary of the fiber bypass testing and in-vessel analysis and resolution is provided below. It is concluded that post-accident long-term core cooling (LTCC) will not be challenged by accumulation of debris within the reactor core for all postulated LOCAs at Seabrook. Note that the discussion on the cold leg breaks and LOCADM analysis has been removed from the submittal in accordance with the NRC review guidance (Reference 9 pp. 2-3).

<u>Seabrook Fiber Bypass Testing</u>

NextEra conducted fiber bypass testing for Seabrook in 2019 at Alden. The purpose of the testing was to collect time-dependent fiber bypass data of the plant strainers. The test parameters were selected to be representative of the conservative plant conditions. The bypass test is described below.

Test Loop Design

The Seabrook fiber bypass test loop layout is shown in Figure 3.n.1-1, which is the same as that used for head loss testing. The main recirculation pump took suction from the test strainer doghouse. Discharge from the recirculation pump first traveled through one of two filter housings, inside which filter bags were installed. Different from head loss testing, one of the two filter bag housings was always online during the fiber bypass test to ensure all flow that passed through the test strainer was filtered by the filter bags. The filter bag housings were outfitted with upstream and downstream isolation valves such that swap between the two housings can be performed during testing without disruption to flow. This allowed for the online filter housing to be switched mid-test in order for clean bags to be brought online while providing continuous filtration.

The overall test loop flow rate was measured by orifice flowmeter “FM1” (see Figure 3.n.1-1), and a portion of the flow downstream of the flow meter can be diverted through a heat exchanger to maintain the test temperature. Afterwards, the flow was split between a debris hopper and the mixing lines. Flow to the debris hopper facilitated introduction of debris into the test tank. Flow through the mixing lines returns to the upstream portion of the test tank, providing turbulence to keep the introduced debris in suspension. The flow to the debris hopper was monitored by orifice flowmeter “FM2”.

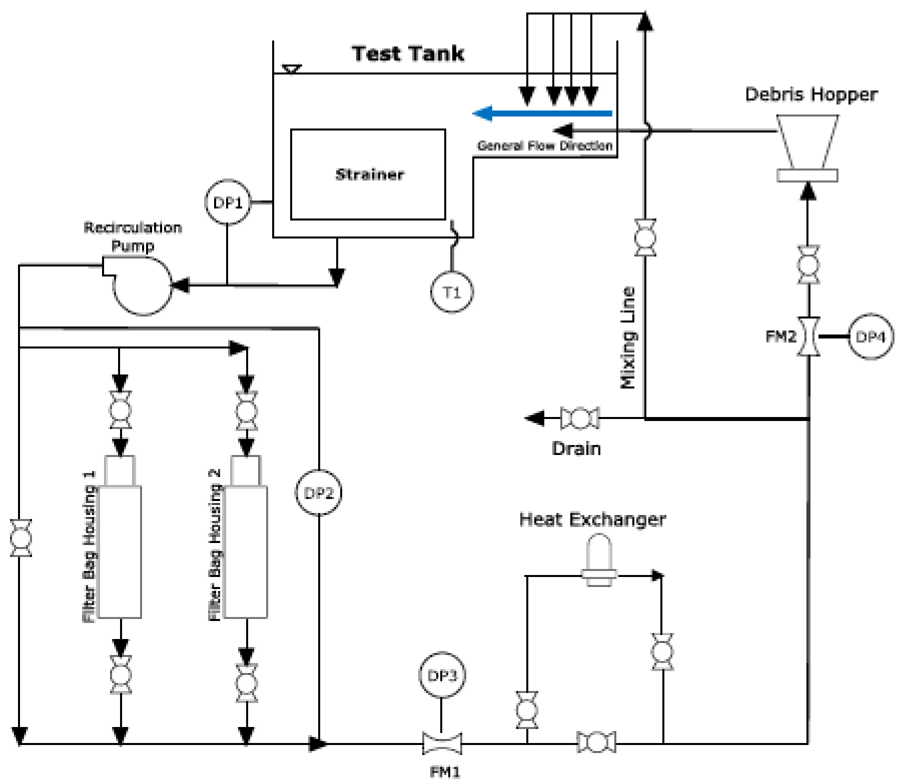

Figure 3.n.1-1: Piping Diagram of Fiber Bypass Test Loop

The test tank, which is illustrated in Figure 3.n.1-2, included two regions: an upstream mixing region where debris was introduced into the tank and a downstream pit where the test strainer was installed. The pit geometry was configured to closely model the containment sump at Seabrook. The depth of the downstream pit region relative to the upstream tank floor was selected such that the fraction of the test strainer above the upstream floor represented the configuration of the plant strainer.

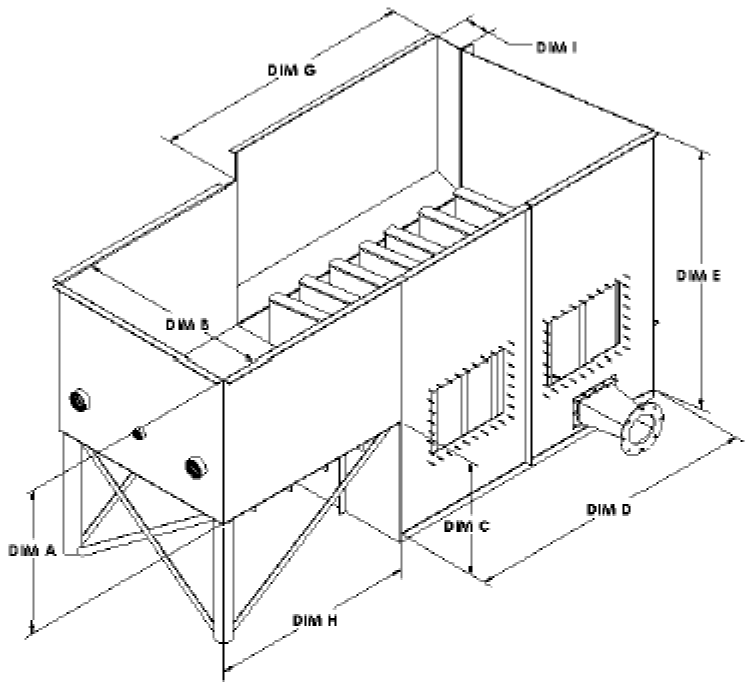

Figure 3.n.1-2: General Arrangement of Seabrook Fiber Bypass Test Tank

Test Strainer

The test strainer used for fiber bypass testing is the same as that for head loss testing. The overall configuration of the test strainer (see Figure 3.n.1-3) is representative of the Seabrook plant strainers, with multiple vertical strainer disks installed on top of a plenum or doghouse. The heights of the plenum and doghouse of the test strainer were properly scaled down to maintain prototypical flow velocities inside and to avoid settling of any debris. The test strainer consisted of 6 disks that model the full-sized disks of the plant strainer and one shorter disk that models the disks on top of the doghouse for the plant strainer. The spacing between adjacent disks reflected the plant strainer condition. The key dimensions of the test strainer disk perforated plates and wire cloth matched those of the plant strainer. The disks of the test strainer were shorter than the plant strainer disks. However, as discussed above, the fraction of the disks extending above the floor of the upstream portion of the test tank was consistent with that of the plant strainer above the containment floor. The test strainer was also designed such that the distribution of approach velocity at clean conditions is consistent with that of the plant strainer. The test strainer has a total surface area of 137.1 ft^2.

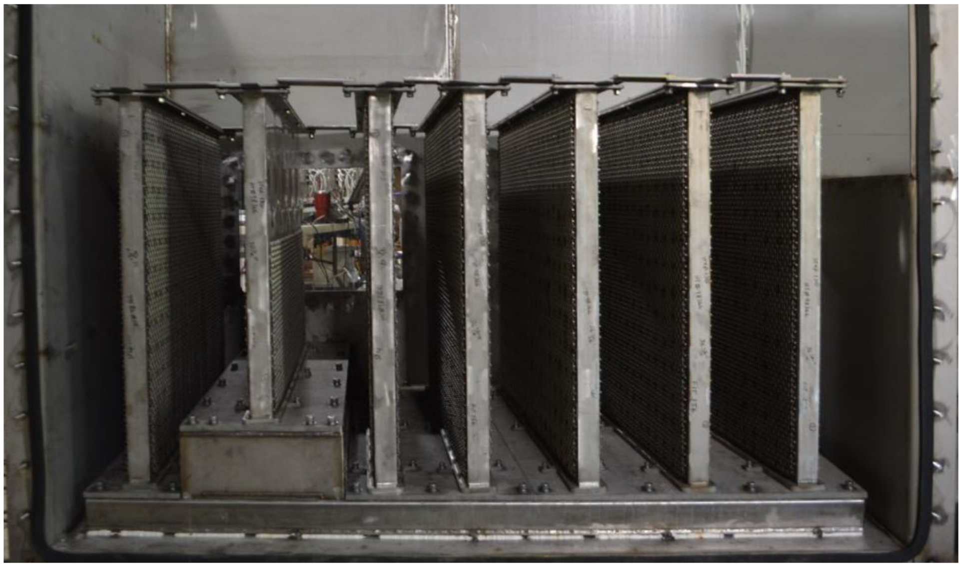

Figure 3.n.1-3: Seabrook Test Strainer inside Test Tank

Debris Types and Preparation

Debris bypass testing used fibrous debris only. The two fibrous debris types at Seabrook are Nukon and latent fiber. Nukon was used as surrogate for latent fiber during testing. Only fiber fines were used during bypass testing.

Heat treated Nukon was procured (see Figure 3.n.1-4) and processed into fiber fines in accordance to the NEI protocol (Reference 27). The insulation was first cut into approximately 2 inch × 2 inch cubes and weighed out into required batches. The fiber was then placed in a preparation vessel that included a manifold with three high pressure nozzles. The debris was wetted with pre-heated test water until the base material was saturated and the pressure washer nozzles were submerged. The debris was then sprayed with test water pressurized to 1500 psi. The duration of the spray was controlled to provide consistent fiber slurry characteristics. The prepared fiber was predominantly Class 2 fibers as defined in NUREG/CR-6224 (Reference 28 pp. B-16), consisting mostly of individual fibers with lesser quantities of fiber shards and small entanglements. Each batch of prepared debris was photographed on top of a light table (see an example in Figure 3.n.1-4).

Figure 3.n.1-4: Nukon Material Before (Left) and After (Right) Preparation

Debris Introduction

Prepared fine Nukon debris was introduced to the test tank in batches via a debris hopper. Before each debris addition, the test tank and debris hopper were visually checked to verify that all debris of the previous batch had transported to the strainer. As shown in Figure 3.n.1-5, debris was added to the hopper from the top opening. The turbulence and mixing resulting from the hopper inflow was sufficient to prevent formation of debris agglomerations within the hopper. The flow with transported debris exited the hopper from its side opening into the test tank. For all batches, the debris introduction rate was controlled to maintain a prototypical debris concentration in the test tank.

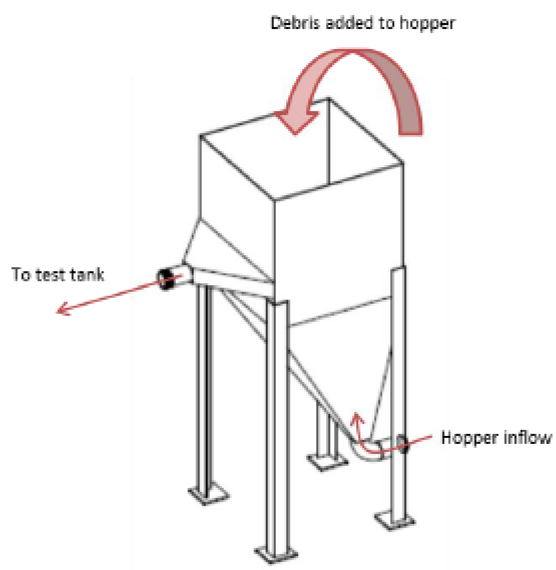

Figure 3.n.1-5: Debris introduction hopper

Test Debris Load and Batching

The prepared debris was introduced in six separate batches. The debris batching size is equivalent to a theoretical uniform bed thickness of approximately 1/16” for the first two batches and increased for the later batches (see Table 3.n.1-1).

Table 3.n.1-1: Fiber Bypass Testing Debris Batch Size

Batch No.	Batch Size (g)	Equivalent Uniform Bed Thickness (inches)
1	810.5	0.065
2	809.7	0.065
3	1618.6	0.130
4	3245.5	0.261
5	3243.3	0.261
6	4923.3	0.396

The total tested fiber debris load at plant scale is determined to be 576.0 lbm by multiplying the total test load (32.3 lbm) by the ratio between the Seabrook plant strainer surface area (2445 ft^2) and test strainer surface area (137.1 ft^2). This testing fiber load bounds the largest transported fiber load for all postulated breaks of 547.3 lbm per strainer (540.84 lbm for insulation fiber plus 6.45 lbm for latent fiber) for two-train operation.

Debris Capture

Fiber can penetrate through the strainer by two different mechanisms: prompt bypass and shedding. Prompt bypass occurs when fiber reaching the strainer travels through the strainer immediately. Shedding occurs when fiber that already accumulated on the strainer migrates through the bed and ultimately travels through the strainer. Both mechanisms were considered during testing.

All of the flow downstream of the test strainer traveled through 5-micron filter bags before returning to the test tank to collect the fibers bypass. The capture efficiency of the filter bags was verified to be above 97%. As discussed above, the filtering system allowed the installation of two sets of filter bags in parallel filter housings such that one of the two sets of filter bags was online at all times, even during periods in which filter bags were swapped.

A clean set of filter bags was placed online before a debris batch was introduced to the test tank and was left online for a minimum of three pool turnovers (PTOs) to capture the prompt fiber bypass. For each batch, at least one additional set of filter bags was used for a minimum of 30 minutes to capture the fiber bypass due to shedding. For the third, fourth and sixth batches, additional filter bag sets were brought online for extended period of time to collect data for long term shedding. At the time when the final shedding filter bag set for Batch 6 was taken offline, the overall test duration is over 24 hours, which exceeds the maximum switchover time for hot leg recirculation for Seabrook (5 – 6 hours after accident). This approach allowed the test to collect time-dependent fiber bypass data, which was used to develop a curve-fit for the rate of fiber bypass as a function of fiber quantity on the strainer.

Before and after the test, all of the filter bags used were uniquely marked and dried, and their weights were recorded. The weight gain of the filter bags was used to quantify fiber bypass. After testing, the debris-laden filter bags were rinsed with deionized (DI) water to remove residual chemicals before being dried and weighed. When processing the filter bags, in either a clean or debris laden state, the bags were placed in an oven for at least an hour before being cooled and weighed inside a humidity-controlled chamber. This process was repeated for each set of bags until two consecutive weights were within 0.05 g of each other.

Test Parameters

The chemistry condition selected for testing had a boron concentration of 0.215 mol/l and a sodium hydroxide (NaOH) buffer concentration of 0.135 mol/l. This water chemistry corresponds to the maximum Seabrook sump pH condition (9.6), which was chosen based on small scale testing results that showed higher pH led to more bypass. Test water was prepared by adding pre-weighed chemicals to DI water per the prescribed concentrations.

During the fiber bypass test, the test flow rate was maintained within -0%/+5% of 337 gpm for over 92% of the test duration. This test flow rate corresponds to an equivalent plant flow rate of 6010 gpm per strainer (337 gpm × 2445 ft^2 / 137.1 ft^2) or a total recirculation flow rate of 12020 gpm for two-train operation. This total flow rate bounded the condition that resulted in the highest in-vessel fiber load with the failure of one CBS pump (see Table 3.n.1-2).

The temperature of test water was maintained between 100.2°F and 107.0°F during the fiber bypass test.

<u>Strainer Bypass Model Development</u>

Data gathered from the Seabrook fiber bypass test were used to develop a model for quantifying the strainer fiber bypass under plant conditions. The model was developed per the following steps:

- General governing equations were developed to describe both the prompt fiber bypass and shedding through the strainer as a function of time and fiber quantity on the strainer. The equations contain coefficients whose values were determined from test results.

- The Seabrook fiber bypass testing results were fit to the governing equations using various optimization techniques to refine the coefficient values.

Figure 3.n.1-6 compares the fiber bypass test results (shown as circles) with the fiber bypass quantities determined from the model for the test conditions (shown as blue solid line). As shown in the figure, the model results adequately represent the test data.

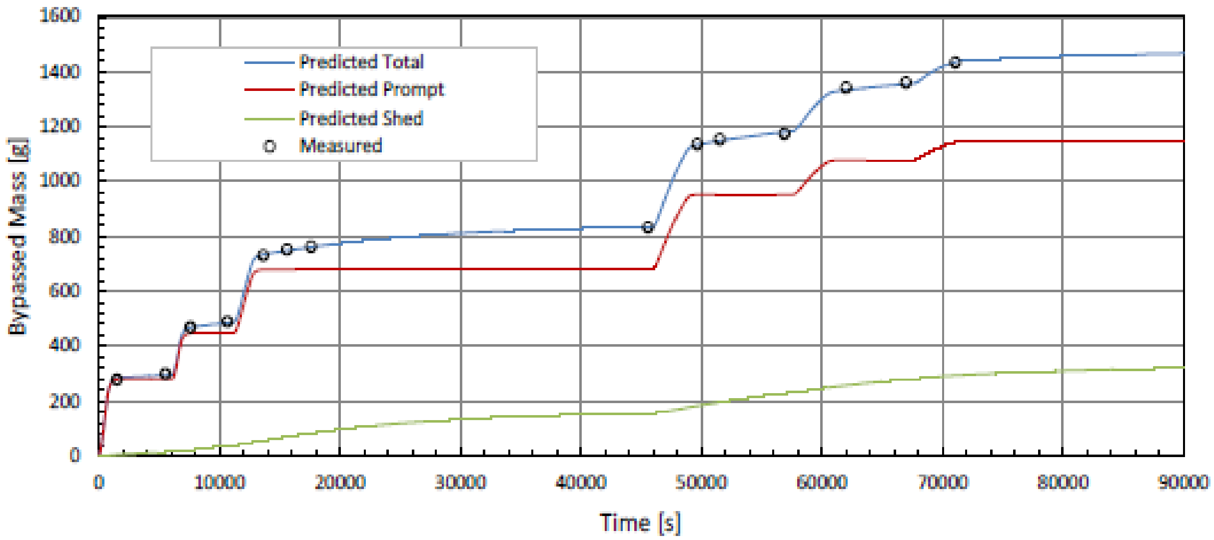

Figure 3.n.1-6: Seabrook Test Bypass Model Fit

The bypass model from the previous step can be used to determine the prompt fiber bypass fraction and shedding fraction for a given time and amount of fiber accumulated on the strainer. Coupled with a fiber transport model, a time-dependent evaluation can be performed to quantify the total amount of fiber that could pass through the strainer under certain plant conditions.

An example application of the model is shown below. For the time-dependent analysis, the recirculation duration was divided into smaller time steps. For each time step, the fiber bypass fractions and quantities were calculated. Figure 3.n.1-7 shows the resulting cumulative fiber bypass through the strainer over time at plant conditions for a 31” break.

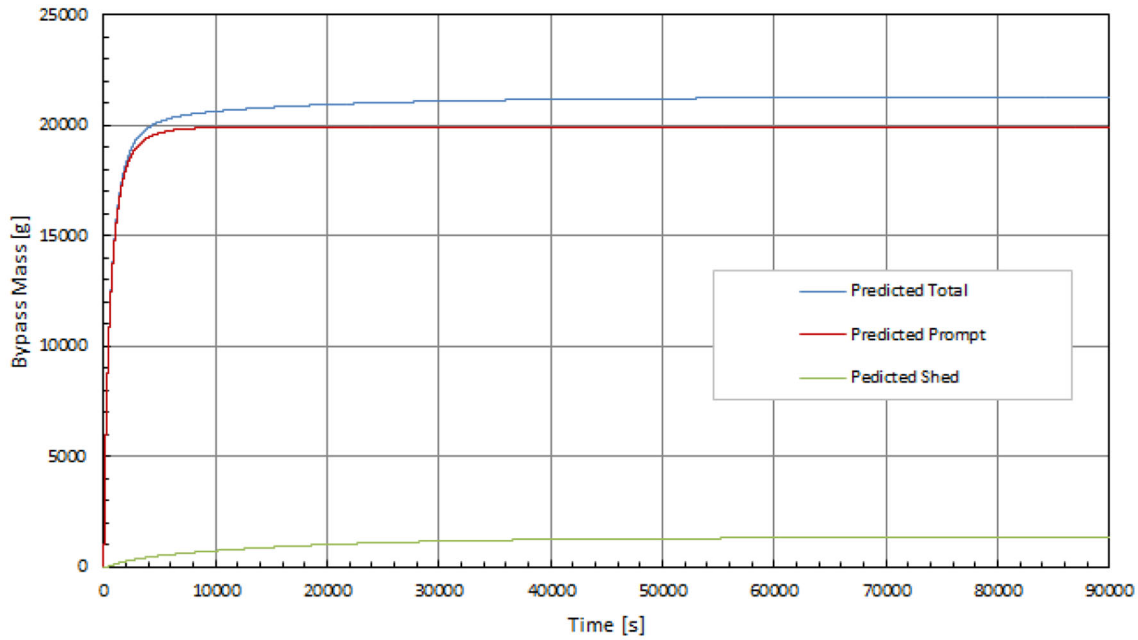

Figure 3.n.1-7: Example Application of Fiber Bypass Model for a 31" Break

Figure 3.n.1-8 shows the prompt fiber bypass fraction as a function of fiber quantity on the strainer derived using the model. As expected, the prompt bypass fraction decreases as a fiber debris bed forms on the strainer.

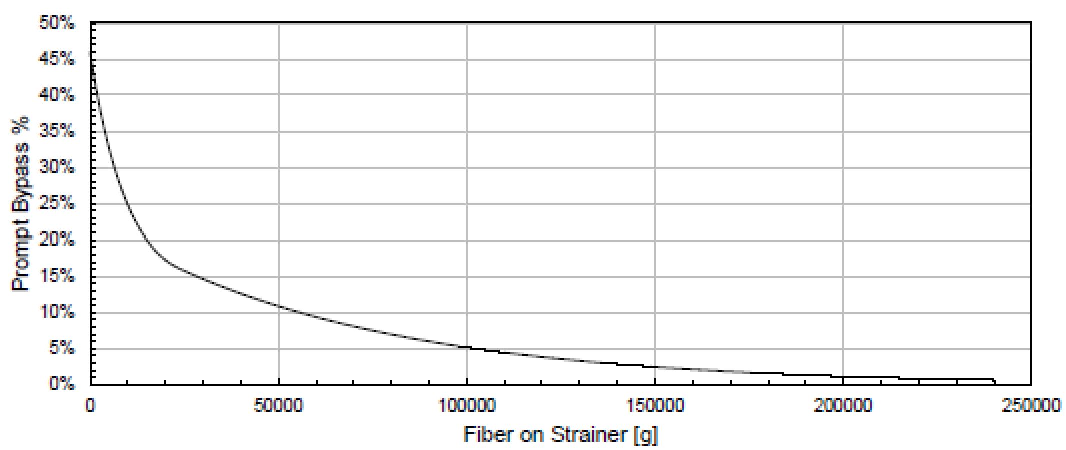

Figure 3.n.1-8: Seabrook Prompt Fiber Bypass Fraction Strainer Model

Figure 3.n.1-9 shows the shedding rate calculated from the model as a function of time. Note that shedding bypass depends on the fiber quantity on the strainer and time. As shown in the figure, the shedding rate decreases over time for a given amount of fiber on the strainer.

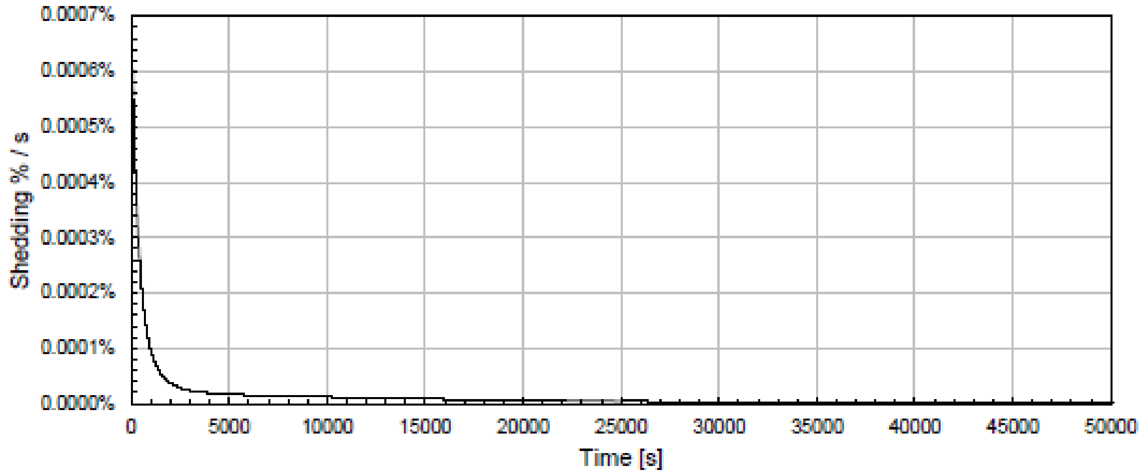

Figure 3.n.1-9: Seabrook Shedding Rate Calculated

Evaluation of Fiber Accumulation inside Reactor Vessel

Accumulation of debris inside the reactor during the post-LOCA recirculation phase was evaluated following the methodology in WCAP-17788 and NRC review guidance on in-vessel effects. Per this guidance, analysis of in-vessel fiber load was performed for the hot leg breaks (HLBs) only (Reference 9 p. 3). To apply the time-dependent fiber bypass fractions, the recirculation duration was divided into small time steps. For each time step, the following computation was performed to quantify the fiber that reaches the reactor:

1. The fractions of prompt and shedding bypass were calculated using the Seabrook fiber bypass model based on the quantity of fine fiber collected on the strainer at the beginning of the time step.
2. The amount of fine fiber that arrived at the strainer during the current time step was calculated using the fine fiber concentration in the pool, strainer flow rate, and time step.
3. The amount of prompt bypass was calculated by multiplying the prompt bypass fraction from Step 1 by the amount of fine fiber arriving at the strainer during the current time step from Step 2.
4. The amount of shedding bypass was calculated by multiplying the shedding bypass fraction from Step 1 by the amount of fiber collected on the strainer at the beginning of the time step.
5. The fiber that passes through the strainer was then split based on the ratio in flow rate between the in-service ECCS and CBS pumps.
6. The fiber transported by the ECCS pump(s) reaches the reactor and is assumed to accumulate at the core inlet only, without crediting the alternate

flow paths (AFPs). This is consistent with the NRC review guidance (Reference 9). The fiber carried by the CBS pump(s) is returned to the sump pool.

7. The pool fiber concentration is updated as an initial condition for the next time step.

The steps shown above were implemented in a spreadsheet, and the total in-vessel fiber load was calculated by summing up the amount of fiber that reaches the reactor during each time step. The calculated total fiber quantity was increased by 2% to account for the uncertainties in the curve fit of the fiber bypass test data. This percentage increase was determined by comparing the measured total fiber bypass with that obtained from the model for the testing conditions.

The analysis was conducted for different pump lineups: all pump in operation, single train failure and single CBS pump failure. Sensitivity runs were performed to ensure the worst combination of input parameters (e.g., pool volume, transport fiber load, RHR and CS pump flow rates, and CS duration) were used for each case. Table 3.n.1-2 shows the resulting in-vessel fiber loads for different pump lineups. The bounding case had two ECCS trains in operation at the maximum flow rate, maximum sump pool volume, maximum fiber load and one CBS pump in operation at minimum flow rate and duration.

Table 3.n.1-2: In-Vessel Results for Largest Transported Fiber Load

Pump Lineup	In-Vessel Fiber Load (g/FA)
All Pumps in Operation	108.48
Single Train Failure	55.13
Failure of One CBS Pump	161.61

<u>Resolution of In-Vessel Downstream Effects per NRC Review Guidance</u>

The NRC review guidance (Reference 9) on in-vessel effects provided four different paths (identified as Box 1 through Box 4 paths) that PWR licensees can use to resolve the issue based on the AFP analysis in WCAP-17788. NextEra chose to use the Box 4 path for the Seabrook resolution. This approach requires the licensee to demonstrate applicability of the WCAP-17788 AFP analysis to plant conditions. To meet this requirement, Table 3.n.1-3 and Table 3.n.1-4 summarize the comparison of key in-vessel parameters between Seabrook and those used in the WCAP analysis. More detailed discussions of these parameters are presented after the table.

Table 3.n.1-3: Summary of In-Vessel Effects Parameters

Parameters	WCAP-17788 Revision 1 Values	Seabrook Values
Nuclear Steam Supply System (NSSS) Design	Various	Westinghouse
Fuel Type	Various	Westinghouse 17 x 17
Barrel/Baffle Configuration	Various	Upflow
Minimum Chemical Precipitation Time	143 minutes t_{block} from WCAP-17788, Volume 1, Table 6-1	24 hours
Maximum Hot Leg Recirculation Switchover (HLSO) Time	N/A	5 to 6 hours
Minimum Sump Switchover (SSO) Time	20 minutes	26 minutes
Maximum Rated Thermal Power	3658 MWt	3648 MWt
Maximum AFP Resistance	[ ]a,c	[ ]a,c
ECCS Flow per Fuel Assembly	8 – 40 gpm/FA	15.77 – 32.77 gpm/FA

Comparison of Seabrook Chemical Precipitation Time with HLSO Time and t_{block}

For Seabrook, chemical precipitation was shown to occur after the latest HLSO time and after the time that complete core inlet blockage can be tolerated, which is defined in WCAP-17788 as t_{block}.

1. Seabrook chemical precipitation time (t_{chem}) – Chemical precipitation is shown not to occur within 24 hours after the accident for containment sump temperatures above 75°F based on the autoclave testing in WCAP-17788, Volume 5 (Reference 11). This was determined using a precipitation map to compare the sump aluminum concentration estimated with the WCAP-16530 methodology with all NaOH group autoclave test results and the WCAP-17788 precipitation boundary equation (see Figure 3.n.1-10). Autoclave tests performed at a pH greater than 10 were omitted as non-representative of Seabrook, which has a maximum final containment sump pool pH of 9.4.

   The aluminum concentration results from the WCAP-17788 autoclave tests that used NaOH buffer are shown in Figure 3.n.1-10 as plus signs. Test results where precipitation was detected are overlaid with red dots. The WCAP-17788 precipitation boundary equation is also plotted on the figure for pH values of 8.8 and 9.4, which is representative of the Seabrook post-LOCA containment sump pH range. The WCAP precipitation boundary at a pH of 8.8 (solid blue curve) is used in this analysis because it conservatively minimizes aluminum solubility (high p[Al]).

   Using the maximum sump aluminum concentration at 24 hours determined from the WCAP-16530 methodology and the minimum sump pH of 8.8, the pH + p[Al] was calculated to be 11.89 (see the red dotted line in Figure 3.n.1-10), which crosses the precipitation boundary at 75°F. Containment sump temperatures below 75°F by 24 hours would be indicative of a significantly less severe accident than simulated using the WCAP-16530 methodology. Therefore, aluminum precipitation will not occur within 24 hours.

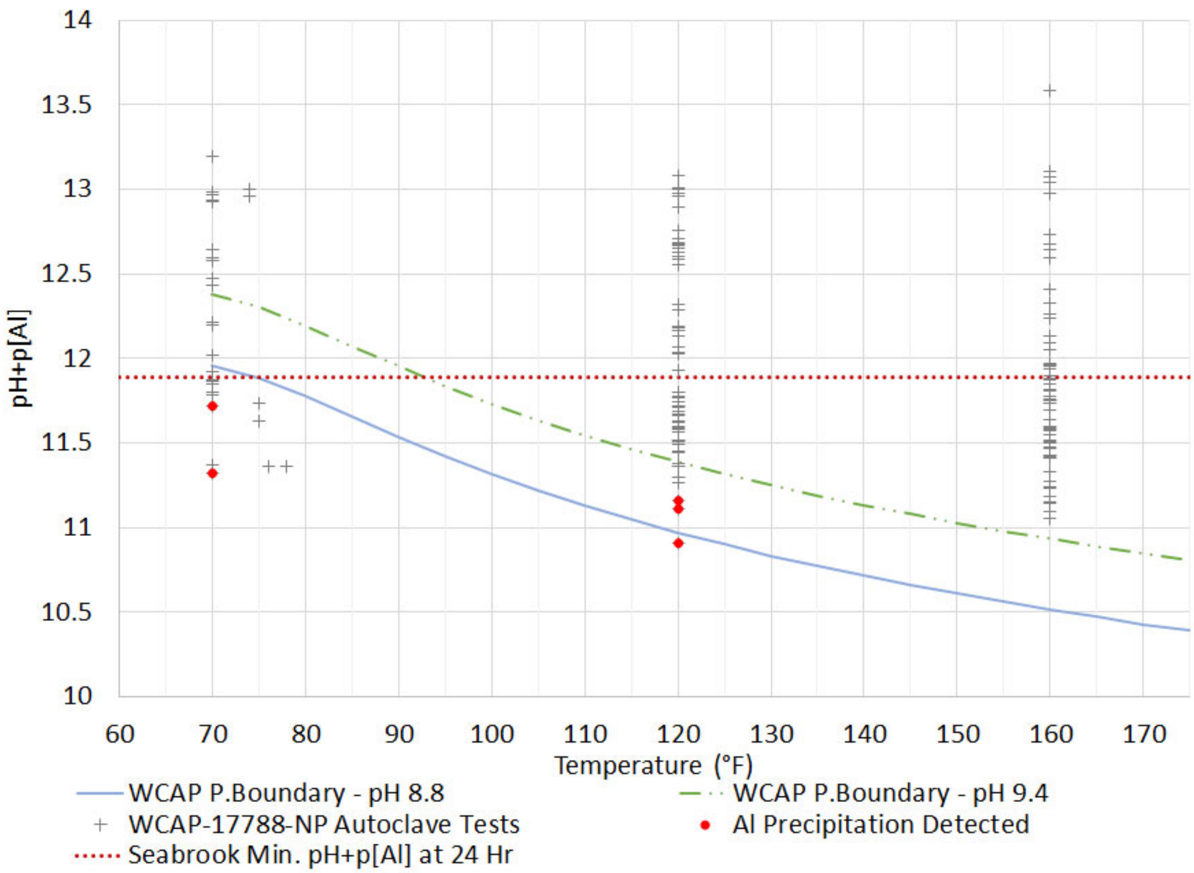

Figure 3.n.1-10: 24 Hours Aluminum Solubility

2. Seabrook HLSO time – Seabrook maximum HLSO time is 5 to 6 hours after the accident.
3. Time of t_{block} used in WCAP-17788 – Seabrook is a Westinghouse NSSS plant with an upflow barrel/baffle design. WCAP-17788 used a t_{block} of 143 minutes for this reactor design (Reference 10).

Comparison of Seabrook SSO Time with that Assumed in WCAP-17788

The earliest SSO time for Seabrook is greater than that assumed in the WCAP-17788 analysis.

1. Seabrook SSO time – The SSO time marks the beginning of sump recirculation and fiber accumulation inside the reactor. For Seabrook, the shortest duration for injection from the RWST is 26 minutes. This duration was determined conservatively by neglecting the volume of the SAT (over 7000 gallons) and the margin in the RWST usable volume (over 2,000 gallons). Additionally, the pump flow rates used were calculated assuming no backpressure.
2. The SSO time assumed in the WCAP-17788 analysis is 20 minutes (Reference 32).

Comparison of Seabrook Maximum Thermal Power with that Assumed in WCAP-17788

Seabrook maximum rated thermal power is less than that analyzed in WCAP-17788 for a Westinghouse NSSS with an upflow barrel/baffle design.

1. Seabrook rated thermal power – Seabrook maximum rated thermal power is 3648 MWt.
2. Thermal power assumed in WCAP-17788 – The WCAP analysis used a thermal power of 3658 MWt for Westinghouse upflow plants, provided in Table 6-1 of WCAP-17788, Volume 4 (Reference 32).

Comparison of Seabrook Reactor AFP Resistance with that Assumed in WCAP-17788

The Seabrook reactor AFP resistance is less than that analyzed in WCAP-17788.

1. Seabrook reactor AFP resistance – The Seabrook AFP resistance is

   [ ]^{a,c}, presented in Table RAI-4.2-24 of WCAP-17788, Volume 4, as "Total Unadjusted K/A^2".
2. Maximum AFP resistance assumed in WCAP-17788 – The maximum AFP resistance used for the WCAP analysis is [ ]^{a,c}, presented in Table 6-1 of WCAP-17788, Volume 4, as "Barrel/Baffle Total K/A^2".

Comparison of Seabrook ECCS Flow Rate with that Analyzed in WCAP-17788

The Seabrook ECCS flow per fuel assembly is within the range of flow rates analyzed in WCAP-17788.

1. Seabrook ECCS flow rate – The Seabrook ECCS flow rate per fuel assembly is between 15.77 gpm/FA and 32.77 gpm/FA, calculated by dividing the minimum flow rate of a single RHR pump and the maximum two-train RHR flow rate by the number of fuel assemblies.
2. ECCS flow rates analyzed in WCAP-17788 – For Westinghouse upflow plants, the analyzed ECCS flow rate is 8 gpm/FA to 40 gpm/FA (Reference 32).

As shown above, all of the in-vessel parameters listed in Table 3.n.1-3 for Seabrook are bounded by those used in the WCAP-17788 AFP analysis. Per the Box 4 path in the NRC review guidance, the only other parameter that needs to be addressed is the in-vessel fiber load, which is discussed next.

<u>Seabrook In-Vessel Fiber Loads and Comparison with WCAP-17788 limits</u>

The maximum Seabrook HLB core-inlet fiber loads for the worst breaks (see Table 3.n.1-2) are compared with the WCAP-17788 fiber limits in Table 3.n.1-4. For the single train failure case, the resulting core inlet fiber load exceeds the WCAP-17788 core inlet fiber limit but is less than the WCAP-17788 total in-core fiber limit. For the other two pump lineups (i.e., with all pumps available and failure of one CBS pump), the Seabrook core inlet fiber loads exceed both limits. Note that the Seabrook fuel assembly has the same pitch as was used in WCAP-17788 Volume 1, and therefore, no adjustment to the core inlet fiber limit is necessary.

Table 3.n.1-4: Maximum In-Vessel Fiber Loads

Pump line up	In-Vessel Fiber Load (g/FA)	Core Inlet Fiber Limit (g/FA)	Total In-Core Fiber Limit (g/FA)
Single Train Failure	55.13	[ ]a,c	[ ]a,c
All Pumps in Operation	108.48		
One CBS Pump Failure	161.61		

The subsections below demonstrate that, although the maximum in-vessel fiber loads exceed the WCAP-17788 limits, LTCC is ensured for all operating scenarios considered for Seabrook.

Single Train Failure Case

The maximum Seabrook core inlet fiber loading with failure of one ECCS and CBS train (55.13 g/FA) is greater than the HLB core inlet fiber limit, but much less than the total in-vessel fiber limit. Per the PWROG guidance, if analysis shows that the fiber reaching the reactor core following an HLB exceeds the core inlet fiber limit but is less than the in-vessel debris limit of [ ][a,c], credit for non-uniform debris buildup at the core inlet should be taken.

Westinghouse's model of predicted flow patterns shows generally upward flow to the high power assemblies at the center of the core while lower powered assemblies on the periphery of the core tend to have downward flows due to coolant entering through the barrel-baffle region. The Seabrook configuration is similar to that shown in the Westinghouse base case analysis for upflow reactors. This is also consistent with the NRC review guidance (Reference 9), which stated that "although the staff does not agree that the core split can be used to calculate an amount of debris that will bypass the core inlet via the AFPs, licensees may justify that a non-uniform debris bed will form at the core inlet allowing adequate flow to assure long term core cooling (LTCC), even though the average debris load per FA metric is exceeded."

All Pumps Available or Failure of One CBS Pump Summary

As shown in Table 3.n.1-4, the worst Seabrook core inlet fiber load with all pumps in operation or failure of one CBS pump exceeds the WCAP-17788 fiber limits. However, numerous sensitivities are performed in WCAP-17788 that demonstrate adequate LTCC for conditions very similar to the Seabrook plant specific configuration. Seabrook's decay heat at time of initial debris arrival is lower than that assumed in the WCAP-17788 base case. Sensitivities with reduced decay heat demonstrate expected core cladding temperature peaks are far below the 800 °F criterion during the initial period of debris arrival. Further, a high fiber case with peak loading nearly identical to Seabrook's and a similar debris buildup curve shows substantial cooling margin for Seabrook's most limiting case. Finally, using plant specific parameters, calculations show that normal core inlet flow is greater than boiloff for the entire event duration, and that AFP activation occurs shortly after debris arrival. These characteristics as well as additional margins described below demonstrate adequate LTCC for Seabrook's limiting fiber case.

For cooling analyses beyond a core inlet resistance of K_{max}, the sensitivity cases summarized above extrapolate the bounding resistance curve, K_{EQ}, in WCAP-17788. While the WCAP fuel assembly testing was performed at fiber loading less than the limiting case, it is conservative to use the limiting debris resistance curve for Seabrook's high flow cases. As described in WCAP-17788 Volume 6 (Reference 33), the K_{EQ} curve is based on experimental data from a subscale test facility. The limiting resistance curve, K_{EQ}, was developed based on testing up to the fiber loads that are acceptable at 20 minutes after shutdown. Testing finds a low flow regime to be the most limiting for K_{EQ} resistances. At middle and high flow regimes, the debris bed is unstable resulting in flattening resistance curves, and the resistance is consistently less than the low flow regime. This is due to a bed breakthrough phenomenon, which was consistently observed during fuel assembly testing at the middle and high flow regimes. The testing also showed that the debris bed and its resistance do not recover with subsequent debris additions. During an actual accident, the declining debris concentration over time will not allow the bed to re-establish. Therefore, it is appropriate and conservative for NextEra to use the most limiting debris loading resistance curve for all two ECCS train scenarios up to the peak fiber quantity.

The following conservatisms and mitigation factors are applicable to Seabrook and provide assurance of LTCC.

1. Lower Decay Heat

The WCAP analysis assumed a sump switchover time of 20 minutes after the initiation of the accident and used the “10 CFR 50 Appendix K” decay heat curve of 1971 ANS Infinite + 20%, along with a thermal power of 3658 MWt for the plant configuration applicable to Seabrook. The decay heat at the sump switchover time for this assumed configuration is 87.4 MWt.

Table 3.n.1-3 shows that the minimum SSO time for Seabrook is 26 minutes after the accident and the thermal power is 3648 MWt. As discussed above, this minimum SSO time was conservatively determined. Additionally, debris will not affect fuel performance until it reaches the reactor. Removing the margins due to rounding of pump flows, neglecting the SAT volume and debris transport time results in the earliest arrival of fiber at the core: 28.25 minutes (or 1695 seconds) following an accident. Using the Appendix K 1971 ANS Infinite + 20% decay heat curve, the decay heat at the earliest fiber arrival time after an accident is 80.6 MWt for Seabrook, which is ~8.4% lower than that analyzed in WCAP-17788.

As discussed in the response to the NRC RAI-4.7 on WCAP-17788, decay heat is the main driver of a debris-induced heatup. A sensitivity run therein demonstrates the reduction in debris-induced heatup as a result from assuming a reduced decay heat. This sensitivity illustrates that reduced decay heat results in less boiling and an increased reactor vessel liquid inventory.

2. Short Term Debris Transport Behavior during Initial Fiber Loading

As debris reaches the reactor and a debris bed forms at the core inlet, flow begins to become partially obstructed. Flow to the core inlet is driven by the downcomer level. As debris gradually builds up at the core inlet, backpressure increases, resulting in higher downcomer level and driving head over time. If the debris arrival is abrupt, downcomer level has less time to rise which can challenge core inlet cooling.

The base thermal hydraulic analysis in WCAP-17788, Volume 4 (Reference 32) assumed an abrupt 60 second arrival of debris at the core to reach the maximum resistance (Kmax) limit associated with a debris loading of [ ]a,c. Seabrook's in-vessel calculation showed that it takes 254 seconds (after start of SSO) for the core inlet fiber load to reach the fiber limit of [ ]a,c. This time is much longer than the 60 seconds assumed in the WCAP analysis. Additionally, as discussed above, debris would not reach the reactor core until at least 28.25 minutes (or 1695 seconds) after the accident for Seabrook, which is 495 seconds later than the 20 minutes assumed in the WCAP analysis.

In the PWROG's response to the NRC RAI-4.19(b) on WCAP-17788, the sensitivity Case 1 and Case 2 demonstrated that delaying sump switchover time by 200 and 400 seconds, respectively, while still ramping up the core inlet resistance within 60 seconds after start of recirculation reduced the peak cladding temperature (see Figure 3.n.1-11) and the potential for debris induced core uncovery and heatup. These cases demonstrate that a SSO similar to Seabrook's demonstrates adequate core cooling during the initial debris arrival period due to reduction in decay heat alone. Sensitivity Case 3 showed that, when the start of core inlet resistance increase is delayed by 200 seconds after SSO (instead of starting promptly at SSO) and the resistance ramps up over a 300-second (instead of 60-second) period, the model predicted a less severe core uncovery and heat-up, and a much lower peak cladding temperature (just over 400°F for Case 3 compared with ~800°F in the base case, see Figure 3.n.1-11). Table 3.n.1-5 compares the specific Seabrook parameters with those in the sensitivity cases from Table RAI-4.19-1 of the WCAP. Seabrook's SSO time and resistance ramp-up time are similar to sensitivity Cases 2 and 3, respectively. As discussed above, either effect is enough to reduce the peak cladding temperature response to just over 400°F.

Table 3.n.1-5: Comparison of Seabrook Parameters with WCAP Cases

Case	SSO Time (sec)	Start of Core Inlet Resistance (sec)	Resistance Ramp Time (sec)
Base Case (2B)	1200	1200	60
Sensitivity Case 1	1400	1400	60
Sensitivity Case 2	**1600**	**1600**	60
Sensitivity Case 3	1200	1400	**300**
Seabrook	**1560** (note 1)	**1560** (note 1)	**254**

Note 1: This is based on the minimum Seabrook SSO time of 26 minutes without fiber transit time.

Note that the sensitivity cases in the response to RAI-4.19(b) were performed for Westinghouse downflow plants because they bound the conditions of the upflow plants.

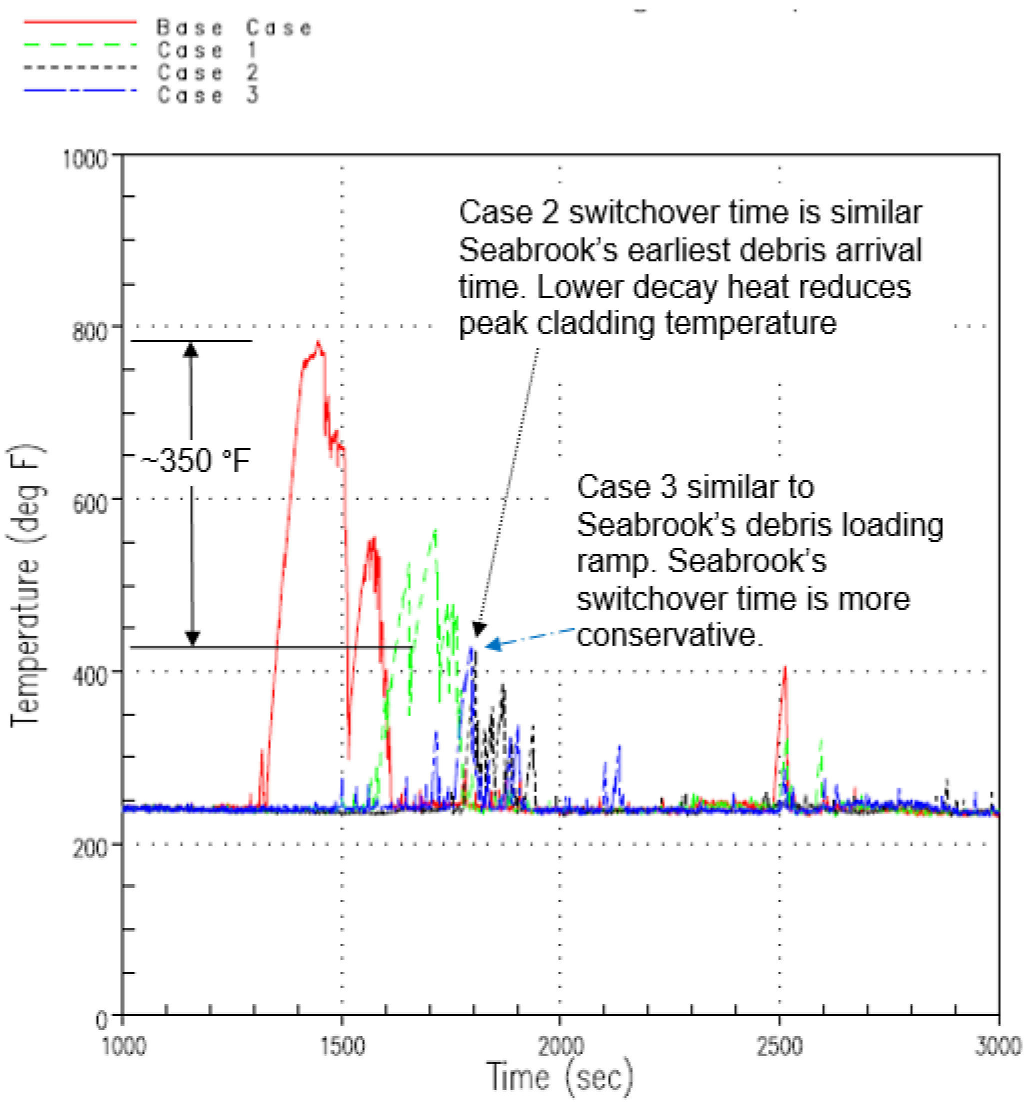

Figure 3.n.1-11: Cladding Temperature Response with Delayed SSO and Longer Debris Ramp (Figure RAI-4.19-1 in WCAP-17788-P, Volume 4)

3. Debris Transport Behavior until Steady State Fiber Loading

As a more substantial debris bed forms on the strainer, debris bypass through the strainer slows down, so does the debris accumulation at the reactor core inlet. Seabrook in-vessel analysis showed that, for the largest breaks with failure of a CBS pump, the core inlet fiber load reaches [ ]^{a,c} at 884 seconds after start of SSO and increases to the maximum fiber load of 161.61 g/FA at 223 minutes after start of SSO.

Section 8.0 and the response to the NRC RAI-4.7 in WCAP-17788 Volume 4 presented two sensitivity cases (Cases 3A and 3B) using the Westinghouse upflow plant model. These two cases applied core inlet loss coefficient that increased linearly over a period of 1 and 2 hours, respectively, after the start of SSO (as opposed to the instantaneous debris at the core) to simulate a more realistic build-up of debris. Figure 3.n.1-12 illustrates the increase in core inlet loss coefficient of Case 3B (see the blue dash dotted line). This sensitivity case resulted in a fiber limit of 163 g/FA when the peak resistance is reached. This fiber limit is very close to the maximum Seabrook in-vessel fiber load of 161.61 g/FA with the failure of one CBS pump. As stated above, it takes 223 minutes for the Seabrook core inlet fiber load to reach this maximum, compared with 120 minutes in Case 3B.

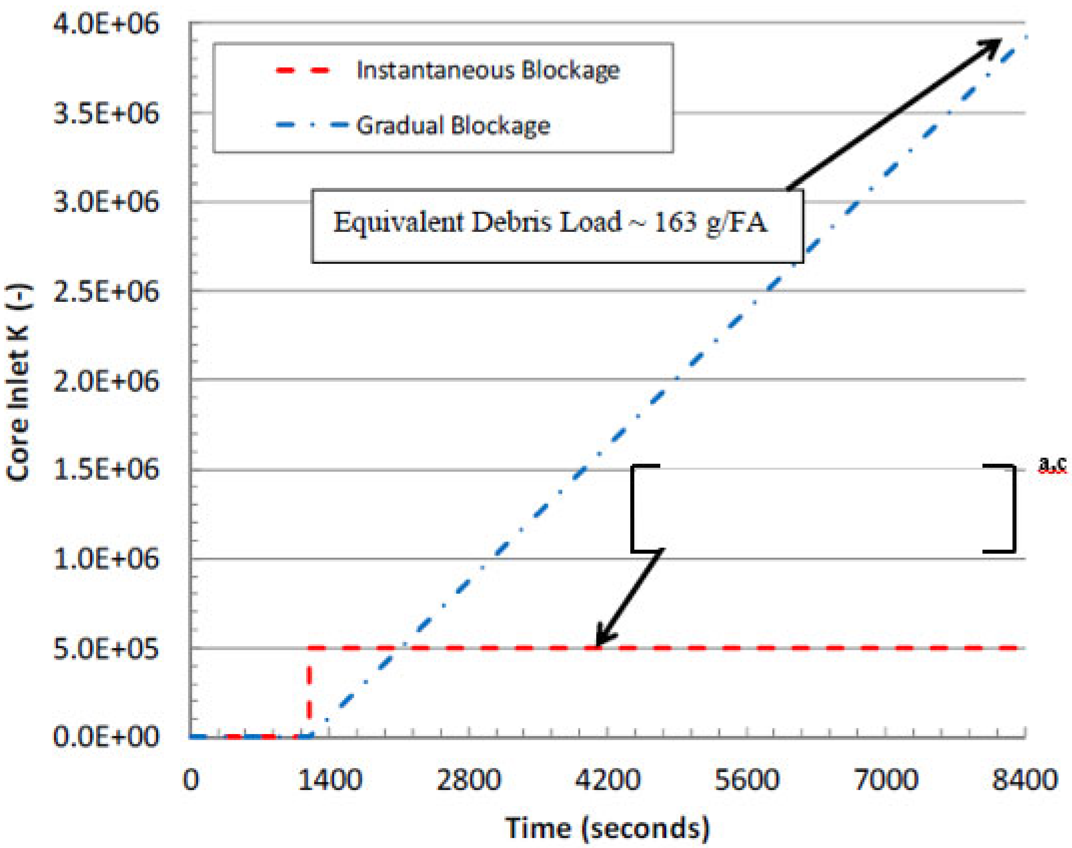

Figure 3.n.1-12: Core Inlet Resistance for RAI-4.7-20 Case 3B (Figure RAI-4.7-20 in WCAP-17788-P, Volume 4)

As shown in Table 8-3 of WCAP-17788 Volume 4, Case 3A and Case 3B result in peak cladding temperatures of <525°F and <500°F, respectively, which are below the acceptance criteria of 800°F. In these cases, a core-wide uncovery does not occur because the downcomer filled as the resistance at the core inlet increased gradually. As such, there is always coolant flow in excess of boil-off reaching the core.

Figure 3.n.1-13 compares Case 3A, which models the one hour linear ramp-up of resistance, with the Seabrook core inlet fiber resistance. The equations in Table 6-2 of WCAP-17788-P, Volume 1 (Reference 10) were used to convert the Seabrook in-

vessel fiber loading to equivalent resistance (K_{EQ}). The Region 3 equation is used to extrapolate for fiber loads beyond the maximum value specified in Table 6-2 of WCAP-17788-P, Volume 1. Because of the timing differences in the start of SSO, the time after shutdown is converted to decay heat (based on the 1971 ANS Standard + 20%) for Case 3A, Case 3B, and Seabrook in-vessel fiber loading. As shown in Figure 3.n.1-13, although Seabrook has a relatively high fiber load, when considering Seabrook's delayed sump recirculation phase (and resultant lower decay heat level) the loading is similar to Case 3A.

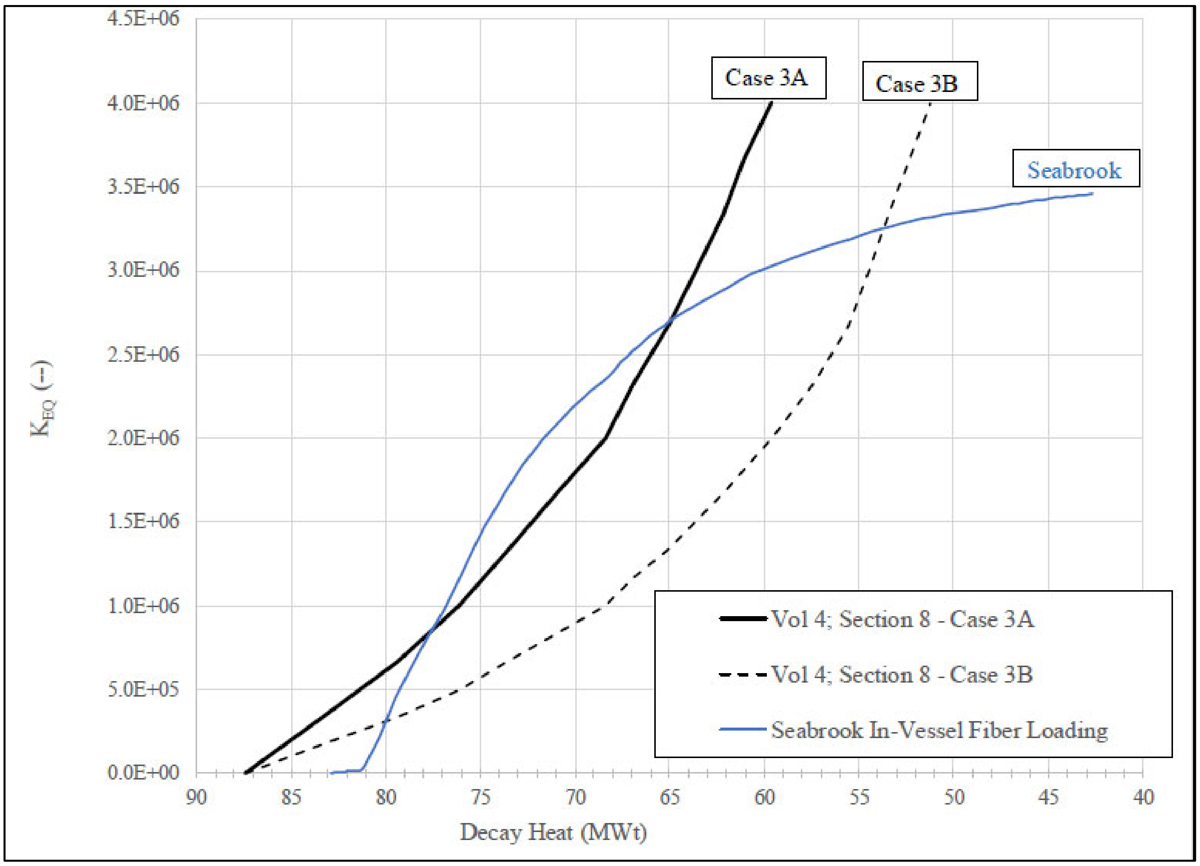

Figure 3.n.1-13: Comparison of K_{EQ} vs Decay Heat from Case 3A and Seabrook In Vessel Fiber Loading

The Seabrook fiber loading condition is similar to that of Cases 3A and 3B, as shown in the table below.

Table 3.n.1-6: WCAP-17788, Volume 4 Case 3A, Case 3B, and Seabrook Comparison

	Recirculation Flow	Resistance Curve Fiber Loading	Peak Cladding Temperature
Case 3A	40 gpm/FA	163 g/FA over 1 hour	<525 °F
Case 3B	18 gpm/FA	163 g/FA over 2 hours	<500 °F
Seabrook Limiting Case	32.77 gpm/FA	161.61 g/FA with similar curve to Case 3A	Expected to be similar to Case 3A

As shown above, Seabrook has a similar resistance curve to Case 3A with 19% less flow. Case 3B demonstrates that a much lower flow with less resistance yields similar peak cladding temperatures. Therefore, should the Seabrook specific conditions be modeled, the resulting peak cladding temperature is expected to be similar to that of Case 3A. The modeled peak cladding temperature over time is shown in the figure below.

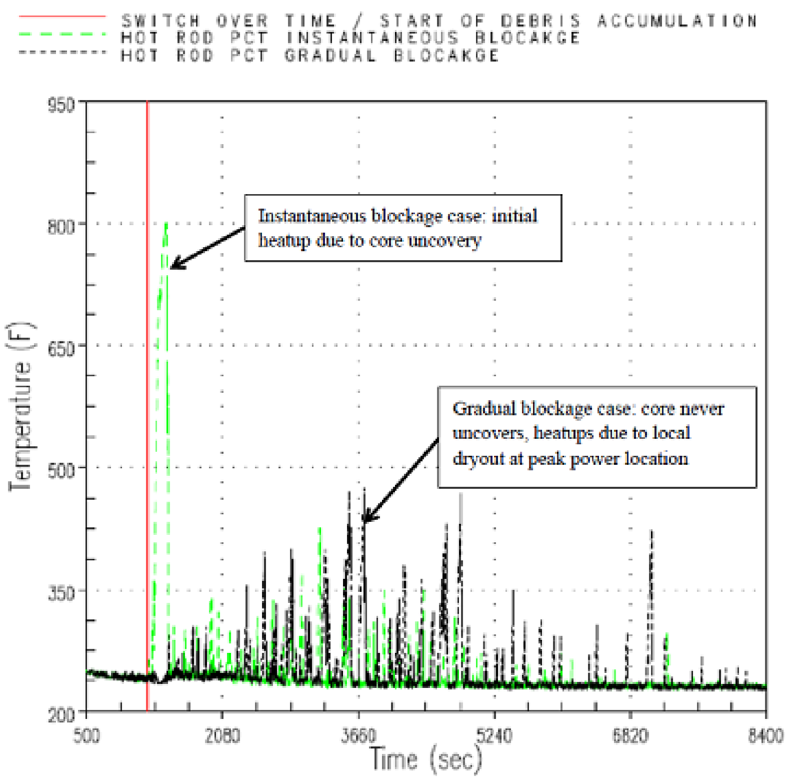

Figure 3.n.1-14: Comparison of Instantaneous Blockage to a Case Similar to Seabrook (Figure RAI-4.7-21 in WCAP-17788, Volume 4)

4. Margin in AFP Resistance and Defense-in-Depth

The analyses in WCAP-17788 Volume 4 indicated that AFPs in the reactor vessel can supply the necessary coolant flow to the core in case of complete blockage of the core inlet. As stated in the NRC review guidance, the staff applied considerable scrutiny to these analyses and expected that AFPs can provide an additional means to ensure adequate LTCC. For Seabrook, the flow resistance of the AFPs in the barrel/baffle (BB) region is 3.4% less than that analyzed in WCAP-17788 (See Table 3.n.1-3). Therefore, should the core inlet be blocked by debris, the AFPs of the Seabrook reactor will allow more flow to reach the core than that analyzed in the WCAP.

Additionally, WCAP-17788 Volume 4, RAI-4.19 analyses were performed to examine a more gradual build-up of debris at the core inlet. The gradual increase in resistance at the core inlet slowly raises the downcomer level and delays the activation of the AFPs. Eventually, the downcomer driving head becomes sufficiently large to change the flow direction in the BB channel. After this point, flow from the lower plenum (LP) is split between the core inlet and the AFPs and, as the core inlet resistance continues to build, the flow fraction to the AFPs continues to increase.

Using a conservatively low Seabrook recirculation flow rate of 31.8 gpm/FA for degraded ECCS pumps, the Seabrook in-vessel debris as a function of time after shutdown, and Figures 6-1 and 6-2 of WCAP-17788-P Volume 1, the AFPs are estimated to activate 30s after SSO time or 26.5 minutes following the accident for Seabrook. At 28 minutes, the flow through the AFPs exceeds boiloff. This is before the time when K_{MAX} is reached (i.e., 30 minutes). The flow to the core inlet is well above boiloff. It is therefore reasonable to conclude that the AFPs provide an effective cooling path should significant core inlet blockage occur. Figure 3.n.1-15 illustrates this calculation.

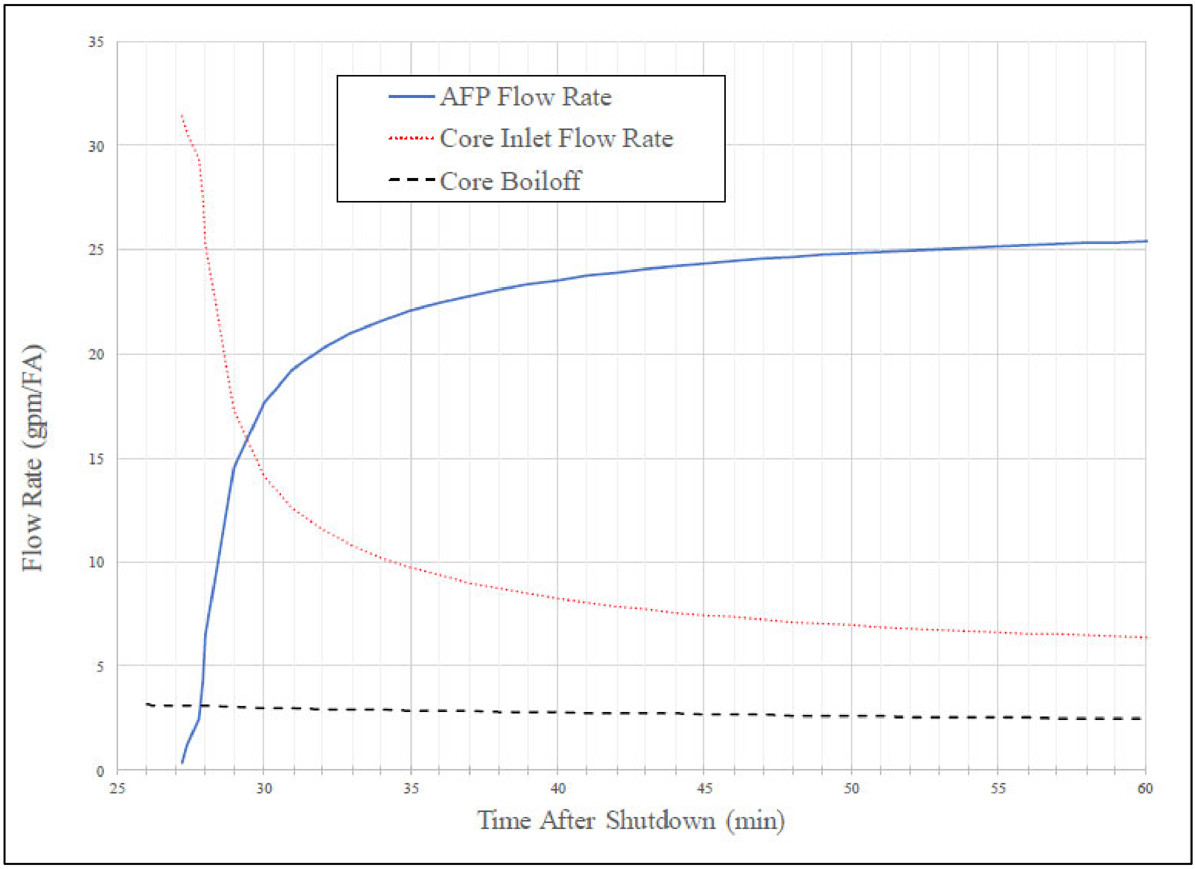

Figure 3.n.1-15: Core Inlet and AFP Flow Rates Compared to Boiloff

5. Recirculation flow margin

The ECCS recirculation flow that resulted in the highest in-vessel fiber load is 32.77 gpm/FA. Note that this flow rate does not consider pump degradation since a higher ECCS flow rate results in higher core inlet fiber loading. If pump degradation is considered, the ECCS flow rate is 31.8 gpm/FA, which is significantly greater than the maximum flow rate of 18 gpm/FA tested in the WCAP for Westinghouse upflow plants. As shown in Figure 3.n.1-15, the core inlet flow provides more than a factor of two over the core boiloff flow rate, and the AFP flow is nearly a factor of 10 above the boiloff flow rate.

6. Injection Phase ECCS Flow Rates

For the Seabrook specific limiting fiber loading scenario, the injection flow rates are high, leading to improved cooling flow above the base model. This double ECCS drain injection flow for Seabrook is 33 gpm/FA. As discussed in WCAP-17788 Volume 4 and shown in Figure 3.n.1-16, high injection flows will significantly decrease the debris-induced peak cladding temperature. The higher flows raise the core collapsed liquid level and reduce void fractions at lower core elevations. The mitigating effects of the higher inventory continues for several minutes following sump switchover as shown in Figure RAI-4.24-12 (Reference 32 pp. A-490). The lower peak temperature is expected as this timing coincides with initial core inlet bed build-up. Further, higher injection flow rates raise downcomer level at switchover which also enhances flow. The Seabrook injection flow rate is substantially higher than those in Figure 3.n.1-16.

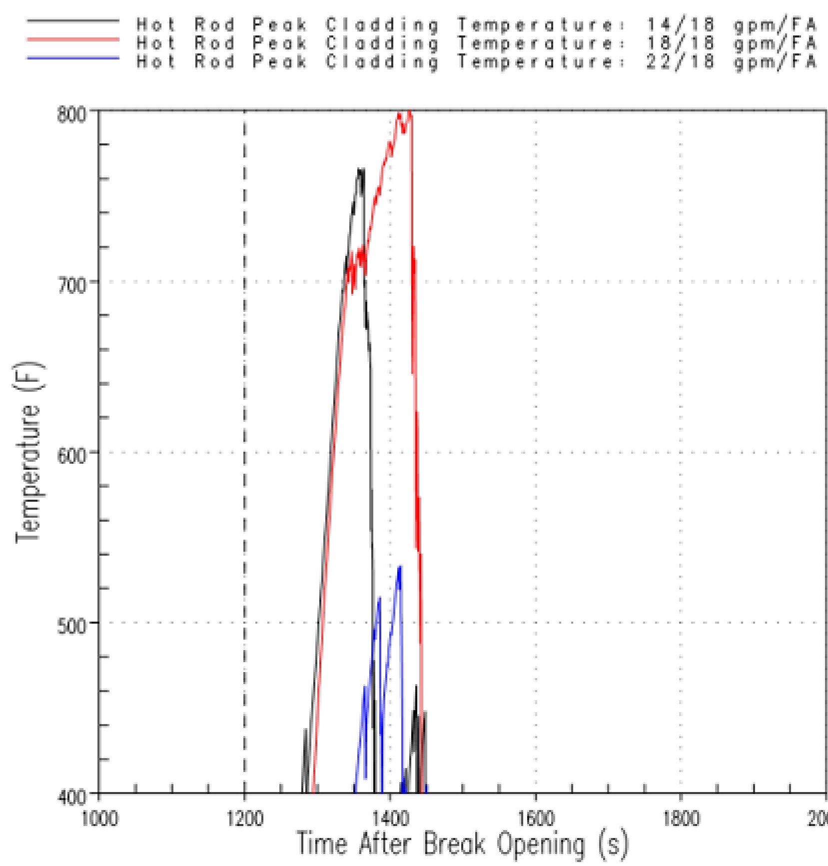

Figure 3.n.1-16: Westinghouse Injection Phase ECCS Flow Sensitivity Fuel (Figure RAI-4.24-8 in WCAP-17788 Volume 4)

Based on the comparisons shown above, the WCAP-17788 AFP analysis for Westinghouse upflow plants is applicable for Seabrook and can be used to show that in-vessel downstream effects due to accumulation of debris inside the reactor core will not challenge LTCC at Seabrook.

Basis for K_{EQ} Resistance Curve in High Fiber Cases with Two ECCS Trains

The WCAP-17788 Section 6 subscale testing examines fiber loading up to K_{max}. This is the amount of fiber that can be tolerated at sump switchover. Testing shows this resistance correlates to a plant equivalent fiber loading of [ ]a,c for a bounding Westinghouse upflow plant. The supporting subscale testing is performed up to a fiber quantity of [ ]a,c. That testing provides the basis for fiber resistance curves as described in WCAP-17788 Volume 1, Section 6.3.2. The limiting curve is based on low flow conditions that would be expected during single ECCS train operation. Testing shows the bed resistance for higher flow, two ECCS train operation is substantially lower as illustrated in Figure 3.n.1-18, Figure 3.n.1-19, and Figure 3.n.1-20. While debris resistance behavior for low flow conditions with high debris quantities are not known, high flow resistance curves flatten following the onset of a phenomenon called bed breakthrough. Seabrook's in-vessel analysis for two ECCS trains uses an extrapolation of the limiting low flow K_{EQ} curve. This is conservative, because testing shows a lower resistance curve is expected for the Seabrook-specific conditions due to an unstable fiber bed.

All of Seabrook's cases with greater than [ ]a,c are with two trains of ECCS, and therefore, have substantially greater ECCS flow than the WCAP-17788 base case resistance curve. For Seabrook, high ECCS flows are necessary to direct a large fraction of the fiber to the core and to exceed [ ]a,c. Due to Seabrook specific recirculation flow rates, the debris bed at the core inlet is unlikely to remain stable leading to substantially lower debris bed resistance. As stated in WCAP-17788 Volume 6 Section 5.3.1.2.2 on flow rate and p:f ratio parametric study with six mid and high flow test sets,

> [
>
>]a,c

Breakthrough occurs when intra-bed hydraulic differences cause localized particulate re-entrainment into the flow stream. After the initial "scouring" effect occurs, the interstitial flow increase results in additional shear stress at the pores. Due to the core inlet differential pressure increase after bed formation, the local velocities at the pores tend to be higher than the core inlet velocity prior to fiber arrival. As a result, high fiber concentrations are required to re-establish the bed. As stated in WCAP-17788 Volume 6 Section 3.3 on flow control,

> *At high interstitial velocities, fluid shear within the debris bed can reach a point in which scouring and potential bed breakthrough occurs. This can result in a dramatic reduction in pressure drop across the bed. This process is very chaotic and test-to-test variation after this occurs is very high. Preservation of the flow and*

pressure boundary conditions is necessary to preserve characteristics of the debris bed, such as porosity and bed compression that influence the onset of scouring.

Different from testing where debris was added incrementally, the concentration of fiber arriving at the reactor core following a LOCA decreases over time as the debris bed on the sump strainer grows, and bypass fraction declines (see Figure 3.n.1-8 and Figure 3.n.1-9). Therefore, an intact debris bed cannot reestablish after bed breakthrough occurs during an actual LOCA.

Breakthrough is also repeatable with different core geometries. The AREVA fuel achieved similar results over eight test series each showing breakthrough. As shown in Figure 3.n.1-20, after the bed becomes unstable, the pressure drop flattens. Pressure drop is typically less at peak fiber additions when compared to the onset of scouring.

Table 3.n.1-7 lists the approximate flow rates for each of the 12 gram fiber loading for tests shown in Figure 3.n.1-17, Figure 3.n.1-18 and Figure 3.n.1-19. The flows are calculated based on the flow profiles in WCAP-17788 Volume 6 Table 3-1 and Equation 3-1 therein. The values are scaled from subscale test to plant geometry. The Seabrook ECCS flow rate with the most limiting fiber loads is approximately 80% higher than the flow rate used during the “Final-Mid” tests.

Table 3.n.1-7: Comparison of Seabrook ECCS Flow with Subscale Test Flows

Flow Profile	Test Flow Rate
Final-Low	9 gpm/FA
Final-Mid	18 gpm/FA
Final-High	39 gpm/FA
Seabrook’s limiting case	32.77 gpm/FA

As shown in Figure 3.n.1-17 and Figure 3.n.1-18, at the maximum test fiber load, the “Final-Mid” tests resulted in pressure drops approximately one third of the “Final-Low” tests. Note that the higher pressure drops from the “Final-Low” tests were used as the base case in WCAP-17788. Therefore, the WCAP analysis base case bounds pressure drops for Seabrook specific conditions for the maximum fiber, two ECCS train case.

Considering that bed breakthrough occurred consistently during the higher flow tests for different debris composition and fuel designs, the fiber bed head loss curves at Seabrook are bounded by the WCAP-17788 base case loss coefficient curves.

a,c

Figure 3.n.1-17: Test Results at the Limiting Flow Profile "Final Low" (Figure 5-43 in WCAP-17788-P, Volume 6)

a,c

Figure 3.n.1-18: Test Results for the "Final-Mid" Flow Profile (Figure 5-45 in WCAP-17788-P, Volume 6)

[ ]a,c

Figure 3.n.1-19: Test Results for the "Final-High" Flow Profile
(Figure 5-46 in WCAP-17788-P, Volume 6)

[ ]a,c

Figure 3.n.1-20: AREVA Fuel Test Results for the "Final-High" Flow Profile
(Figure 5-57 in WCAP-17788 Volume 6)

3.o Chemical Effects

The objective of the chemical effects section is to evaluate the effect that chemical precipitates have on head loss and core cooling.

3.o.1 Provide a summary of evaluation results that show that chemical precipitates formed in the post-LOCA containment environment, either by themselves or combined with debris, do not deposit at the sump screen to the extent that an unacceptable head loss results, or deposit downstream of the sump screen to the extent that long-term core cooling is unacceptably impeded.

Response to 3.o.1:

The chemical effects strategy for Seabrook includes:

1. Quantification of maximum chemical precipitates using the WCAP-16530-NP-A methodology. The limitations and conditions of this WCAP were addressed as part of the evaluation and it was shown that the WCAP-16530-NP-A methods and values were appropriate to use for Seabrook.
2. Introduction of those pre-prepared precipitates in prototypical strainer testing.
3. Application of an aluminum solubility correlation to determine the maximum precipitation temperature.
4. Time-based determination of acceptable head losses.

As discussed in the response to Section 3.a.1, NextEra has determined the debris generated at all ISI welds on the primary RCS piping inside containment for Seabrook. The amount/mass of chemical precipitate was quantified for bounding quantities of LOCA generated debris. Other plant-specific inputs such as pH, temperature, aluminum quantity, and spray times were selected to maximize the generated amount of precipitates. The precipitate amount was scaled by the ratio of the test strainer area to the plant strainer surface area and was compared with the chemical debris quantities used in the prototypical strainer tests to determine the resulting head loss across the strainers. Before the chemical debris portions of the tests were conducted, the AlOOH was prepared according to the WCAP-16530-NP-A recipe and was verified to meet the settling criteria. During the test, a fiber and particulate debris bed was established on the strainer surfaces, the stabilization criteria was satisfied, and the pre-prepared precipitates were added to the test tank in batches. See the response to Section 3.f.4 for further details on the head loss measured after introduction of chemical precipitates.

See the response to Section 3.n.1 for the evaluation of impact of chemical precipitation on the in-vessel downstream effects.

3.o.2 Content guidance for chemical effects is provided in Enclosure 3 dated March 2008 to a letter from the NRC to NEI (Reference 7).

Response to 3.o.2:

The NRC identified evaluation steps in "NRC Staff Review Guidance Regarding Generic Letter 2004-02 Closure in the Area of Plant-Specific Chemical Effect Evaluations" in March of 2008 (Reference 7). NextEra's responses for Seabrook to the GL supplemental content evaluation steps are summarized below. The numbering of the following subsections to the response to Section 3.o.2 follow the numbering scheme provided in Section 3 and Figure 1 of the March 2008 guidance (Reference 7 pp. 8-23). Figure 3.o-1 highlights the Seabrook chemical effects evaluation process using the flow chart in Figure 1 of the March 2008 guidance (Reference 7 p. 8).

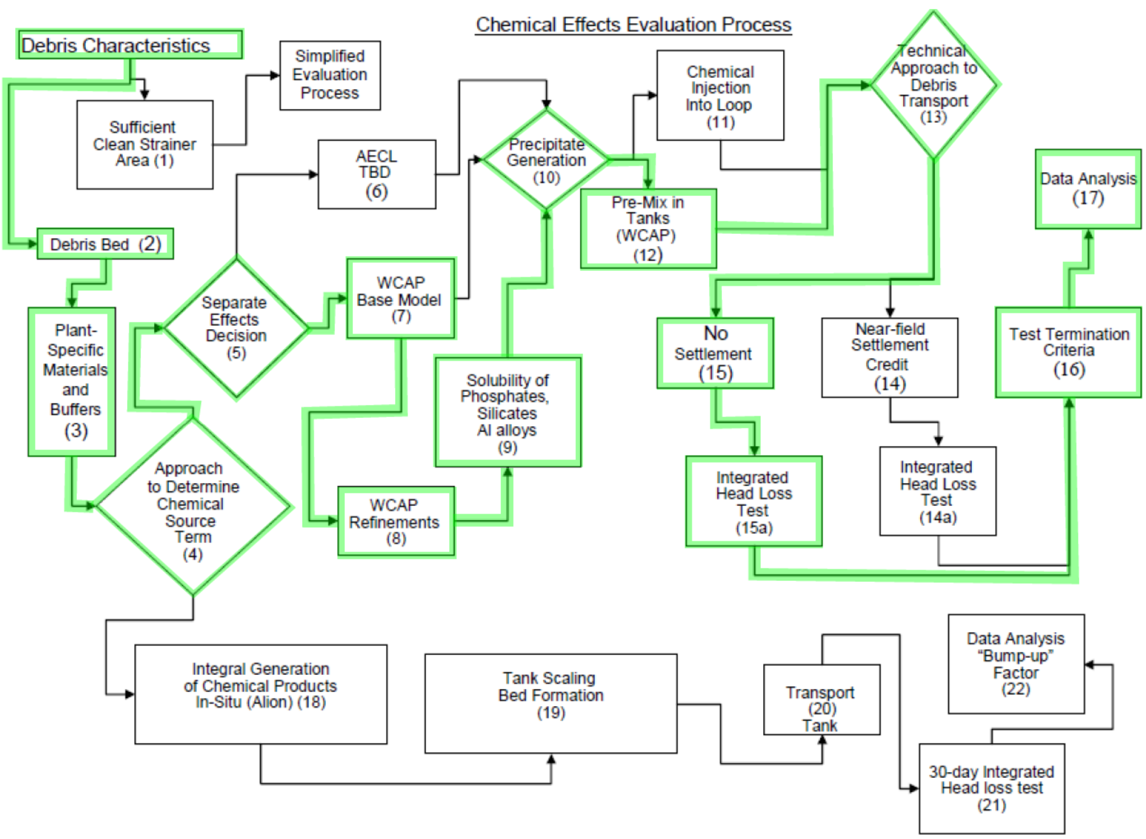

Figure 3.o-1: Chemical Effects Evaluation Process for Seabrook

1. *Sufficient 'Clean' Strainer Area: Those licensees performing a simplified chemical effects analysis should justify the use of this simplified approach by providing the amount of debris determined to reach the strainer, the amount of bare strainer area and how it was determined, and any additional information that is needed to show why a more detailed chemical effects analysis is not needed.*

   Response to 3.o.2.1:

   NextEra is not crediting clean strainer area to perform a simplified chemical effects analysis for Seabrook. See Figure 3.o-1.

2. *Debris Bed Formation: Licensees should discuss why the debris from the break location selected for plant-specific head loss testing with chemical precipitate yields the maximum head loss. For example, plant X has break location 1 that would produce maximum head loss without consideration of chemical effects. However, break location 2, with chemical effects considered, produces greater head loss than break location 1. Therefore, the debris for head loss testing with chemical effects should be based on break location 2.*

   Response to 3.o.2.2:

   Full load and thin bed head loss tests were completed for Seabrook to determine the conventional and chemical head losses. The tests evaluated the head loss response for a debris load bounding all breaks. Head loss contributions from conventional debris sources (fibrous insulation debris, latent debris, and particulate debris originating from coatings) as well as chemical precipitate sources (AlOOH) were evaluated in the test campaign. One test used a thin bed protocol, adding all particulates to the test prior to any fibrous debris additions. The other test followed the full debris load protocol, which added a mixture of particulates and fibrous debris. Chemical precipitate was added to these tests after the conventional debris as described in the response to Section 3.f.4. The response to Section 3.f.7 shows that the tested chemical debris loads bound the predicted plant load.

3. *Plant-Specific Materials and Buffers: Licensees should provide their assumptions (and basis for the assumptions) used to determine chemical effects loading: pH range, temperature profile, duration of containment spray, and materials expected to contribute to chemical effects.*

   Response to 3.o.2.3:

   The chemical model requires a number of plant-specific inputs. Each input was chosen to maximize the calculated quantity and minimize the solubility (aluminum only) of the chemical precipitates.

   NextEra uses sodium hydroxide (NaOH) for Seabrook to buffer the post-LOCA containment sump pool to a final pH between 8.8 and 9.4. The injection spray delivers the NaOH to the containment sump pool and is buffered to a maximum pH of 9.6. The pH value used for chemical release was conservatively high, and the pH value used for aluminum solubility was conservatively low. Different pH values for release and solubility were combined in a non-physical way, bounding the effects of all potential pH profile variations.

The pH values are summarized in Table 3.o.2.3-1:

Table 3.o.2.3-1: Seabrook pH Values

Injection Spray pH Used To Determine Chemical Release Rates	9.6
Sump and Recirculation Spray pH Used To Determine Chemical Release Rates	9.4
Sump pH Used To Determine Aluminum Solubility	8.8

The containment building sprays are initiated at 65 s (1.08 min) post-LOCA during the injection phase. The recirculation phase starts at 2755 s (45.92 min) for the minimum ECCS case, after which, the containment spray pH will be the same as the containment sump pool pH. The containment sprays were assumed to be active to the end of the 30-day post-LOCA event.

Conservative containment sump pool and containment temperature profiles were used to maximize chemical release rates. The temperature profiles are shown in Figure 3.o.2.3-1.

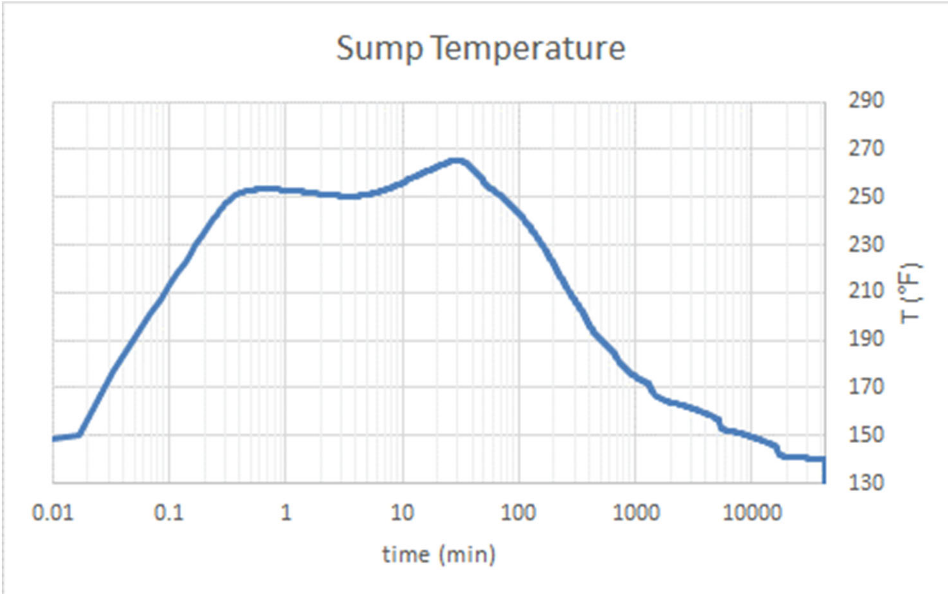

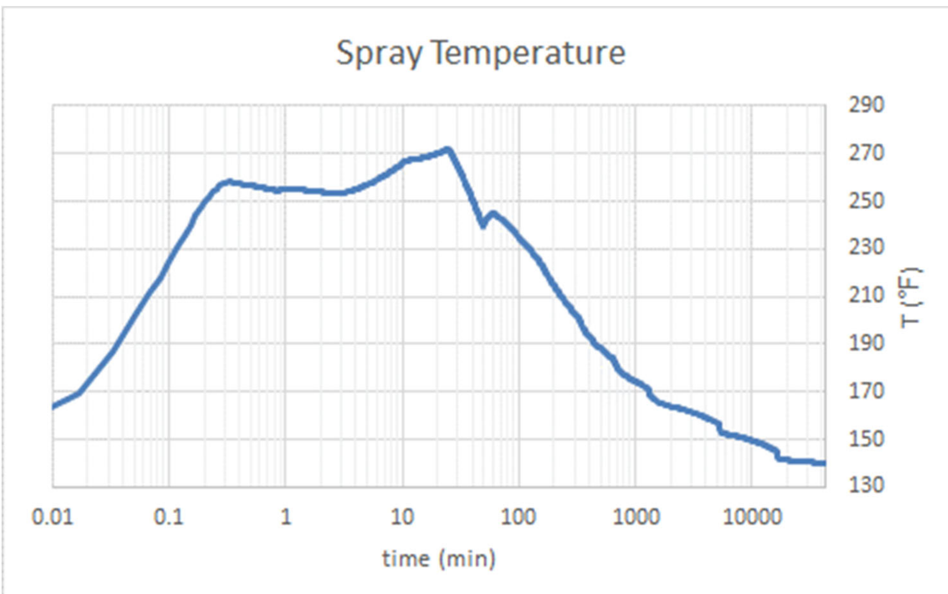

Figure 3.o.2.3-1: Sump Pool and Containment Spray Temperature Profiles used to Determine Chemical Release Rates

The total amount of concrete assumed to be exposed and submerged in the containment sump pool was 10,000 ft². The quantity of chemical precipitates was negligibly impacted by this large assumed surface area of exposed concrete. Therefore, exposed concrete is not a significant impact to chemical product generation in the Seabrook post-LOCA containment sump pool and is not tracked for this purpose.

The containment sump pool was assumed to be well mixed. This assumption conservatively maximized aluminum release by not considering the concentration gradient that will form around submerged source materials at low pool velocity conditions.

At Seabrook, the total amount of unsubmerged aluminum exposed to containment sprays is 776.2 ft^2 (including contingency). The total amount of submerged aluminum exposed to the containment sump fluid at Seabrook is 190.1 ft^2 (including contingency). The mass of these unsubmerged and submerged aluminum metals was in excess of the total aluminum that would be released into the containment sump pool, and therefore, no limit was set on the quantity released from these sources.

At Seabrook, the maximum containment sump pool mass that is available for chemical dissolution is 4,367,000 lbm. The maximum containment sump pool mass was used to conservatively maximize the mass of aluminum released from sources with concentration dependent release rates. The minimum containment sump pool mass that is available for chemical dissolution is 3,692,000 lbm. Given the conservatively maximized amount of aluminum released, the minimum containment sump pool mass was conservatively used to determine the concentration of aluminum for the solubility equation. Consistent with the WCAP-16530-NP-A methodology, the total mass was assumed to be present immediately post-LOCA.

The maximum amount of Nukon destroyed by the LOCA and assumed to be submerged was 2,809 ft^3 (including contingency) with an as-fabricated bulk density of 2.4 lbm/ft^3. The amount of latent fiber debris in containment is 15 lbm.

4. *<u>Approach to Determine Chemical Source Term (Decision Point)</u>: Licensees should identify the vendor who performed plant-specific chemical effects testing.*

Response to 3.o.2.4:

NextEra is using the separate chemical effects approach for Seabrook to determine the chemical source term. Alden performed the testing in their test lab in Holden, MA.

5. *<u>Separate Effects Decision (Decision Point)</u>: Within this part of the process flow chart, two different methods of assessing the plant-specific chemical effects have been proposed. The WCAP-16530-NP-A study (Box 7 WCAP Base Model) uses predominantly single-variable test measurements. This provides baseline information for one material acting independently with one pH-adjusting chemical at an elevated temperature. Thus, one type of insulation is tested at each individual pH, or one metal alloy is tested at one pH. These separate effects are used to formulate a calculational model, which linearly sums all of the individual effects. A second method for determining plant-specific chemical effects that may rely on single-effects bench testing is currently being developed by one of the strainer vendors (Box 6, AECL).*

Response to 3.o.2.5:

NextEra is using the WCAP-16530-NP-A chemical effects base model for Seabrook to determine the chemical source term. The application of an aluminum solubility correlation to determine a maximum precipitate formation temperature is discussed in the Responses to 3.o.2.8 and 3.o.2.9.i.

6. *<u>AECL Model</u>:*

   i. *Since the NRC is not currently aware of the complete details of the testing approach, the NRC staff expects licensees using it to provide a detailed discussion of the chemical effects evaluation process along with head loss test results.*

   Response to 3.o.2.6.i:

   This question is not applicable because NextEra is not using the AECL model for Seabrook. See Figure 3.o-1.

   ii. *Licensees should provide the chemical identities and amounts of predicted plant-specific precipitates.*

   Response to 3.o.2.6.ii:

   This question is not applicable because NextEra is not using the AECL model for Seabrook. See Figure 3.o-1.

7. *<u>WCAP Base Model</u>:*

   i. *Licensees proceeding from block 7 to diamond 10 in the Figure 1 flow chart [in Enclosure 3 dated March 2008 to a letter from the NRC to NEI* (Reference 7 p. 8)*] should justify any deviations from the WCAP base model spreadsheet (i.e., any plant specific refinements) and describe how any exceptions to the base model spreadsheet affected the amount of chemical precipitate predicted.*

   Response to 3.o.2.7.i:

   The Seabrook chemical model quantifies chemical precipitates using the WCAP-16530-NP-A (Reference 29) methodology with the following two deviations:

   1. The application of an aluminum solubility correlation to determine a maximum precipitate formation temperature (see the response to Section 3.o.2.9.i).
   2. The use of a new base model spreadsheet that follows the WCAP-16530-NP-A methodology.

An aluminum solubility correlation was used to determine a maximum precipitate formation temperature, which effectively delays the onset of aluminum precipitation. Therefore, to allow for time-based head loss acceptance criteria, a new spreadsheet was developed to include the requirement in the SE to double the aluminum release rate from aluminum metal over the initial 15 days. Additionally, the aluminum solubility was used to conservatively decrease the aluminum concentration after precipitation occurs, which increases the rate of release from insulation materials and concrete post-precipitation. As shown in Figures 3.o.2.7-1 and 3.o.2.7-2, the ICET 1 test results were simulated using the new spreadsheet and compared with the measured aluminum concentrations. The results verify that the new spreadsheet accurately predicts ICET 1 aluminum release and, therefore, can be used for time-based acceptance criteria in accordance with the WCAP-16530-NP-A SE.

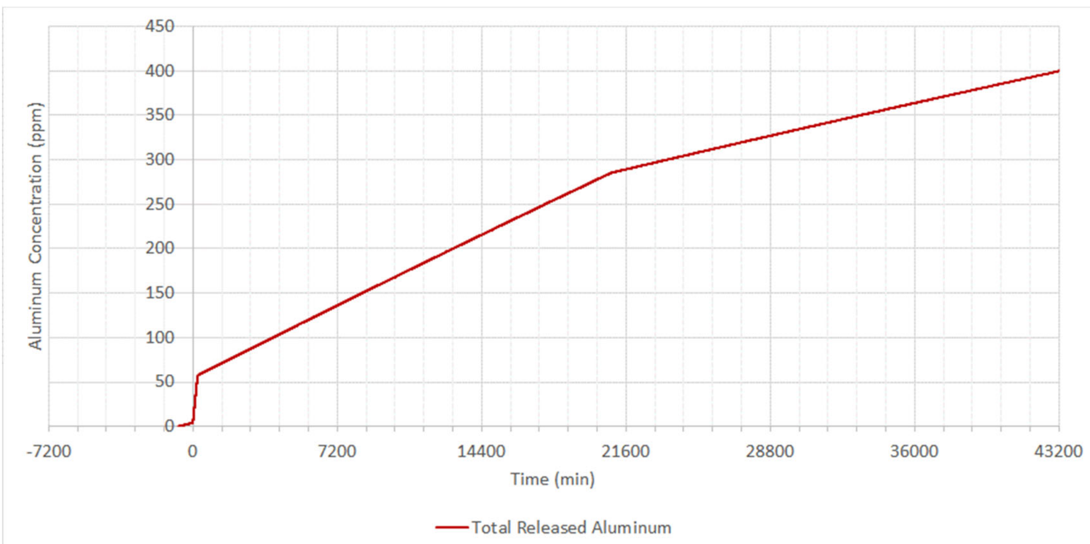

Figure 3.o.2.7-1: Simulation of ICET 1 Al Concentration

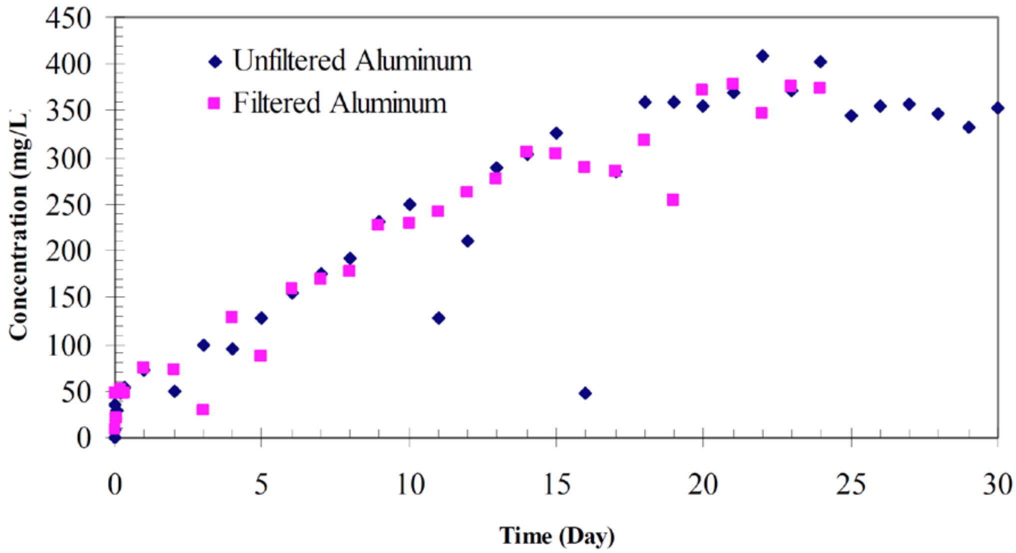

Figure 3.o.2.7-2: Measured Aluminum Concentrations in ICET 1

The chemical precipitates assumed by the WCAP-16530-NP-A methodology for plants that use NaOH buffer are AlOOH and sodium aluminum silicate ($NaAlSi_3O_8$). Per the WCAP-16530-NP-A SE, both aluminum precipitates are acceptable surrogates for aluminum precipitate in head loss testing. Therefore, to simplify head loss testing, only AlOOH is predicted to form by the new spreadsheet.

ii. *Licensees should list the type (e.g., AlOOH) and amount of predicted plant-specific precipitates.*

Response to 3.o.2.7.ii:

A bounding AlOOH precipitate mass of 182 kg (81.5 kg elemental aluminum) was calculated for Seabrook. The maximum temperature where aluminum precipitation could occur in the containment sump pool is 117.6°F.

The design contingency applied to the Nukon and aluminum quantities (discussed in the response to Section 3.o.2.3) results in an AlOOH precipitate mass margin of 18 kg.

8. *<u>WCAP Refinements</u>: State whether refinements to WCAP-16530-NP-A were utilized in the chemical effects analysis.*

Response to 3.o.2.8:

Refinement to the model for aluminum solubility is discussed in the response to Section 3.o.2.9.i. No other refinements to the WCAP-16530-NP-A methodology were used.

9. *Solubility of Phosphates, Silicates and Al Alloys:*

   i. *Licensees should clearly identify any refinements (plant-specific inputs) to the base WCAP-16530-NP-A model and justify why the plant-specific refinement is valid.*

Response to 3.o.2.9.i:

The base WCAP-16530-NP-A model assumes that aluminum precipitates form immediately upon the release of aluminum into solution. However, as justified in the response to Section 3.o.2.7.i, the Seabrook chemical model includes the following application of an aluminum solubility correlation to determine formation temperature and timing.

The aluminum solubility limit was determined using Equation 3.o.2.9-1, developed by Argonne National Laboratory (ANL).

$$\mathrm{C_{Al,sol}} = \begin{cases} 26980 \cdot 10^{(\mathrm{pH}+\Delta\mathrm{pH})-14.4+0.0243\mathrm{T}}, & \text{if } \mathrm{T} \leq 175\ °\mathrm{F} \\ 26980 \cdot 10^{(\mathrm{pH}+\Delta\mathrm{pH})-10.41+0.00148\mathrm{T}}, & \text{if } \mathrm{T} > 175\ °\mathrm{F} \end{cases} \qquad \text{(Equation 3.o.2.9-1)}$$

Nomenclature:

$\mathrm{pH} + \Delta\mathrm{pH}$ = sump pH including the change due to radiolysis acids
T = solution temperature, °F

The aluminum solubility limit equation was used to determine the temperature and timing of aluminum precipitation and to determine the aluminum concentration in solution for use in the aluminum release equations for concrete and insulation. When precipitation was predicted by this equation, the full amount of aluminum released was assumed to precipitate. The aluminum solubility limit equation was not used to reduce the predicted quantity of precipitate by crediting the amount remaining in solution.

A precipitation boundary function was developed by Westinghouse in WCAP-17788, Volume 5 to determine aluminum solubility in a PWR containment sump (Reference 11). Between pH 8.6 and 9.6, the ANL function is more conservative (lower aluminum solubility) at low temperatures (< 160°F), and the WCAP function is more conservative at higher temperatures. NextEra used a conservatively low pH of 8.8 (pH + ΔpH) for Seabrook to determine aluminum solubility (see Table 3.o.2.3-1). The maximum temperature where aluminum precipitation could occur in the containment sump pool is very low at 117.6°F (see the response to Section 3.o.2.7.ii). Although the WCAP function is more conservative at higher temperatures, both the WCAP and ANL functions would result in a higher aluminum solubility at higher temperatures and higher pH values. Therefore, the ANL equation is acceptable for use by NextEra for Seabrook.

ii. *For crediting inhibition of aluminum that is not submerged, licensees should provide the substantiation for the following: (1) the threshold concentration of silica or phosphate needed to passivate aluminum, (2) the time needed to reach a phosphate or silicate level in the pool that would result in aluminum passivation, and (3) the amount of containment spray time (following the achieved threshold of chemicals) before aluminum that is sprayed is assumed to be passivated.*

Response to 3.o.2.9.ii:

Silicon and phosphate inhibition of aluminum release were not credited. See the response to Section 3.o.2.9.i.

iii. *For any attempts to credit solubility (including performing integrated testing), licensees should provide the technical basis that supports extrapolating solubility test data to plant-specific conditions. In addition, licensees should indicate why the overall chemical effects evaluation remains conservative when crediting solubility given that small amount of chemical precipitate can produce significant increases in head loss.*

Response to 3.o.2.9.iii:

Reductions in precipitate quantity due to residual solubility of aluminum after precipitation occurs was not credited. See the response to Section 3.o.2.9.i.

iv. *Licensees should list the type (e.g., AlOOH) and amount of predicted plant-specific precipitates.*

Response to 3.o.2.9.iv:

The type and amount of plant-specific precipitates are provided in the response to Section 3.o.2.7.ii.

10. *<u>Precipitate Generation (Decision Point)</u>: State whether precipitates are formed by chemical injection into a flowing test loop or whether the precipitates are formed in a separate mixing tank.*

Response to 3.o.2.10:

NextEra pre-made surrogate chemical precipitates in a separate mixing tank for Seabrook chemical head loss testing. The direct chemical injection method was not used in head loss testing.

11. *<u>Chemical Injection into the Loop</u>:*

    i. *Licensees should provide the one-hour settled volume (e.g., 80 ml of 100 ml solution remained cloudy) for precipitate prepared with the same sequence as with the plant-specific, in-situ chemical injection.*

    Response to 3.o.2.11.i:

    The direct chemical injection method was not used in head loss testing for Seabrook. See Figure 3.o-1.

    ii. *For plant-specific testing, the licensee should provide the amount of injected chemicals (e.g., aluminum), the percentage that precipitates, and the percentage that remains dissolved during testing.*

    Response to 3.o.2.11.ii:

    The direct chemical injection method was not used in head loss testing for Seabrook. See Figure 3.o-1.

    iii. *Licensees should indicate the amount of precipitate that was added to the test for the head loss of record (i.e., 100 percent, 140 percent of the amount calculated for the plant).*

    Response to 3.o.2.11.iii:

    The direct chemical injection method was not used in head loss testing for Seabrook. See Figure 3.o-1.

12. *<u>Pre-Mix in Tank</u>: Licensees should discuss any exceptions taken to the procedure recommended for surrogate precipitate formation in WCAP-16530-NP-A.*

    Response to 3.o.2.12:

    Surrogate chemical debris preparation was performed according to the requirements of WCAP-16530-NP-A for AlOOH with no exceptions.

13. *<u>Technical Approach to Debris Transport (Decision Point)</u>: State whether near-field settlement is credited or not.*

    Response to 3.o.2.13:

    NextEra did not credit near field settlement for Seabrook in head loss testing. The Seabrook head loss test tank was designed to discourage settling to ensure that essentially all chemical debris analyzed to reach the strainer in the plant reached the strainer in head loss testing.

14. *Integrated Head Loss Test with Near-Field Settlement Credit:*

    i. *Licensees should provide the one-hour or two-hour precipitate settlement values measured within 24 hours of head loss testing.*

    Response to 3.o.2.14.i:

    NextEra is not crediting near field settlement of chemical precipitate for Seabrook in chemical head loss testing. See Figure 3.o-1.

    ii. *Integrated Head Loss Test with Near-Field Settlement Credit: Licensees should provide a best estimate of the amount of surrogate chemical debris that settles away from the strainer during the test.*

    Response to 3.o.2.14.ii:

    NextEra is not crediting near field settlement of chemical precipitate for Seabrook in chemical head loss testing. See Figure 3.o-1.

15. *Head Loss Testing Without Near Field Settlement Credit:*

    i. *Licensees should provide an estimate of the amount of debris and precipitate that remains on the tank/flume floor at the conclusion of the test and justify why the settlement is acceptable.*

    Response to 3.o.2.15.i:

    The test tank was designed to keep debris suspended and transportable to the test strainer, preventing notable settling of debris. Refer to the response to Section 3.f.12 for details.

    ii. *Licensees should provide the one-hour or two-hour precipitate settlement values measured and the timing of the measurement relative to the start of head loss testing (e.g., within 24 hours).*

    Response to 3.o.2.15.ii:

    Settling tests were executed immediately upon preparing the chemical precipitate solution. A given chemical precipitate solution could be used for 24 hours after passing a settling test; after that point, re-execution of the settling test was required to document the continued acceptability of the precipitate. All the precipitates met the acceptance criteria provided in the Safety Evaluation to WCAP-16530-NP-A.

16. *<u>Test Termination Criteria</u>: Licensees should provide the test termination criteria.*

Response to 3.o.2.16:

As shown in the response to Section 3.f.4, head loss was stabilized at the conclusion of conventional debris introduction and chemical debris introduction. Additional head loss stabilization periods were also implemented when a stabilized head loss measurement was desired. Head loss was considered stable when head loss was neither increasing nor decreasing at a rate greater than 0.5% over at least 30 minutes.

17. *<u>Data Analysis</u>:*

i. *Licensees should provide a copy of the pressure drop curve(s) as a function of time for the testing of record.*

Response to 3.o.2.17.i:

The pressure drop curves as a function of time for the head loss tests are shown in Figure 3.f.4-7 through Figure 3.f.4-11.

ii. *Licensees should explain any extrapolation methods used for data analysis.*

Response to 3.o.2.17.ii:

As discussed in the response to Section 3.o.2.16, head loss was stabilized before critical head loss values were obtained. Therefore, no extrapolation methods were necessary.

18. *<u>Integral Generation (Alion)</u>: Licensees should explain why the test parameters (e.g., temperature, pH) provide for a conservative chemical effects test.*

Response to 3.o.2.18:

NextEra is using the separate chemical effects approach for Seabrook to determine the chemical source term. This section is not applicable to the Seabrook chemical effects analysis. See Figure 3.o-1.

19. *Tank Scaling / Bed Formation:*

i. *Explain how scaling factors for the test facilities are representative or conservative relative to plant-specific values.*

Response to 3.o.2.19.i:

NextEra is using the separate chemical effects approach for Seabrook to determine the chemical source term. This section is not applicable to the Seabrook chemical effects analysis. See Figure 3.o-1.

ii. *Explain how bed formation is representative of that expected for the size of materials and debris that is formed in the plant specific evaluation.*

Response to 3.o.2.19.ii:

NextEra is using the separate chemical effects approach for Seabrook to determine the chemical source term. This section is not applicable to the Seabrook chemical effects analysis. See Figure 3.o-1.

20. *Tank Transport: Explain how the transport of chemicals and debris in the testing facility is representative or conservative with regard to the expected flow and transport in the plant-specific conditions.*

Response to 3.o.2.20:

NextEra is using the separate chemical effects approach for Seabrook to determine the chemical source term. This section is not applicable to the Seabrook chemical effects analysis. See Figure 3.o-1.

21. *30-Day Integrated Head Loss Test: Licensees should provide the plant-specific test conditions and the basis for why these test conditions and test results provide for a conservative chemical effects evaluation.*

Response to 3.o.2.21:

NextEra is using the separate chemical effects approach for Seabrook to determine the chemical source term. This section is not applicable to the Seabrook chemical effects analysis. See Figure 3.o-1.

22. *Data Analysis Bump Up Factor: Licensees should provide the details and the technical basis that show why the bump-up factor from the particular debris bed in the test is appropriate for application to other debris beds.*

Response to 3.o.2.22:

NextEra is using the separate chemical effects approach for Seabrook to determine the chemical source term. This section is not applicable to the Seabrook chemical effects analysis. See Figure 3.o-1.

3.p Licensing Basis

The objective of the licensing basis is to provide information regarding any changes to the plant licensing basis due to the sump evaluation or plant modifications.

3.p.1 Provide the information requested in GL 2004-02 Requested Information Item 2(e) regarding changes to the plant-licensing basis. The effective date for changes to the licensing basis should be specified. This date should correspond to that specified in the 10 CFR 50.59 evaluation for the change to the licensing basis.

GL 2004-02 Requested Information Item 2(e)
A general description of and planned schedule for any changes to the plant licensing bases resulting from any analysis or plant modifications made to ensure compliance with the regulatory requirements listed in the Applicable Regulatory Requirements section of this GL. Any licensing actions or exemption requests needed to support changes to the plant licensing basis should be included.

Response to 3.p.1:

As discussed in Section 2 of this response, various physical plant changes and procedural changes have been made at Seabrook to resolve GL 2004-02 concerns. The Seabrook UFSAR has previously been updated to incorporate the effects of plant modifications and evaluations performed in accordance with the requirements of 10 CFR 50.59.

There is one regulatory commitment. NextEra plans to modify the refueling canal drain and drain lines for Seabrook during the fall 2021 outage, and will update relevant UFSAR sections accordingly. Details of the modification are summarized in the response to Section 3.e.1.

Following receipt of a GL 2004-02 final closure letter, the UFSAR will be updated in accordance with 10 CFR 50.12(e).

The TS surveillance procedure was updated to expand the recirculation sump inspection requirements to include the entire sump strainer system. This change ensures that the entire system will come under the TS requirements for sump inspection and control. No further revision of the TS or TS Bases is anticipated.

The existing SR 4.5.2.d.2 mentions trash racks as potential sump components that should be included in the sump inspection. Although the new strainers installed at Seabrook do not include trash racks, in the context of TS surveillance, the debris interceptors in the vicinity of the sumps are viewed as “trash racks”. To ensure that these debris interceptors are available during Modes 1-4, the surveillance procedure was revised to include inspections of these debris interceptors in accordance with SR

4.5.2.d.2. NextEra has no current plans for Seabrook to revise the TS surveillance requirement since it ensures that the current design is in a condition ready to support operation of the ECCS recirculation sumps. Note that no credit was taken for debris holdup by the debris interceptors.

4. References

1. **NRC Generic Letter 2004-02 ML042360586.** Potential Impact of Debris Blockage on Emergency Recirculation During Design Basis Accidents at Pressurized Water Reactors. September 13, 2004.
2. **NRC Correspondence ML18031B248.** Seabrook, Unit 1 - Updated Final Response to NRC Generic Letter 2004-02. January 31,2018.
3. **PWROG-16073-P.** TSTF-567 Implementation Guidance, Evaluation of In-Vessel Debris Effects, Submittal Template for Final Response to Generic Letter 2004-02 and FSAR Changes. February 2020. Revision 0.
4. **NRC Correspondence ML073110278.** Revised Content Guide for Generic Letter 2004-02 Supplemental Responses. November 2007.
5. **NRC Correspondence ML080230038.** NRC Staff Review Guidance Regarding Generic Letter 2004-02 Closure in the Area of Strainer Head Loss and Vortexing. March 2008.
6. **NRC Correspondence ML080230462.** NRC Staff Review Guidance Regarding Generic Letter 2004-02 Closure in the Area of Coatings Evaluation. March 2008.
7. **NRC Correspondence ML080380214.** *NRC Staff Review Guidance Regarding Generic Letter 2004-02 Closure in the Area of Plant-Specific Chemical Effects Evaluation.* March 2008.
8. **NRC Correspondence ML19217A003.** Audit Report Regarding Generic Letter 2004-02, "Potential Impact of Debris Blockage on Emergency Recirculation During Design Basis Accidents at Pressurized Water Reactors" Closure Methodology. December 2, 2019.
9. **NRC Correspondence ML19228A011.** U.S. Nuclear Regulatory Commission Staff Review Guidance for In-Vessel Downstream Effects Supporting Review of Generic Letter 2004-02 Responses. September 4, 2019.
10. **Westinghouse WCAP-17788-P, Volume 1.** Comprehensive Analysis and Test Program for GSI-191 Closure (PA-SEE-1090). Revision 1, December 2019.
11. **Westinghouse WCAP-17788-NP, Volume 5.** Comprehensive Analysis and Test Program for GSI-191 Closure (PA-SEE-1090) – Autoclave Chemical Effects Testing for GSI-191 Long-Term Cooling. Revision 1, December 2019.
12. **NRC Correspondence ML18136A905.** Summary of April 25, 2018, Meeting with Florida Power & Light Company/NextEra Energy Regarding Planned Submittal of Exemption Requests to Support Closure of NRC Generic Safety Issue 191/NRC Generic Letter 2004-02. May 31, 2018.
13. **NRC Correspondence ML18243A043.** Exemption Request to Support Updated Final Response to NRC Generic Letter 2004-02. August 30, 2018.
14. **NRC Correspondence ML18331A033.** Audit Plan for NextEra Methodologies for Closure of Generic Letter 2004-02. November 26, 2018.

15. **NRC Correspondence ML20324A623.** Withdrawal of Exemption Request Supporting Updated Final Response to NRC Generic Letter 004-02. November 19,2020.
16. **NRC Correspondence ML20346A089.** Withdrawal of an Exemption Request Supporting Updated Final Response to NRC Generic Letter 2004-02 (EPID L-2018-LLE-0015). December 21, 2020.
17. **ASME Boiler and Pressure Vessel (B&PV) Code.** ASME Boiler and Pressure Vessel Code. *Section III, Subsection NC, Class 2 Components and Subsection NF Supports.*
18. **NEI Guidance Report NEI 04-07 Volume 1.** Pressurized Water Reactor Sump Performance Evaluation Methodology 'Volume 1 - Pressurized Water Reactor Sump Performance Evaluation Methodology'. December 2004. Revision 0.
19. **NEI Guidance Report NEI 04-07 Volume 2.** Pressurized Water Reactor Sump Performance Evaluation Methodology 'Volume 2 - Safety Evaluation by the Office of Nuclear Reactor Regulation Related to NRC Generic Letter 2004-02'. December 2004. Revision 0.
20. **NUREG-1829 Volume 1.** Estimating Loss-of-Coolant Accident (LOCA) Frequencies Through the Elicitation Process. April 2008.
21. **NRC Correspondence ML082210425.** Final Response and Notice of Completion for NRC Generic Letter 2004-02, "Potential Impact of debris Blockage on Emergency recirculation During Design Basis Accidents at Pressurized-Water Reactors". August 4, 2008.
22. **NRC Correspondence ML100960495.** Revised Guidance Regarding Coatings Zone of Influence for Review of Final Licensee Responses to Generic Letter 2004-02, "Potential Impact of Debris Blockage on Emergency Recirculation During Design Basis Accidents at Pressurized-Water Reactors". April 6, 2010.
23. **ANSI/ANS 58.2-1988.** Two-Phase Jet Model (ADAMS Accession No. ML050830344). September 15, 2004.
24. **NUREG/CR-6772 ML022410104.** *GSI-191: Separate Effects Characterization of Debris Transport in Water.* August 2002.
25. **NUREG/CR-6808 ML030780733.** *Knowledge Base for the Effect of Debris on Pressurized Water Reactor Emergency Core Cooling Sump Performance.* February 2003.
26. **Correspondence ML082050433.** Indian Point Energy Center Corrective Actions for Generic Letter 2004-02.
27. **NEI Correspondence ML120481057.** *ZOI Fibrous Debris Penetration: Processing, Storage and Handling.* Revision 1 : January 2012.
28. **NUREG/CR-6224 ML083290498.** Parametric Study of the Potential for BWR ECCS Strainer Blockage Due to LOCA Generated Debris. October 1995.

29. **Westinghouse WCAP-16530-NP-A.** Evaluation of Post-Accident Chemical Effects in Containment Sump Fluids to Support GSI-191. March 2008.

30. **Correspondence ML070950240.** San Onofre Nuclear Generating Station Unit 2 and Unit 3 GSI-191 Generic Letter 2004-02 Corrective Actions Audit Report.

31. **Westinghouse WCAP-16406-P-A.** Evaluation of Downstream Sump Debris Effects in Support of GSI-191. August 2007. Revision 1.

32. **Westinghouse WCAP-17788-P, Volume 4.** Comprehensive Analysis and Test Program for GSI-191 Closure (PA_SEE-1090) - Thermal-Hydraulic Analysis of Large Hot Leg Break with Simulation of Core Inlet Blockage. Revision 1, December 2019.

33. **Westinghouse WCAP-17788-NP, Volume 6.** Comprehensive Analysis and Test Program for GSI-191 Closure (PA-SEE-1090) - Subscale Head Loss Test Program Report. Revision 1, December 2019.

Enclosure 3 - Application for Withholding Proprietary Information from Public Disclosure

COMMONWEALTH OF PENNSYLVANIA:
COUNTY OF BUTLER:

(1) I, Camille T. Zozula, have been specifically delegated and authorized to apply for withholding and execute this Affidavit on behalf of Westinghouse Electric Company LLC (Westinghouse).

(2) I am requesting the proprietary portions of NextEra Energy Seabrook Document SBK-L-21049 be withheld from public disclosure under 10 CFR 2.390.

(3) I have personal knowledge of the criteria and procedures utilized by Westinghouse in designating information as a trade secret, privileged, or as confidential commercial or financial information.

(4) Pursuant to 10 CFR 2.390, the following is furnished for consideration by the Commission in determining whether the information sought to be withheld from public disclosure should be withheld.

(i) The information sought to be withheld from public disclosure is owned and has been held in confidence by Westinghouse and is not customarily disclosed to the public.

(ii) The information sought to be withheld is being transmitted to the Commission in confidence and, to Westinghouse's knowledge, is not available in public sources.

(iii) Westinghouse notes that a showing of substantial harm is no longer an applicable criterion for analyzing whether a document should be withheld from public disclosure. Nevertheless, public disclosure of this proprietary information is likely to cause substantial harm to the competitive position of Westinghouse because it would enhance the ability of competitors to provide similar technical evaluation justifications and licensing defense services for commercial power reactors without commensurate expenses. Also, public disclosure of the information would enable others to use the information to meet NRC requirements for licensing documentation without purchasing the right to use the information.

(5) Westinghouse has policies in place to identify proprietary information. Under that system, information is held in confidence if it falls in one or more of several types, the release of which might result in the loss of an existing or potential competitive advantage, as follows:

(a) The information reveals the distinguishing aspects of a process (or component, structure, tool, method, etc.) where prevention of its use by any of Westinghouse's competitors without license from Westinghouse constitutes a competitive economic advantage over other companies.

(b) It consists of supporting data, including test data, relative to a process (or component, structure, tool, method, etc.), the application of which data secures a competitive economic advantage (e.g., by optimization or improved marketability).

(c) Its use by a competitor would reduce his expenditure of resources or improve his competitive position in the design, manufacture, shipment, installation, assurance of quality, or licensing a similar product.

(d) It reveals cost or price information, production capacities, budget levels, or commercial strategies of Westinghouse, its customers or suppliers.

(e) It reveals aspects of past, present, or future Westinghouse or customer funded development plans and programs of potential commercial value to Westinghouse.

(f) It contains patentable ideas, for which patent protection may be desirable.

(6) The attached documents are bracketed and marked to indicate the bases for withholding. The justification for withholding is indicated in both versions by means of lower-case letters (a) through (f) located as a superscript immediately following the brackets enclosing each item of information being identified as proprietary or in the margin opposite such information. These lower-case letters refer to the types of information Westinghouse customarily holds in confidence identified in Sections (5)(a) through (f) of this Affidavit.

I declare that the averments of fact set forth in this Affidavit are true and correct to the best of my knowledge, information, and belief.

I declare under penalty of perjury that the foregoing is true and correct.

Executed on: 06 May 2021

Camille Zozula

Camille T. Zozula, Manager
Regulatory Compliance & Corporate Licensing